UNIVERSITY OF ALBERTA

NUCLEOBASE INTERACTIONS WITH SOLVENTS AND SUNSCREENS FROM RAMAN SPECTROSCOPY

by LUCIO HAYFORD BEYERE

A thesis submitted to the Faculty of Graduate Studies and Research in partial fulfillment of the requirements for the degree of Master of Science

DEPARTMENT OF CHEMISTRY

EDMONTON, ALBERTA

SPRING, 2000

National Library of Canada
Acquisitions and Bibliographic Services
395 Wellington Street
Ottawa ON K1A 0N4
Canada

Bibliothèque nationale du Canada
Acquisitions et services bibliographiques
395, rue Wellington
Ottawa ON K1A 0N4
Canada

Your file Votre référence

Our file Notre référence

The author has granted a non-exclusive licence allowing the National Library of Canada to reproduce, loan, distribute or sell copies of this thesis in microform, paper or electronic formats.

The author retains ownership of the copyright in this thesis. Neither the thesis nor substantial extracts from it may be printed or otherwise reproduced without the author's permission.

L'auteur a accordé une licence non exclusive permettant à la Bibliothèque nationale du Canada de reproduire, prêter, distribuer ou vendre des copies de cette thèse sous la forme de microfiche/film, de reproduction sur papier ou sur format électronique.

L'auteur conserve la propriété du droit d'auteur qui protège cette thèse. Ni la thèse ni des extraits substantiels de celle-ci ne doivent être imprimés ou autrement reproduits sans son autorisation.

0-612-60094-7

Canada

UNIVERSITY OF ALBERTA

LIBRARY RELEASE FORM

NAME OF AUTHOR: Lucio Hayford Beyere

TITLE OF THESIS: Nucleobase Interactions with Solvents and Sunscreens from Raman Spectroscopy

DEGREE: Master of Science

YEAR THIS DEGREE GRANTED: 2000

Permission is hereby granted to the University of Alberta Library to reproduce single copies of this thesis and to lend or sell such copies for private, scholarly, or scientific research purposes only.

The author reserves all other publication and other rights in association with the copyright in the thesis, and except as herein before provided, neither the thesis nor any substantial portion thereof may be printed or otherwise reproduced in any material form whatever without the author's prior written permission.

Lucio Hayford Beyere

Nandom Catholic Mission, Post Office Box 14

Nandom-Ketuo, Wa, Upper-West Region, Ghana

Date: Jan. 18, '00

UNIVERSITY OF ALBERTA

FACULTY OF GRADUATE STUDIES AND RESEARCH

The undersigned certify that they have read, and recommend to the Faculty of Graduate Studies and Research for acceptance, a thesis entitled

Nucleobase Interactions with Solvents and Sunscreens from Raman Spectroscopy

submitted by **Lucio Hayford Beyere** in partial fulfillment of the requirements for the degree of **Master of Science**.

Dr. G. R. Loppnow Supervisor

Dr. A. Mar Committee Chair

Dr. X. C. Le Committee Member

Date: Jan. 14, '00

Abstract

In this thesis, Raman spectra of nucleobases and sunscreen active ingredients are measured in an attempt to determine DNA-sunscreen interactions. The Raman spectra of thymine and thymidine in nine solvents, acid and base show frequency shifts and intensity changes in specific N-H and C=O Raman modes as a function of solvent hydrogen bonding strength. The Raman spectra of five sunscreen active ingredients in ten solvents also show frequency shifts in the C=O Raman mode of para-amino benzoic acid (PABA) and cinnamate derivatives with increasing solvent hydrogen bonding strength and mode-specific Raman intensity changes for PABA, cinnamate and benzophenone derivatives. Surprisingly, Raman spectra of sunscreen:DNA with concentration ratios from 2:1 to 1:10 show no frequency shifts nor intensity changes upon addition of DNA. These results are discussed in terms of the DNA molecular environment.

Dedication

"So *faith, hope, love* remain, these three; but the greatest of these is **love**"

(1 Corinthians 13:13)

I dedicate this work to:

Daria Nopoe (Mother)

Jane Francis Hai (Brother)

Esther Segta Aasirenifaa-wuo (Sister)

and Emmanuel Aagangngmen Aasirenifaa-wuo(Son)

(*N Māāā, fo yaane; Janee, ta zore dambieh; Esther ne Emmaa, ne zaane velaa*)

Preface

"...for you (God) have made us for yourself, and our heart is restless until it rests in you."

("*...quia fecisti nos ad te et inquietum est cor nostrum, donec requiescat in te.*")

[The Confessions of St. Augustine]

Serenity Prayer

God grant me the **serenity**

to *accept* the things I cannot change,

the **courage** to *change* the things I can,

and the **wisdom** to *know* the difference.

(Pastor Reinhold Niebuhr Prayer)

Acknowledgments

Thanks be to God Almighty, author of my being, source of my might, strength, and wisdom; with whom "nothing is impossible," who has made all things possible in my life and brought me to a successful completion of this program. Praise, glory and honor to you Loving Father. Yet since God does not work in 'vacuum,' but uses feeble/mortal humans to unfold His divine will and purpose in my life, I thank Him for the gift of parents, family, relatives, friends, teachers, benefactors and well-wishers through whom He has worked and continues to reveal the miracle/mystery of my life.

I will first like to thank all my teachers from primary one to date especially Teachers Zob and Willie (P1), Teacher Maurice (P4), and Mr. Charles Gornah (P6), who from the onset have taught me that "Education is not the filling of a hole/bucket, but the lighting of a fire/flame." I also wish to express my deepest appreciation to Rev. Fr. John Kwame Owiredu (SJ), the F.I.C. Brothers and Mr. T. C. L. Brew for their tremendous and indispensable advice, spiritual guidance, encouragement, prayers and financial support that made it possible for me to come to Canada for this graduate studies program. Fr. Kwame, *me daa wase, Nyame nhyira woooh.* Bro Methodius Kuusoru *ne* F.I.C. Brothers, *nye barka barka yaga zaa.* Finally to Mr. Brew, my favorite Chemistry Lecturer, who has convinced me that 'Chemistry is life and life is Chemistry, I say thank you for all the encouragement and financial assistance.

Yet, since this work would not have been possible without a research group and a Supervisor, I will like to thank Dr. Glen R. Loppnow for making me a part of his research group and putting at my disposal his resources and research facilities, as well as for generous use of his time to supervise this work. It has been a pleasure knowing and working in/with the group. Thank you Glen. Special thanks to Dr. Ester Fraga and to my colleagues Musilli M. Mitambo and Adam M. Webb for all the support, assistance, discussions, and for the pleasant moments shared. *Gratias Ester; Musilli, Assantee; Adam, merci beaucoup.* I am particularly grateful to Miss Vishakha Monga (1997 RISE Student) with whom I did all the thymine and thymidine work. *VISH, bahut, bahut.* I thank Dr. Shuliang Zhang, Sarah Eisler and Jayan Nagendran for their work on

thymine/thymidine which was very useful to me. I would also like to acknowledge financial support from the Department of Chemistry.

I am also greatly indebted to Mr. and Mrs. Robert H. and Phyllis J. Cook (My Canadian Parents) who welcomed me into their home and for all the help during my stay. Bob and Phyllis, God Bless you, *barka*. I would also like to thank the Basilian Fathers and parishioners of St. Joseph's College for nourishing my faith all these years, and especially for the Antioch and Montée retreats where I made many great friends. Next, special thanks to my wonderful apartment mates Dr. Rohit Patwardhan, Jaishankar Thayyoor and Eshetu Atenafu for a memorable and pleasant stay, as well as for all the encouragement and cultural exchanges. To Dr. Peter Imoro, a brother and friend who was never tired of my complaining and would not let me give up when I wanted to on this program, I say *naagoodeeee*. I am very grateful to Dr. Kingsley Donkor who used his experiences to encourage and urge me on anytime I was at the point of giving up. *Onua Panyin Donkor, asidaaa ka Oo*. Also to Bernd Keller and David Naanang for the many encouraging moments and relaxing weekends, I say *danke, amisiere*.

Finally, my sincerest gratitude to my mother, brothers and sisters and Uncle Eugene for your prayers and especially to you Mother, Jane and Esther, who when you needed me most I had to be away for this program. God bless you all. I am greatly indebted to my friends Peter Latuo, Lucius Zaukuu and Dr. Alexis Nangbei-fubah and their families for support, prayers, encouragement and taking care of my family affairs all these years that I have been out here.

To you all and numerous others that I have not mentioned, I say *BARKA BARKA YAGA ZAA, NAANGMEN MAALE NYE ZAAAA*.

TABLE OF CONTENTS

CHAPTER		PAGE
1	General Introduction	1
	1.1 Overview	2
	1.2 DNA Composition and Photochemistry	3
	1.3 Sunscreen active ingredients	17
	1.4 Vibrational spectroscopy	21
	1.5 Summary of Research	25
	1.6 References	26
2	Solvent-Dependence of Thymine Raman Spectrum	29
	2.1 Introduction	30
	2.2 Experimental	33
	2.3 Results	38
	2.4 Discussion	49
	2.5 Conclusion	60
	2.6 References	61
3	Solvent-Dependence of Thymidine Raman Spectrum	63
	3.1 Introduction	64
	3.2 Experimental	66
	3.3 Results	67
	3.4 Discussion	76
	3.5 Conclusion	84
	3.6 References	85

4 DNA-Sunscreen Interactions from Raman Spectroscopy....88
4.1 Introduction....89
4.2 Experimental....92
4.3 Results....97
4.4 Discussion....130
4.4.1 Solvent Interactions....130
4.4.2 Sunscreen Interaction with DNA....137
4.5 Conclusion....139
4.6 References....140

5 Conclusions and Future Work....144
5.1 Thymine and Thymidine Raman Spectra....145
5.2 DNA and Sunscreen Interaction....146
5.3 Future Work....147
5.4 References....149

LIST OF TABLES

TABLE		PAGE
2.1	Selected empirical parameters of solvents used in this study	34
2.2	Selected derived parameters of solvents used in this study	35
2.3	Thymine peaks in various solvents spectra	45
2.4	Correlation coefficients for thymine	50
2.5	Selected Correlations between observed Raman frequencies and solvent properties for thymine	51
3.1	Thymidine peaks in various solvents spectra	72
3.2	Correlation coefficients for thymidine	78
3.3	Selected Correlations between observed Raman frequencies and solvent properties for thymidine	79
4.1	Selected empirical parameters of solvents used in this study	96
4.2	UV-absorption maximum peaks of sunscreens	100
4.3	ODPABA peaks in various solvents from the spectra in Figure 4.7	114
4.4	OMC peaks in various solvents from the spectra in Figure 4.8	117
4.5	BZ3 peaks in various solvents from the spectra in Figure 4.9	120

LIST OF FIGURES

FIGURE		PAGE
1.1	Structure of DNA and constituent nucleobases	5
1.2	UV-absorption spectra of thymine derivatives	8
1.3	General Jablonski diagram	11
1.4	Photoproducts of dTpdT, dTpdC, and dTpdU	14
1.5	Raman spectroscopy	24
2.1	Thymidine/thymine structure and numbering convention	32
2.2	Schematic diagram of experimental set-up	37
2.3	Raman spectra of thymine in water	40
2.4	Raman spectra of various solvents used in this study	42
2.5	Raman spectra of thymine in various solvents	44
2.6	Raman spectra of thymine in acid, basic and aqueous solution	48
2.7	Good and poor correlations of Raman frequency with solvent parameter	54
2.8	Zwitterionic structure of thymine	59
3.1	Raman spectra of thymidine in water	69
3.2	Raman spectra of thymidine in various solvents	71
3.3	Raman spectra of thymidine in acid, basic and aqueous solution	75
3.4	Good and poor correlations of Raman frequency with solvent parameter	81
4.1	Structure of sunscreen active ingredients	94
4.2	UV-absorption spectra of sunscreen active ingredients in methanol	99
4.3	Raman spectra of neat liquid sunscreen active ingredients	103
4.4	Raman spectra of BZ3 and DBM in hexane	106
4.5	Raman spectra of solvents used in this study	108
4.6	Raman spectra of DBM solutions	110
4.7	Raman spectra of ODPABA solutions	113
4.8	Raman spectra of OMC solutions	115

4.9 Raman spectra of BZ3 solutions....119
4.10 Raman spectra of ODPABA-DNA solutions....123
4.11 Raman spectra of ODPABA-DNA solutions....125
4.12 Raman spectra of OMC-DNA solutions....127
4.13 Raman spectra of OMC-DNA solutions....129
4.14 Resonance structures of ODPABA and OMC....134

Chapter 1 - General Introduction

1.1 Overview

Most of the chemical, physical and biological processes of interest to humans occur in the solution or liquid phase. However, a detailed molecular picture of the role of the environment in these processes has not been obtained due to a lack of structural probes of solute-solvent interactions. My research is aimed at the elucidation of these interactions and their effect on chemical reactivity in DNA and related model systems using a structurally-specific probe. The technique of choice is Raman and resonance Raman spectroscopy.

Interaction of light with biological molecules plays a central role in such beneficial processes as photosynthesis in plants, vision, and tanning in humans. Unfortunately, the absorption of light can also have harmful effects. In humans, absorption of solar UV-radiation leads to DNA damage of the skin cells. Several photoproducts are formed, of which the cyclobutane pyrimidine dimers are the most prevalent. Incomplete repair of these dimers is thought to eventually lead to skin cancer. Sunscreens have been used to protect human skin from this UV-solar radiation damaging effect. Recently, however, sunscreens have been reported to have adverse effects.

The goal of this work is to have a better understanding at the molecular level of the interactions between DNA and exogenous substances that in the presence of light may lead to harmful or beneficial health effects. Raman spectroscopy will be used to obtain a better understanding of the light-induced DNA damage and repair mechanism, as well as the beneficial or adverse effects of sunscreens on DNA in the presence of solar UV radiation. As a preliminary step, a study of the solvent effects on the Raman spectra of thymine and thymidine with visible excitation was undertaken. A similar study was done for five sunscreen active ingredients, as well as for the interaction of sunscreens and DNA.

1.2 DNA Composition and Photochemistry

The primary structure of nucleic acids consist of monomeric units called nucleotides that contain predominantly five heterocyclic purine and pyrimidine bases (1-3). The nucleotide subunit consists of a base, a sugar and a phosphate group, while the base and sugar unit alone makes up a nucleoside. The sugars are normally ribose or 2'-deoxyribose, the purine bases are adenine (A) and guanine (G), and the pyrimidine bases are uracil (U), thymine (T), and cytosine (C). DNA (deoxyribonucleic acid) is composed of A, T, G, and C bases (Figure 1.1), while RNA (ribonucleic acid) contains A, U, G, and C bases. The bases in DNA are attached to C-1' of 2'-deoxyribose via the N-9 of the purines or the N-1 of the pyrimidines. Phosphate groups link these nucleoside monomers by forming phosphoester bonds with the -OH groups at C-3' and C-5' of each sugar. Since the nucleobases (or base moieties of the nucleosides and nucleotides) contain two to four nitrogen atoms and one to two exocyclic amino groups or oxo groups, the question of tautomerism and ionization is of prime importance in understanding their structure (1, 4, 5). The purine bases can exist in the amino and imino tautomeric forms, while the pyrimidine bases can exist in the keto and enol tautomeric forms. It has been established that these DNA bases and their nucleoside and nucleotide derivatives exist exclusively in the keto-amino forms, rather than the enol-imino tautomers in neutral aqueous solutions (1, 4). The effects of pH on the structure of these bases is observed in the protonation of the bases at low pH and deprotonation at high pH. The bases all have two or more sites for protonation, i.e., the ring nitrogens and exocyclic groups. Protonation of the base moieties takes place at the ring nitrogens instead of the exocyclic groups. This attachment of protons at the ring nitrogens appears to favor localization of ring π-electrons in various double bonds, while detachment of protons appears to cause delocalization of the π-electrons. Thus, in the pH range 2-11, A and C are positively charged in acid and electrically neutral in alkali, U and T are electrically neutral in acid and negatively charged in alkali, and G is positively charged in acid and negatively charged in alkali (1, 4, 5).

The absorption of UV light by DNA is determined by its constituents. The sugar-

Figure 1.1 - Structure of DNA and constituent nucleobases; adenine (A), thymine (T), cytosine (C), and guanine (G).

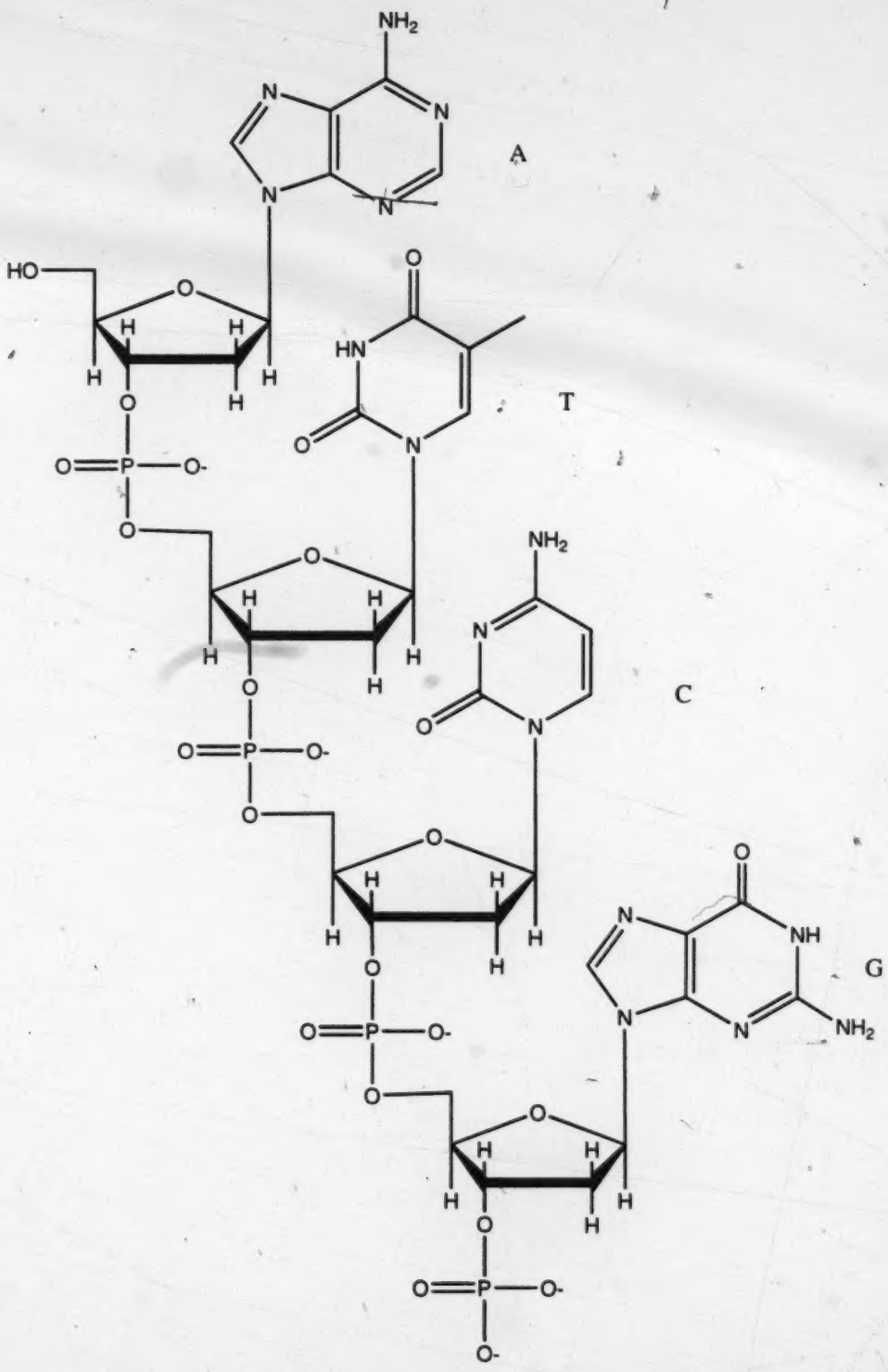
A
T
C
G

the bases absorb significantly in the 200-300 nm region. The absorption spectrum of the bases and their derivatives are similar, an indication that the attachment of the sugar and phosphate groups to the bases do not greatly modify the absorption properties of the bases. Hence the absorption spectrum of thymine, thymidine, thymidine monophosphate and thymidine dinucleotide (dTpdT) all have an absorption maximum around 266 nm, in addition to a peak around 210 nm (Figure 1.2). These absorptions arise from a complex mixing of π,π^* transitions from the C=C, C=O, and C=N double bonds. In addition, n,π^* transitions from non-bonding electron pairs from O and N atoms may also give rise to bands in the absorption spectrum. The π,π^* transitions are more intense with an extinction coefficient of about 10,000 $M^{-1}cm^{-1}$, while the n,π^* transitions are very weak, with an extinction coefficient of around 100 $M^{-1}cm^{-1}$, and do not appear in the absorption spectrum of the bases and DNA. Hence, several different π,π^* and n,π^* transitions occur for each base in the region of the spectrum between 200-300 nm. However, the intense transitions giving rise to bands in the absorption spectra of the nucleobases can be confidently assigned to π,π^* transitions. Of course, two or more transitions may overlap giving the appearance of a single band. Hence, for A and U(T), the band around 260 nm is a composite of more than one electronic transition. G and C also show clear evidence of at least two bands, although more are probably hidden (6).

Several photophysical and photochemical processes occur on exposure of DNA to UV light. In the short time between the absorption of a UV photon by one of the DNA bases and final formation of a damage center, many electronic rearrangements can take place, various excited states of different spin multiplicities may be populated, energy may be transferred between different regions of DNA, and some covalent bonds may be formed while others may be broken (7-9). As described above, the nucleobase UV chromophores in DNA all exhibit π,π^* and n,π^* transitions. The lowest excited singlet state in all the bases is a π,π^*, and all the bases also have a π,π^* state as the lowest excited triplet state. The DNA is excited to the lowest singlet (π,π^*) excited state, upon absorption of a photon. The electronic excitation may dissipate in a number of ways. The Jablonski diagram (Figure 1.3) shows the lowest lying energy levels of a typical

Figure 1.2 - UV absorption spectra of thymine (T), thymidine (TM), thymidine monophospate (TMP), and thymidine dinucleotide (dTpdT).

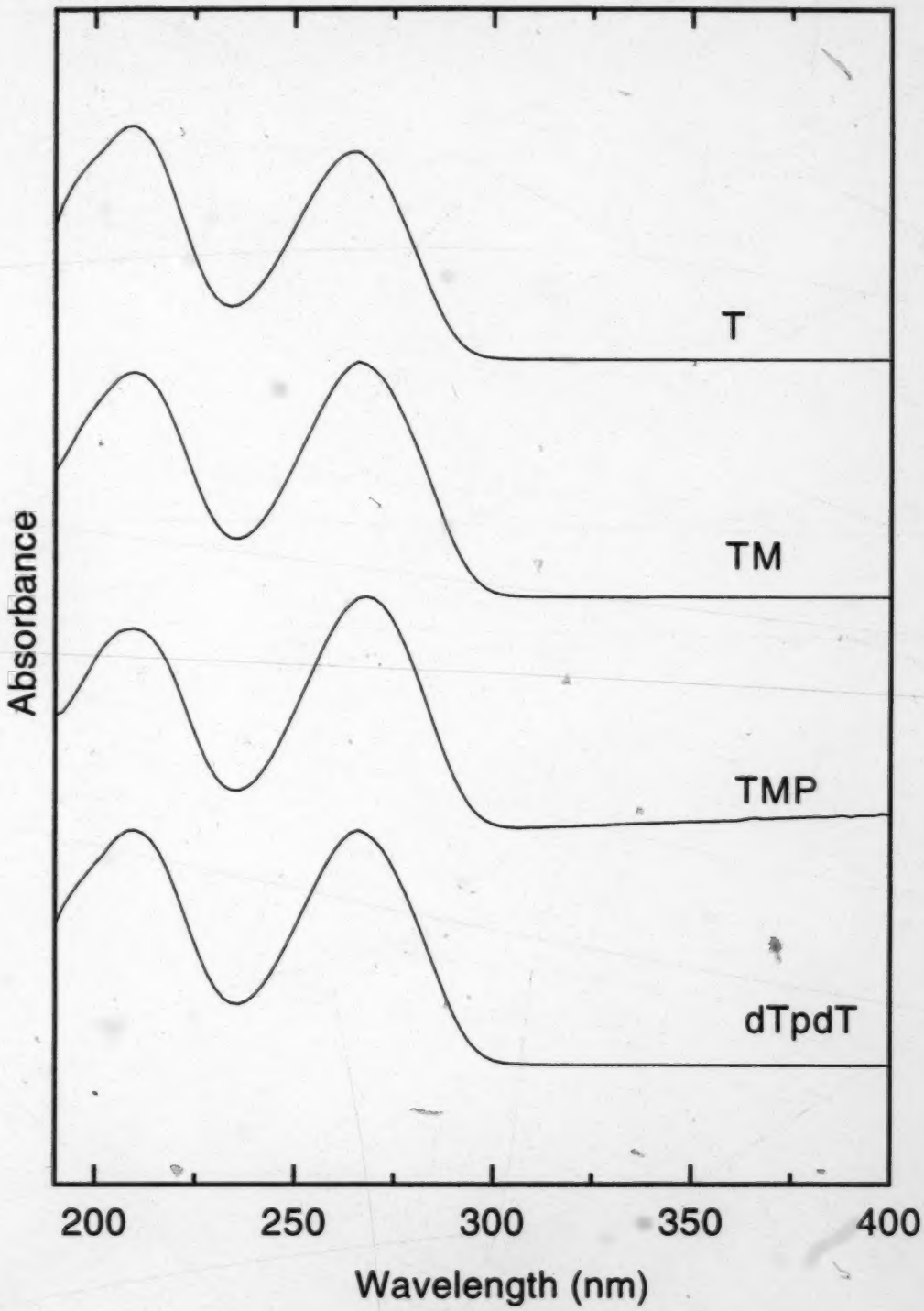
T
TM
TMP
dTpdT
Absorbance
200
250
300
350
400
Wavelength (nm)

organic molecule such as a purine or pyrimidine and indicates the various radiative and non-radiative transitions which may occur. The two excited states of greatest importance are the lowest excited singlet and triplet states. Absorption of a light photon (occurs in 10^{-15}-10^{-12} s) promotes the molecule from the ground electronic state S_0 to one of the excited vibrational levels of excited electronic states, S_1 and S_n (higher states). Spin multiplicity is conserved, as the promoted electron is still spin-paired with the one left in the lower energy level. Considering the S_1 state, the excited molecule vibrationally relaxes in a short time of 10^{-12}-10^{-10} s to the S_1,v_0 state followed by several processes. The molecule can emit a photon and return directly to the S_0 state via fluorescence (a radiative process which occurs in 10^{-10}-10^{-6} s), or by internal conversion (IC, a very rapid non-radiative process which occurs in 10^{-12} s) move from S_1,v_0 to S_0,v_{high} followed by vibrational relaxation to the S_0,v_0 (a non-radiative process). The molecule could also move from the S_1,v_0 state to a higher triplet vibrational level by intersystem-crossing (ISC, occurs in 10^{-12}-10^{-4} s depending on the molecule). This occurs by a spin inversion, hence a change in spin multiplicity. From here it vibrationally relaxes to the T_1,v_0 state, followed by phosphorescence (a radiative process) or ISC followed by vibrational relaxation again (non-radiative processes) to the S_0 state. Phosphorescence involves states of different spin ($T_1 \rightarrow S_0$) and thus occurs in a long time range of 10^{-3}-10 s.

Fluorescence in DNA has been observed, and is thought to increase with A-T content. DNA has a very weak phosphorescence, although the triplet state quantum yield and lifetime has also been observed to increase with A-T content. Typical fluorescence quantum yields of thymine, thymidine and thymidine monophosphate at 77° K are 0.21, 0.22 and 0.16, respectively, while the yield for thymine at 300° K has been estimated as 1.8×10^{-4}, with a rate constant of 1.0×10^8, 7.1×10^8, 1.8×10^8, and 5.7×10^{11} s^{-1}, respectively, for fluorescence, ISC, chemical reactions and IC. Finally, the molecule could undergo some type of reaction from the S_1,v_0 state, as well as from the T_1,v_0 state which is generally termed photochemistry. The S_1 and T_1 states are involved in the formation of photoproducts in DNA photochemistry.

On exposure of DNA to solar UV radiation (200-400 nm), several photochemical processes occur causing damage. The purine bases are generally less sensitive to UV-

Figure 1.3 - A general Jablonski diagram; absorption (A), fluorescence (F), phosphorescence (P), vibrational relaxation (VR), internal conversion (IC), and intersystem crossing (ISC). Lines indicate radiative processes (A, F, P), while broken lines indicate non-radiative processes (VR, IC, ISC).

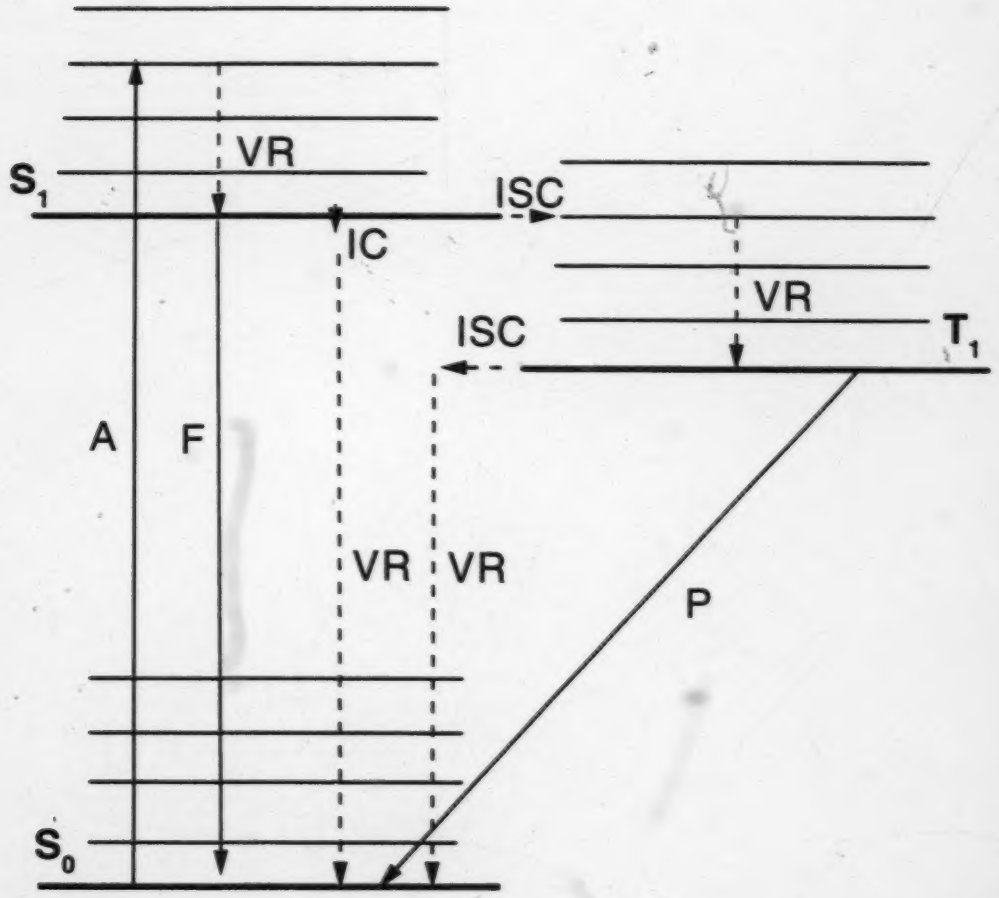
VR
S1
ISC
IC
VR
ISC
T1
A
F
VR
VR
P
S0

irradiation than their pyrimidine counterparts. The main photochemistry involves the formation of pyrimidine photoproducts, the most important and stable ones being cyclobutane dimers, (6-4) photoadducts and photohydrates (Figure 1.4). The first excited singlet electronic state (S_1) is the principal intermediate involved in the formation of these photoproducts.

The major damage to DNA on UV exposure is due to the formation of pyrimidine cyclobutane dimers (9-13). This damage is subject to repair by an enzyme (DNA photolyase) which binds to DNA and splits the dimers back to monomeric bases using near-UV or visible light. The incomplete repair of this damage causes inactivation of cells and may eventually lead to skin cancer. Dimerization results from a [2+2] photocycloaddition reaction between the C_5=C_6 double bonds of two adjacent pyrimidine bases to give the well known cylobutane dimers. Thymidine dimers are formed with the greatest efficiency compared to the other bases (e.g. C<>C dimers form only 50-75% of T<>T). Out of eight potential isomers, only two are formed due to steric constraints; the *cis-syn* (Figure 1.4A) isomer forms with a higher efficiency than the *trans-syn* isomers (Figure 1.4B). Typical quantum yields (Φ) are 0.016, 0.0082, 0.0072 and 0.0075, respectively, for the *cis-syn* dimers of dTpdT, dTpdU, dTpdC and dUpdU, and 0.001, 0.0002, 0.0011 and 0.0002, respectively, for the *trans-syn* isomers. The Φ for *cis-syn* dimer for DNA has been reported as 0.018, which compares favorably with the value for dTpdT. The T_1 state is thought to be a precursor for dimer formation for monomeric bases, nucleosides and nucleotides; i.e., by reaction of one pyrimidine molecule in the T_1 with another in the S_0 (9, 12, 13). This has been proven by the fact that dimer yields are reduced in uracil, uridine, thymine and thymidine in the presence of O_2 (a triplet state quencher). However, O_2 has no influence on dimer yields in dinucleotides, as shown by results from thymine and uracil dinucleotides (dTpdT, dTpdU and dUpdU), an indication that S_1, rather than T_1 states are involved. All evidence indicates that the *cis-syn* isomer is due to excitation of ground state complexes leading to photoproduct via $^1(\pi,\pi^*)$ states with the required singlet excimers observable as discrete intermediates (9, 12, 13). Hence, the main photoproducts of dinucleotides arise from excitation of ground state complexes. Dimers undergo retrocycloaddition on photolysis (e.g., at 240 or 313 nm) to

Figure 1.4 - Photoproducts of dTpdT, dTpdC and dTpdU; *cis-syn* dimers (A), *trans-syn* dimers (2 isomers, B), photohydrates (2 isomers, C), (6-4) adducts (D), and Dewar isomer (E). Figure 6 of ref. 12.

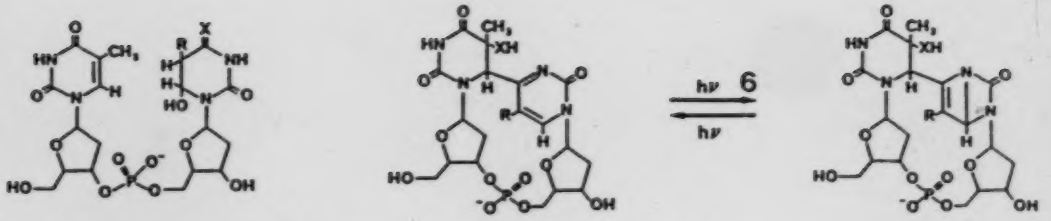

C (2 isomers) D E

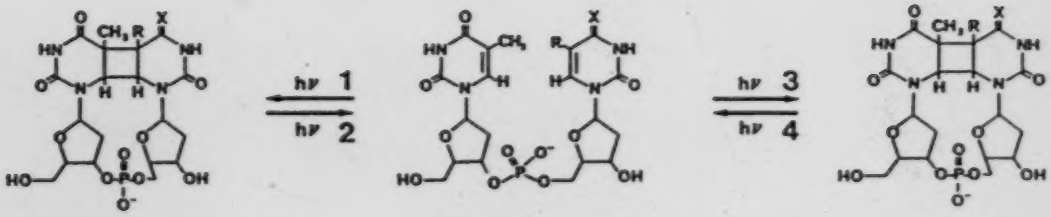

cis-syn A trans-syn B

	X	R
I dTpdT	O	CH_3
II dTpdC	NH	H
III dTpdU	O	H

original bases (greater with C<>C dimers).

The (6-4) photoadducts (9, 10, 12, 13), the next in abundance, are also formed by a [2+2] photocycloaddition of either the C_4=O carbonyl or C_4=N_4 imino groups with the C_5=C_6 double bond of the adjacent 5' base to give oxetane and azetidine intermediates, respectively. These intermediates rearrange by ring-opening mechanisms into 4-(5,6-dihydropyrimidin-6-yl)-2-pyrimidone adducts (Figure 1.4D). These are known to play a role in UV-induced cytotoxic damage of DNA. The 6-4 adducts of the dinucleotides dTpdT, dTpdC, and dTpdU are formed with a much lower yield of 5-10% of the *cis-syn* dimers. Their quantum yields are 0.0005, 0.00075, and 0.00045, respectively, (i.e., TC adducts are 50% higher than TT or TU), compared to 0.016 for the *cis-syn* dimer in dTpdT. The products are not formed by photosensitization reactions and their yields are not affected by the presence of triplet quenchers, an indication that lowest triplet states are not involved. The reaction occurs via $^1(n,\pi^*)$ states. Typical Φ values obtained from DNA irradiation for T<>T:T<>C:T(6-4) adducts are 0.019:0.0027:0.0015, compared to 0.016:0.0074:0.0012 for dTpdT dimers:dTpdC dimers:(dTpdT+dTpdC adducts), respectively. The yield increases with irradiation time for a while but decreases with longer times, an indication of secondary products formation. Photolysis of the product at 312-327 nm leads to an electrocyclization reaction resulting in a substituted 2-oxo-1,3 diazabicyclo-[2.2.0]hex-5-ene moiety called the Dewar isomer (Figure 1.4E).

The photohydrates (9, 10, 12-14) are formed in the least amounts, only 6% of the dimer yield. This class of products are formed from the nucleophilic addition of water onto the C_5=C_6 double bond to give pyrimidine photohydrates (6-hydroxy-5,6-dihydropyrimidines, Figure 1.4C). These have low biological inactivation effects. The photohydration reaction does not involve neighboring bases, but is rather restricted to the excited base. The reaction proceeds by nucleophilic addition of water exclusively onto the C_6 position of an intermediate derived from the singlet excited state, hence triplet states are not involved as the presence of O_2 (a triplet quencher) does not affect the yields. The overall reaction also involves the nonstereospecific addition of water across the C_5=C_6 double bond, and the nucleophilic attack can occur on either side of the pyrimidine ring to result in two diastereoisomers, formed in a 1.3:1 ratio for cytosine and

uracil. Finally, the relative efficiency for photohydrate formation at neutral pH among the pyrimidine nucleosides is Cyd = Urd >> Thd (an indication of low hydration in TT compounds). Photohydrate quantum yields in dTpdC and dTpdU are 0.00074 and 0.00065, respectively. In both acid and base catalyzed media photohydrate dehydration occurs back to the original bases (greater extent with cytosine products).

These photoproducts have all been isolated and characterized by various chromatographic and spectroscopic methods, as described in the review of Cadet and Vigny (9). For example, from UV-Visible absorption spectroscopy, the unirradiated DNA and model compounds show an absorbance maximum around 260 nm. On irradiation, a decrease in intensity of this band is observed as photoproducts are formed. New absorption bands show up in the spectrum with time at different wavelengths corresponding to the various photoproducts. The appearance of a strong band around 204 nm is an indication of the dimer formation. On photolysis of the dimer with 240 or 193 nm light, the 260 nm band reappears and increases with time due to the conversion of the dimers back to base monomers. The (6-4) adducts absorb strongly in the 312-327 nm region due to the 2-pyrimidone chromophore. Hence, the appearance of bands in this region and around 214 nm are an indication of their formation. Further irradiation of the product at 313 nm shows the disappearance of the strong band in the 325 nm region, an indication of the conversion of the (6-4) adducts to the Dewar valence isomers. However, irradiation of both products at 193 or 240 nm shows the appearance of the 260 nm band due to their conversion back to the monomer bases. The appearance of a band with a maximum around 267 nm on irradiation of dTpdU, which doubles on heating the purified products in acidic (pH 2.0) aqueous solution at 65°C, indicates the formation of the photohydrates. With dTpdC the band is seen at 245 nm which disappears upon standing at room temperature. Hence, the extent of increase and decrease in the absorbances in these regions can be used to characterize the products. In addition to the formation of these photoproducts, single strand breaks, crosslinkages and formation of free radical species also occur all contributing to DNA damage, which eventually leads to skin cancer. Several preventive measures have been suggested, of which the use of sunscreens is the most effective.

1.3 Sunscreen active ingredients

The alarming worldwide increase in skin cancer is a major cause for concern and center of much research. Although the causes of skin cancer are complex, there is now enough evidence that exposure to solar UV radiation is a major environmental trigger (15, 16). Of the total solar energy reaching the earth's surface, 15% is in the UV region (100-400 nm), 60% in the visible range (400-800 nm) and the remaining 25% is in the form of infrared radiation or heat (800-5000 nm). Although the UV radiation accounts for the smallest fraction of terrestrial solar energy, this radiation has the shortest wavelengths. Consequently, it is the most energetic and may induce the most biological damage. The solar UV region is divided into three categories: UVC or germicidal region (100-290 nm), UVB or erythemal (290-320 nm) and the UVA or tanning region (320-400 nm). The most energetic UVC photons are absorbed by atmospheric ozone, nitrogen and oxygen, and thus have little biological consequences. Although part of the UVB region is also absorbed by stratospheric ozone, it is the most damaging region of the solar UV radiation and causes dimer and other photoproduct formation, as well as single strand breaks in the DNA. The longer wavelength UVA region, which was once thought to be harmless because of its low energy, has now been shown to have biological consequences. Because of its greater skin penetration and 10- to 100-fold abundance compared to UVB, it has been known to induce single strand breaks, DNA-to-protein crosslinks and oxidative damage due to photosensitization processes.

To protect humans from the damaging effects of UVB and UVA solar radiation, several preventatives are in place such as reducing/avoiding sunlight exposure when possible, wearing protective clothing, hats and glasses, and the use of sunscreen preparations to protect against these adverse effects of the sun (15, 17). A sunscreen may be defined worldwide as a topically applied product (cosmetic) meant to reduce the impact of the solar UV (mainly UVB/A) radiation on the skin in order to prevent sunburn. The efficacy of sunscreens are normally described by the "sunscreen protection factor" (SPF)

$$SPF = \frac{MED(protected)}{MED(unprotected)} \qquad 1.1$$

where MED (minimal erythema dose) is the UV dose required to produce minimal erythema (sunburn) for protected and unprotected skin. SPF values can be improved by an increase in concentration of one sunscreen or by combining several sunscreens. The higher the SPF value, the more efficient the sunscreen is at protecting the skin from UV irradiation (18). The first reported use of sunscreens in the world was in 1928 in the United States with the commercial introduction of an emulsion containing two sunscreen active ingredients, benzyl salicylate and benzyl cinnamate (19). From then on, there was slow progress in the development of sunscreens. In 1943, para-amino benzoic acid (PABA) was first patented, leading the way to the incorporation of a number of PABA derivatives in sunscreens. Since then, the sunscreen industry has developed rapidly worldwide to include a variety of other chemicals. Sunscreen formulations today include emulsions, oils, gels, sticks, mousses, aerosols and ointments.

Sunscreen active ingredients are divided into two categories depending on their mode of action; physical blockers (inorganic/mineral agents) and chemical absorbers (organic agents) (15, 16, 19, 20). Physical blockers minimize or prevent DNA damage by solar UV-radiation by physically blocking UV-light, i.e., they are opaque enough to reflect or scatter the incident radiation. The two most common ones used today worldwide are titanium dioxide (TiO_2) and zinc oxide (ZnO). They are thought to be inert and non-toxic.

The chemical absorbers used worldwide in the sunscreen industry today can be classified as derivatives of (a) anthranilates, (b) benzophenones, (c) camphors, (d) cinnamates, (e) dibenzoyl methanes, (f) PABA, (g) salicylates, and (h) miscellaneous chemicals (15, 16, 19, 20). In turn, these absorbers can further be subdivided into either UVA (benzophenones, anthranilates and dibenzoyl methanes) or UVB (PABA, salicylates, cinnamates and camphors) absorbers depending on which type of radiation they predominantly absorb. Five of these, i.e., benzophenones, cinnamates, dibenzoyl methanes, PABA and salicylates, comprise the majority of sunscreen products worldwide. The molecular structure of these organic absorbers all contain aromatic moieties in

conjugation with a carbonyl group (15, 19, 20). Often an electron-donating group such as an amine or methoxyl group is substituted in the ortho- or para-position of the aromatic ring.

This high degree of conjugation implies that the electrons are delocalized over the molecule. This high degree of electron delocalization gives rise to intense absorption bands in the UVB and UVA regions of the spectrum. Quantum mechanical calculations have shown that the energy of the radiation present in the UVB and UVA region lies in the same order of magnitude as that of the electronic transitions in these aromatic compounds (19, 20). Therefore, the molecule in the ground state absorbs high energy solar UV radiation (250-350 nm), becomes excited to a higher energy state, and finally releases the energy, effectively shielding the skin from damage.

As the energy of the UV radiation absorbed by the sunscreens causing electronic excitation is of the same order of magnitude as typical bond dissociation energies, the absorbing molecules can dissociate into reactive fragments (such as free radicals) or molecular species. Photoexcitation of a molecule can also lead to direct reaction if the excited state produced is of sufficient energy for the molecule to cross the activation energy barrier for that reaction. Hence, a number of reactions which are not feasible at ambient temperatures can now take place. Also, as electronically excited species have considerably more energy than ground-state species, internal rearrangement of bonds and atomic positions can occur, leading to photoisomerization processes. Finally, electronic energy transfer processes can cause deactivation of the initially produced excited state, via bimolecular interactions with the ground state of another molecule.

The formation of fragments in several sunscreens on UV irradiation has been reported. Photofragmentation causes a loss of the active ingredient which can lead to a reduction in the efficacy of the sunscreen preparation. Photofragmentation may also lead to the formation of short-lived reactive intermediates (e.g. free radicals) and photoproducts. The formation of free radicals and other short-lived intermediates in illuminated sunscreen solutions and their toxicity has previously been reported in literature (21-23). These species include carbon centered radicals ($RC^{\bullet}$), organic peroxyl radicals ($RCOO^{\bullet}$), solvated electrons ($e_{solvated}^{-}$), superoxide radical anion ($O_2^{\bullet -}$) and

hydroxyl radical ($^{\bullet}OH$). These either react directly with DNA or generate other species that can lead to DNA damage via single strand breaks. There are also numerous reports of the various reactive intermediates and stable photoproducts of PABA and its derivatives (24-26) and few reports of the other sunscreens (27, 28).

Direct reaction of sunscreen agents with other biomolecules is also possible. Gasparro and Batissa (29) have reported that PABA covalently binds to DNA, while Shaw, et al. (30), more recently isolated and characterized thymine-PABA and thymidine-PABA photoadducts. There have also been reports (31, 32) that cinnamates photobind to DNA and that binding occurs through [2+2] cyclobutane adduct formation. Photoisomerization has been observed for the cinnamates and dibenzoyl methanes, resulting in decrease in maximum absorbance and lower efficiency. The cinnamates undergo *trans-cis* photoisomerization across the ethylenic double bond (21, 33, 34), while the dibenzoyl methanes exhibit keto-enol tautomerism (34, 35).

Chemical absorbers also act as photosensitizers, a process which involves energy transfer to another molecule. While in some cases this is a desirable process for energy dissipation, in other cases, it can lead to the formation of undesirable products. One of such products is singlet molecular oxygen ($^1O_2$), a potentially toxic oxidant. Allen, et al. (22, 36), reported from the illumination of aqueous sunscreen solutions, that for individual solutions of PABA, cinnamate and benzophenone, singlet molecular oxygen was formed extensively. However, radiationless decay of excited sunscreens via energy transfer can lead to DNA base damage. As already discussed above, the cyclobutane dimers are the most stable and abundant photoproducts formed on absorption of UVB/A radiation by DNA. While these can be formed by direct irradiation at short wavelengths, significant amounts of dimers have also been obtained at longer wavelengths in the presence of triplet state photosensitizers. Photosensitizers which have been shown to induce DNA damage by dimer formation include acetone, acetophenone and benzophenone. Several researchers have reported (37-39) that PABA derivatives photosensitize the formation of thymine dimers in DNA and related compounds.

Several researchers have reported the protective effects against damage by UVB/A radiation of the sunscreens on human and mice skin (40-43). However, from the

discussion above, we observe that, in addition to the beneficial protective effects of sunscreens by absorbing solar UV radiation, several photoproducts, free radicals and intermediate species may also be formed, some of which may have adverse effects and contribute to DNA damage. In some cases, the active ingredients are themselves scavengers of some of these reactive intermediates/species. It has been suggested and demonstrated experimentally (44) that PABA forms as well as reacts rapidly with $^1O_2$ and $^{\bullet}OH$, but does not scavenge $O_2^{\bullet-}$ or react with H_2O_2. It has therefore been speculated that sunscreen active ingredients exert additional protective effects (22) by rapid reaction with toxic oxidant/reactive species and by quenching excited state triplets of other molecules. Sunscreens have been tested, analyzed and characterized by several analytical methods such as chromatography and various spectroscopic methods (UV absorption, infrared, NMR and mass spectrometry) leading to a substantial amount of spectroscopic, chemical and physical data on sunscreen chemicals in the literature (45, 46). However these methods do not probe the effect of environment on sunscreens as well as their interaction with DNA and other biomolecules. For a better understanding of the beneficial and adverse effects of sunscreens and their interaction with DNA and other biomolecules, Raman spectroscopy, a mode specific and sensitive vibrational technique, will be used.

1.4 Vibrational spectroscopy

Vibrational spectroscopy has become a powerful tool for characterizing the structure, molecular environment and dynamics of molecules. It is a sensitive indicator of the chemical properties of molecules, since vibrational spectra reflect the disposition of atomic nuclei and chemical bonds within a molecule and interactions between the molecule and its environment. Although molecular vibrational information is obtained from both infrared (IR) and Raman spectroscopy, the two techniques differ greatly. While IR is an absorption process in which the absorption of IR light by the sample is measured as a function of frequency, the origin of Raman spectra is markedly different. In Raman spectroscopy, light (normally in the UV-visible region) is inelastically scattered

off a molecule and the scattered photons observed in the direction perpendicular to the incident beam (47, 48).

The scattered light consists of two types: one, called *Rayleigh scattering*, is strong and has the same frequency as the incident beam (υ_0), and the other, called *Raman scattering*, is very weak (10^{-5} of the incident beam) and has frequencies $\upsilon_0 \pm \upsilon_m$, where υ_m is a vibrational frequency of the molecule. The $\upsilon_0 - \upsilon_m$ and $\upsilon_0 + \upsilon_m$ lines are called *Stokes* and *anti-Stokes* lines, respectively (Figure 1.5). Normally, the Stokes lines are measured, since they originate from the ground vibrational state (S_0,v_0) and therefore are more intense. The Raman scattering effect arises from electric field-induced polarization, which in turn, depends on a change in molecular polarizability with vibration. This process is different than IR absorption, which arises from a change in the permanent dipole moment with molecular vibration.

In normal Raman spectroscopy, the exciting line (υ_0) is chosen so that its energy is far below that of the first electronic excited state. In this technique, the photon inelastically scatters off a "virtual" state. Resonance Raman (RR) scattering occurs when the sample is irradiated with an exciting wavelength corresponding to an electronic transition of a particular chromophoric group in a molecule. In this process, the incident light scatters inelastically off a real state of the molecule. This results in extremely strong intensity enhancement of the Raman modes coupled to this particular electronic transition by 10^3-10^5 fold.

Raman spectroscopy has several advantages over IR in that (a) water is a weak Raman scatterer and interferes only minimally with the spectra of solutes, (b) Raman can be performed on samples in any phase and (c) with RR, it is possible to selectively enhance vibrations of a particular chromophoric group in a molecule. Because of these advantages, Raman spectroscopy is a sensitive, mode-specific probe and an ideal technique for the study of biological molecules. As a result, the biological applications of Raman spectroscopy have increased explosively in recent years and several studies have established the utility of Raman spectroscopy in determining chromophore structure in DNA and its interaction with environment (49-52). Raman spectroscopy has also become a powerful technique in elucidating drug-DNA interactions (52, 53), since the drug

1.5 - Raman spectroscopy; Stokes lines (S), anti-Stokes lines (AS), Rayleigh lines (R), and infrared absorption (IR).

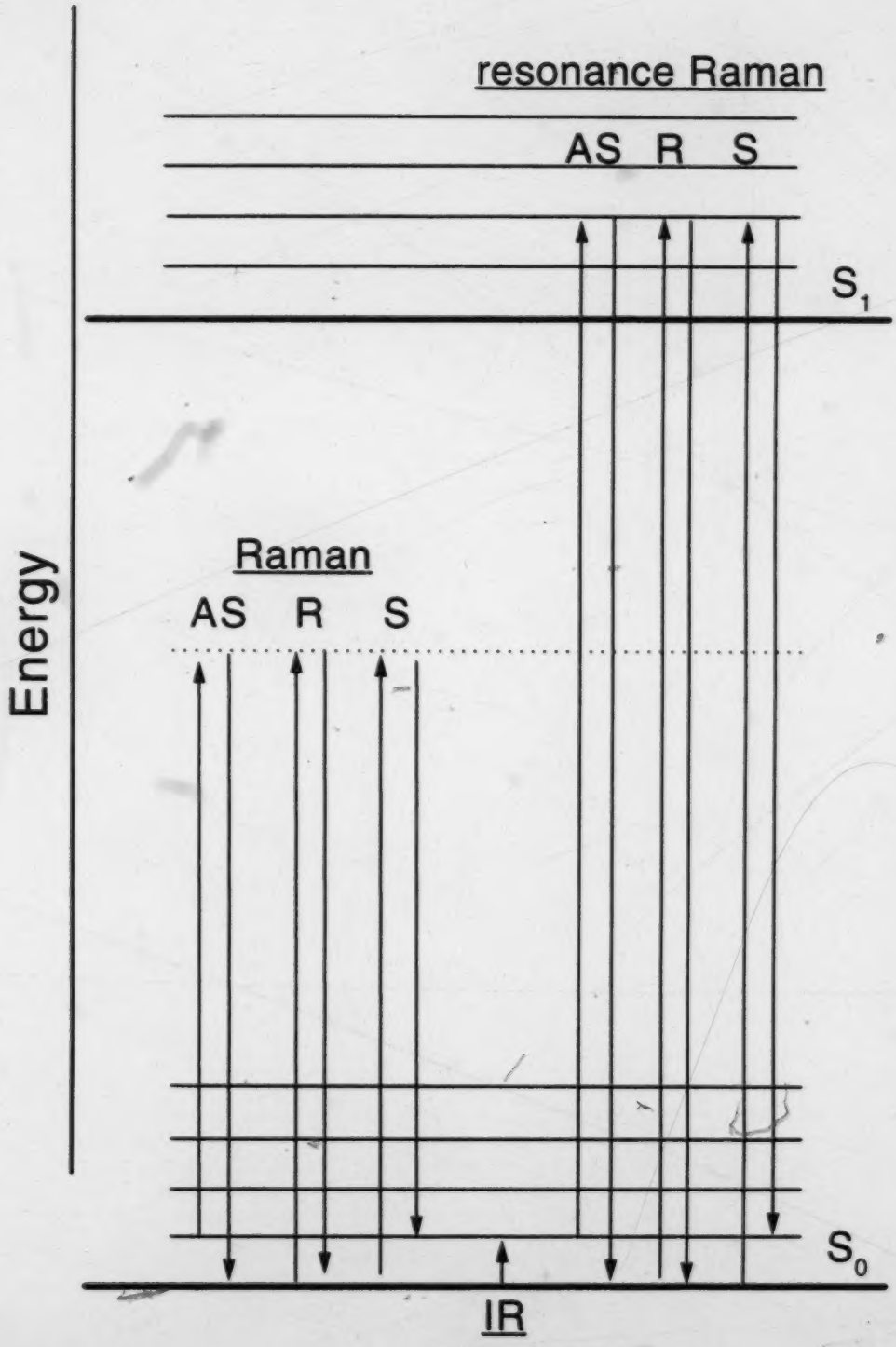
resonance Raman
AS R S
S1
Raman
AS R S
Energy
S0
IR

vibrations can be selectively resonance-enhanced. The technique is therefore suitable in this work to probe DNA structure and dynamics, and the interaction of DNA with sunscreens.

1.5 Summary of Research

Direct exposure of human skin to solar UV radiation causes a variety of damage to DNA which may lead to skin cancer. The mechanisms of this DNA damage are of great biological and biomedical importance. Various sunscreens have been formulated for skin cancer treatment and prevention. On irradiation of DNA and related model compounds with low intensity UV-light (200-300nm range) the most important and stable photoproducts formed are: (1) cyclobutane pyrimidine dimers, (2) pyrimidine (6-4) pyrimidone adducts and (3) pyrimidine photohydrates. Raman spectroscopy, a sensitive and non-invasive vibrational technique will be used in this work to probe DNA structure and environment, sunscreens, and the interaction of DNA and sunscreens. In Chapter 2, we present Raman spectra of thymine in eight solvents using visible excitation. The frequency shifts in some Raman modes and intensity changes observed as a function of solvent polarity are explained. Chapter 3 contains the Raman spectra of thymidine in nine solvents, in which similar frequency shifts and intensity changes are observed and explained as for thymine. The Raman spectra of five active sunscreen ingredients in different solvents are presented in Chapter 4. Frequency shifts are observed for the C=O stretching mode in ODPABA and OMC, as well as some intensity changes. The Raman spectra of the interaction of these two sunscreens with calf thymus DNA at different concentrations are also presented and the results discussed. Chapter 5 draws some conclusions from the results presented in Chapters 2-4 and gives some directions for future work.

1.6 - REFERENCES

1. Ts'o, P. O. P. In *Basic Principles in Nucleic Acid Chemistry*; Ts'o, P. O. P., Ed.; Academic Press: New York, 1974; Vol. 1, p. 453.
2. Saenger, W. In *Principles of Nucleic Acid Structure*; Cantor, C. R., Ed.; Springer Verlag: New York, 1984, p. 9.
3. Carey, P. R. *Biochemical Applications of Raman and Resonance Raman Spectroscopies*; Academic Press: New York, 1982, p. 184.
4. Hartman, K. A.; Lord, R. C.; Thomas, G. J., Jr. In *Physico-chemical Properties of Nucleic Acids*, Duchesne, J., Ed.; Academic Press: New York, 1973; Vol. 2, p. 1.
5. Saenger, W. In *Principles of Nucleic Acid Structure*; Cantor, C. R., Ed.; Springer Verlag: New York, 1984, p. 105.
6. Cantor, C. R.; Schimmel, P. R. *Biophysical Chemistry*.; W. H. Freeman and Company: New York, 1980; Vol. 2, p.343.
7. Eisinger, J.; Shulman, R. G. *Science* **1968**, *161*, 1311.
8. Gueron, M.; Eisinger, J.; Lamola, A. A. In *Basic Principles in Nucleic Acid Chemistry*; Ts'o, P.O.P., Ed.; Academic Press: New York, 1974; Vol. 1, p. 311.
9. Cadet, J.; Vigny, P. In *Bioinorganic Photochemistry: The Photochemistry and the Nucleic Acids*; Morrison, H., Ed.; Wiley Interscience: New York, 1990; vol. 1, p.1.
10. Patrick, M. H.; Rahn, R. O. In *Photochemistry and Photobiology of Nucleic Acids*; Wang, S. Y., Ed.; Academic Press: New York, 1976; Vol. 2, p. 35.
11. Fisher, G. J.; Johns, H. E. In *Photochemistry and Photobiology of Nucleic Acids*; Wang, S. Y., Ed.; Academic Press: New York, 1976; Vol. 1, p. 225.
12. Lemaire, G. E. D.; Ruzsicska, P. B. *Photochem. Photobiol.* **1993**, *57*, 755.
13. Görner, H. J. *Photochem. Photobiol. B: Biol.* **1994**, *26*, 117.
14. Fisher, G. J.; Johns, H. E. In *Photochemistry and Photobiology of Nucleic Acids*; Wang, S. Y., Ed.; Academic Press: New York, 1976; Vol. 1, p.169.
15. Martincigh, B. S.; Aleen, J. M.; Allen, S. K. In *Sunscreen Photobiology*; Gasparro, F. P., Ed.; Landes Press: Georgetown, TX., 1997, chapter 2.
16. Gasparro, F. P.; et al. *Photochem. Photobiol.* **1998**, *68*, 243.

17. Hidaka, H.; et. al. *J. Photochem. Photobiol. A: Chem.* **1997**, *111*, 205.

18. Roberts, L. K.; Learn, D. B. In *Sunscreen Photobiology*; Gasparro, F. P., Ed.; Landes Press: Georgetown, TX., 1997, chapter 8.

19. Shaath, N. A. In *Sunscreens Development, Evaluation, and Regulatory Aspects*; Lowe, N. J.; Shaath, N. A., Eds.; Marcel Dekker: New York, 1990; p 3.

20. Shaath, N. A. In *Sunscreens Development, Evaluation, and Regulatory Aspects*; Lowe, N. J.; Shaath, N. A., Eds.; Marcel Dekker: New York, 1990; p 211.

21. Morliere, P.; Avice, O.; Melo, T. S. E.;et. al. *Photochem. Photobiol.* **1982**, *36*, 395.

22. Allen, J. M.; Gossett, C. J.; Allen, S. K. *J. Photochem. Photobiol. B: Biol.* **1996**, *32*, 33.

23. Halliwell, B.; Gutteridge, J. M. C. *Free Radicals in Biology and Medicine*; 2nd. Ed., Clarendon Press: Oxford, 1995, p. 1.

24. Gasparro, F. P. *Photodermatology*, **1985**, *2*, 151.

25. Shaw, A. A.; Wainschel, L. A.; Sheltar, M. D. *Photochem. Photobiol.* **1992**, *55*, 647.

26. Knowland, J.; McKenzie, E. A.; McHugh, P. J.; Cridland, N. A. *FEBS*, **1993**, *324*, 309.

27. Roscher, N. M. ; Lindemann, M. K. O.; Kong, S. B.; et al. *Photochem. Photobiol.* **1994**, *80*, 417.

28. Schallreuter, K. U.; Wood, J. M.; Farewell, D. W.; et al. *J. Invest. Dermatol.* **1996**, *106*, 538.

29. Gasparro, F. P.; Battista, J. *Photochem. Photobiol.* **1987**, *45*, 49S.

30. Shaw, A. A.; Wainschel, L. A.; Sheltar, M. D. *Photochem. Photobiol.* **1992**, *55*, 657.

31. Broadbent, J. K.; Martincigh, B. S.; Raynor, M. W.; et al. *J. Of Chromatography A* **1996**, *732*, 101.

32. Mohammad, T.; Baird, W. M.; Morrison, H. *Bioorganic Chem.* **1991**, *19*, 88.

33. Kammeyer, A.; Westerhof, W.; Bolhuis, P. A. *Cos. Sc.* **1987**, *9*, 125.

34. Shaath, N. A.; Fares, H. M.; Klein, K. *Cosmetics and Toiletries*, **1990**, *105*, 41.

35. Deflandre, A.; Lang, G. *Cos. Sci.* **1988**, *10*, 53.

36 Allen, J. M.; Gossett, C. J.; Allen, S. K. *Chem. Res. Toxicol.* **1996**, *9*, 605.

37. Rutherford, C. E.; Salter, L. F.; Thomas, R. C. *Photochem. Photobiol.* **1990**, *52*, 337.

38. Bolton, K.; Martincigh, B. S.; Salter, L. F. *Photochem. Photobiol. A: Chem.* **1992**, *63*, 241.

39. Sutherland, B. M. *Photochem. Photobiol.* **1982**, *36*, 95.

40. Kligman, L. H.; Akin, F. J.; Kligman, A. M. *J. Invest. Dermatol.* **1982**, *78*, 181.

41. Whitmore, S. E.; Morison, W. L. *Arch. Dermatol.* **1995**, *131*, 1128.

42. Wolf, P.; Donawho, C. K.; Kripke, M. L. *J. Invest. Dermatol.* **1993**, *100*, 254.

43. Naylor, M. F.; et. al. *Arch. Dermatol.* **1995**, *131*, 170.

44. Allen, J. M.; Engenolf, S.; Allen, S. K. *Biochem. Biophys. Res. Commun.* **1995**, *212*, 1145.

45. Shaath, N. A. In *Sunscreens Development, Evaluation, and Regulatory Aspects*; Lowe, N. J.; Shaath, N. A., Eds.; Marcel Dekker: New York, 1990; p 537.

46. Shaath, N. A. *Cosmet. Toilet.* **1987**, *102*, 21.

47. Nakamoto, K.; Ferraro, J. R. *Introductory Raman Spectroscopy*; Academic Press Inc.: San Diego, 1994, p. 1.

48. McHale, J. L. *Molecular Spectroscopy*; Prentice Hall: New Jersey, 1999, p. 364.

49. See: Carey, P. R. "*Biochemical Applications of Raman and Resonance Raman Spectroscopies*"; Academic Press: New York, 1982.

50. Tsuboi, M.; Nishimura, Y.; Hirakawa, A. Y.; Peticolas, W. L. In *Biological Applications of Raman Spectroscopy*; Spiro, T. G., Ed.; Wiley-Interscience: New York, 1987; Vol. 2, p. 109.

51. Peticolas, W. L.; Kubase, W. L.; Thomas, G. A.; Tsuboi, M. *In Biological Applications of Raman Spectroscopy*; Spiro, T. G., Ed.; Wiley-Interscience: New York, 1987; Vol. 1, p. 81.

52. Nakamoto, K.; Ferraro, J. R. *Introductory Raman Spectroscopy*; Academic Press Inc.: San Diego, 1994, p. 195.

53. Manfait, M.; Theophanides, T. In *Advances in Infrared and Raman Spectroscopy*; Clark, R. J. H.; Hester, R. E., Eds.; John Wiley: Brisbane, 1986; Vol 13, p. 311.

Chapter 2 - Solvent-Dependence of Thymine Raman Spectrum

2.1 Introduction

Thymidine is composed of a 2'-deoxyribose sugar covalently attached to thymine (Figure 2.1), 2,4-dioxo-5-methylpyrimidine, and forms one of the four monomeric building blocks of DNA. Thymine in nucleic acids is particularly prone to damage by UV light, forming a variety of photoproducts such as cyclobutane photodimers, 6-4 photoproducts, and photohydrates (1-3). Because of thymine's susceptibility to photodamage, organisms have developed repair enzymes such as DNA photolyase (4-7), and T4 endonuclease (4, 8-10). Most methods for detecting DNA damage, such as gel electrophoresis (11-13), are invasive and destructive. To follow DNA damage and repair in real time, a non-invasive probe is needed. In this Chapter, we report the first step at developing Raman spectroscopy as a non-invasive probe of DNA structure.

Raman spectroscopy is the inelastic scattering of light off a molecule and usually yields vibrational information (14, 15). Raman spectroscopy has been applied to DNA by a number of groups, in an effort to understand its structure and dynamics (16-22). Although a significant body of work has already been performed on DNA, these studies have suffered from a lack of detail, due to a lack of an adequate understanding of the normal mode properties of the bases in DNA and of the spectroscopic signatures characteristic of particular interactions between DNA and its environment.

In this Chapter, we explore the Raman frequency shifts of thymine as a function of solvent environment. Guided by a recent experimental assignment of the normal modes in thymine and by solvent parameter scales, we attempt to elucidate the specific interaction sites of solvent molecules with thymine in the condensed phase. Several of the observed thymine modes exhibit frequency shifts as a function of solvent parameters. Interestingly, the magnitude of the shifts in a particular solvent are different for different modes, suggesting Raman spectroscopy is a structurally-specific probe of solvent-thymine interactions. In addition, intensity changes in thymine C=O stretch-containing modes indicate particularly strong interactions with solvent. These results suggest Raman spectroscopy may be a useful probe of DNA structure and dynamics.

Figure 2.1 - Thymidine structure and numbering convention. For thymine, a H-atom is attached at the N_1 in place of the 2'-deoxyribose sugar in thymidine.

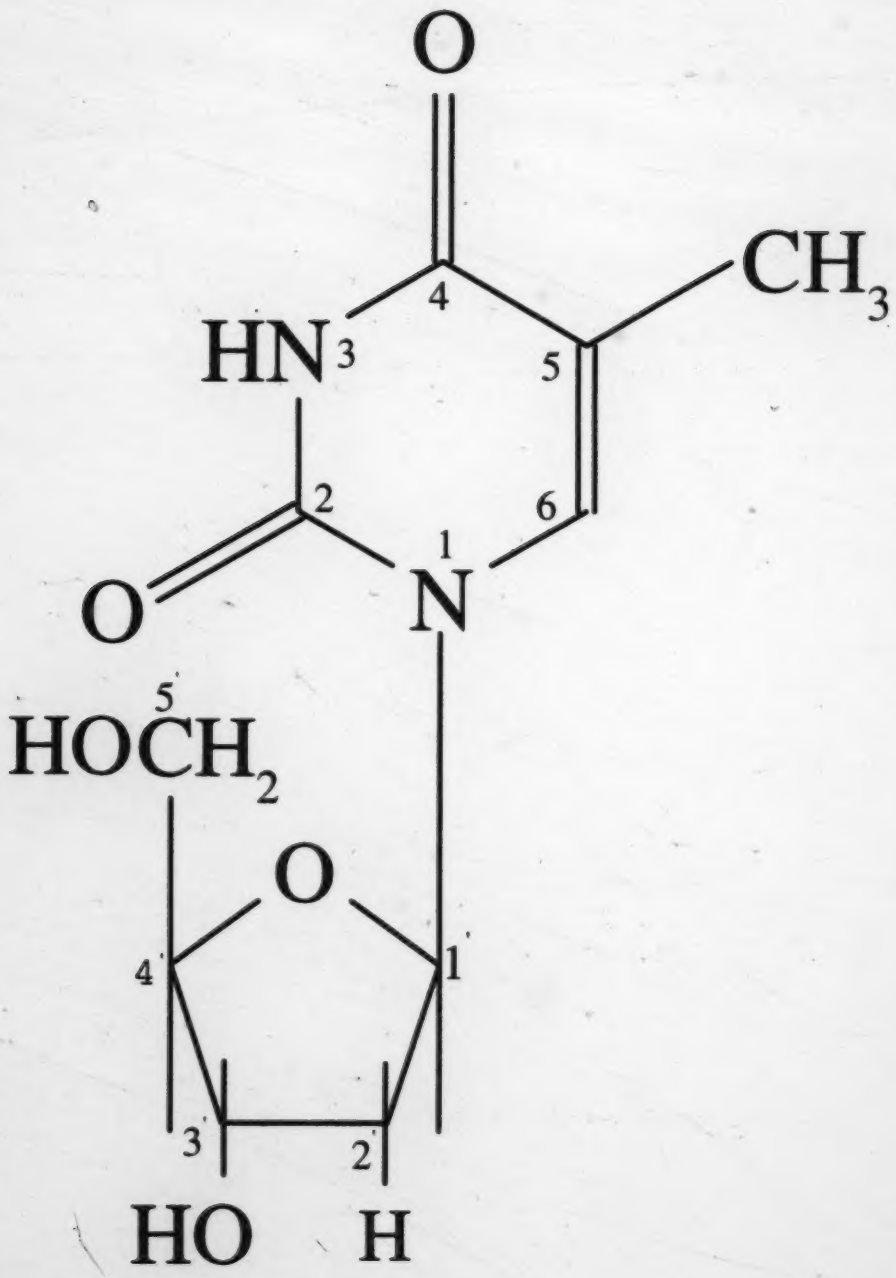
O
CH3
4
HN3
5
2
6
1
O
N
5'
HOCH2
O
4'
1'
3'
2'
HO
H

2.2 Experimental

Thymine (2,4-dioxo-5-methylpyrimidine) was used as received (Sigma, St. Louis, MO). Acetic acid (glacial), N,N-dimethylformamide, ethylene glycol, formamide, formic acid (88%), pyridine, trifluoroacetic acid, and water (deionized, 18 MΩ) were reagent grade or better from freshly-opened bottles and were used without further purification. The important solvent parameters are collected in Tables 2.1 and 2.2.

Room-temperature Raman spectra were obtained of freshly prepared saturated solutions of thymine in various solvents. Due to the differences in solubility of thymine in the various solvents used, the concentration varied from a high range of 0.5-1.5 M for the acidic solvents, to a low range of 1-20 mM in the other solvents (highest concentration of 1.5 M was in trifluoroacetic acid and lowest of ~1 mM in pyridine), as determined from the ultraviolet-visible absorption measurements of the saturated solutions using ε = 10,200 $M^{-1}cm^{-1}$ at 260 nm. Raman spectra were excited by 250 mW of 457.9-nm light from an Ar^+ ion laser (Coherent, Santa Clara, CA) spherically-focused on a spinning NMR tube containing the solution. Figure 2.2 shows a schematic of the experimental set-up. Multichannel detection of the resulting Raman scattering was accomplished with a liquid nitrogen-cooled, charged-coupled device (CCD) detector (Princeton Instruments, Trenton, NJ) coupled to the first half of a double monochromator (Spex, Metuchen, NJ). Spectral slitwidths were 5-7 cm^{-1}. A solvent spectrum has been subtracted from the spectrum of each solution, and the resulting spectrum has been frequency calibrated by measuring the Raman scattering of solvents with known frequencies (acetone, benzene, carbon tetrachloride, and chloroform). The reported frequencies are accurate to ±1.5 cm^{-1}. The baselines have been leveled by subtraction of multiple joined line segments. Raman spectra of freshly prepared saturated solutions of thymine in acid (0.31 M, H_2O, pH~3) and base (0.60 M, H_2O, pH~11) were also obtained under similar conditions.

TABLE 2.1: Selected Empirical Parameters for the Solvents Used in this Study[a]

Solvent	Type of Solvent	n	ε	AN	DN	π*/π*II
acetic acid	A/D	1.3716	6.15^{20}	52.9	12.7[d]	0.664/0.64
benzyl alcohol	A/D	1.5396	13.1	34.5	15.8	0.984/-
N,N-DMF	A[b]	1.4305	36.5[d]	16.0	26.6	0.882[b]/0.88
ethanol	A/D	1.3611	24.3	37.9	20	0.54/-
ethylene glycol	A/D	1.4318	37.7^{25}	-	-	0.932/0.92
formamide	A/D	1.4472	109^{20}	39.8	24.0	1.118/0.97
formic acid	A/D[c]	1.3714	58.5^{16}	-	-	-
pyridine	Ar, A	1.5095	12.3^{25}	14.2	33.1	0.867/0.87
trifluoroacetic acid	A/D[c]	1.6506[d]	8.6[d]	105.3	7.1[d]	0.50[e]
water	A/D	1.333	80.37^{20}	54.8	18.0	1.090/1.09

[a]Type of solvent (A, D, and Ar are hydrogen bond acceptor, hydrogen bond donor and aromatic, respectively), n (refractive index), and ε (dielectric constant, superscripts represent temperature in °C) data from ref. 25. AN (acceptor number) data from ref. 26. DN (donor number) from ref. 27. π*/π*II (Kamlet-Taft dipolarity numbers) data from ref. 28. [b]Used value for N,N-dimethylacetamide. [c]Used value for acetic acid. [d]From ref 29. [e]From ref. 30.

TABLE 2.2: Selected Derived Parameters for the Solvents Used in this Study[a]

Solvent	Y	Π	B	K	Θ	ε_p	M'	M	L	KL
acetic acid	0.649	0.227	0.163	0.387	0.263	5.27	0.369	0.405	0.185	0.0717
benzyl alcohol	0.801	0.314	0.0764	0.429	0.826	11.73	0.345	0.488	0.314	0.153
N,N-DMF	0.922	0.259	0.0274	0.480	0.444	35.5	0.461	0.663	0.205	0.0986
ethanol	0.886	0.221	0.0411	0.460	0.573	23.45	0.499	0.665	0.221	0.147
ethylene glycol	0.924	0.259	0.0265	0.480	0.446	36.7	0.461	0.665	0.206	0.0989
formamide	0.973	0.267	9.2×10^{-5}	0.500	0.716	10900	0.477	0.732	0.211	0.105
formic acid	0.950	0.227	0.0171	0.487	0.481	57.6	0.515	0.723	0.185	0.0901
pyridine	0.790	0.299	0.0811	0.442	0.342	11.0	0.358	0.492	0.230	0.102
trifluoroacetic acid	0.717	0.365	0.116	0.418	0.302	6.88	0.251	0.352	0.267	0.112
water	0.964	0.206	0.0124	0.491	0.504	79.6	0.550	0.758	0.171	0.0837

[a] $Y = (\varepsilon - 1)/(\varepsilon + 2)$ and $\Pi = (n^2 - 1)/(n^2 + 2)$ from ref. 29. $B(\varepsilon) = 1/\varepsilon$, $K(\varepsilon) = (\varepsilon - 1)/(2\varepsilon + 1)$, $\Theta(\varepsilon) = [(3\varepsilon \ln \varepsilon)/(\varepsilon \ln \varepsilon - \varepsilon + 1)] - (6/\ln \varepsilon) - 2$, $\varepsilon_p = \varepsilon - n^2 + 1$, $M'(\varepsilon, n^2) = 1/n^2 - 1/\varepsilon$, $M(\varepsilon, n^2) = [(\varepsilon - 1)/(\varepsilon + 2)] - [(n^2 - 1)/(n^2 + 2)]$, and $L(n^2) = (n^2 - 1)/(2n^2 + 1)$ from ref. 31.

Figure 2.2 - A schematic diagram of the experimental set-up and backscattering geometry used.

Experimental Set-up

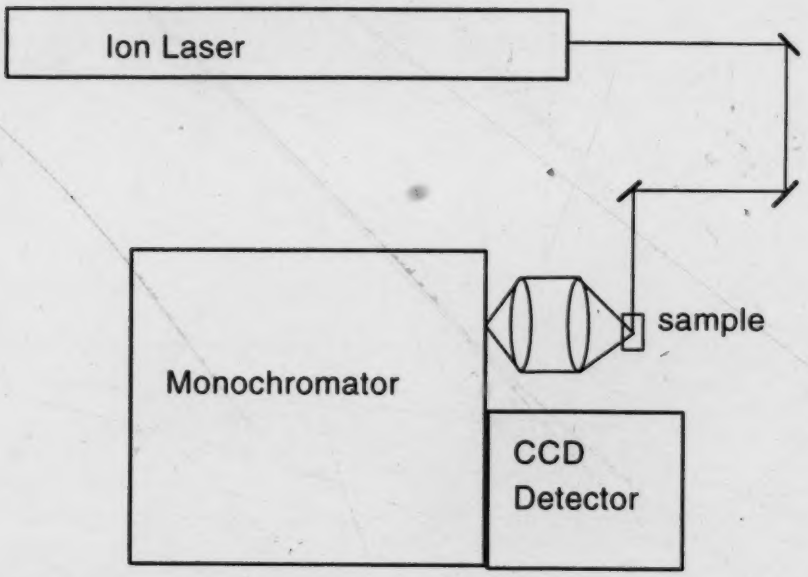

Back-Scattering Geometry

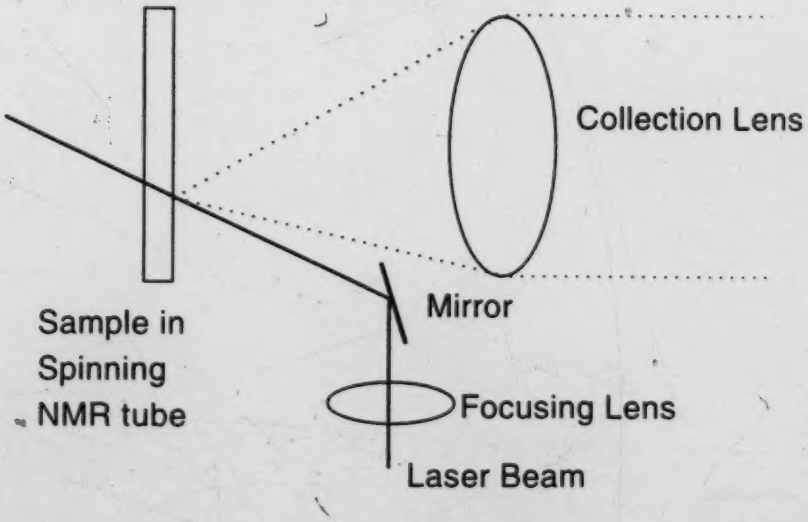

2.3 Results

Figure 2.3 shows the Raman spectrum and vibrational assignments of thymine in water for the 700-1800 cm^{-1} region. The vibrational assignments had been determined earlier from an extensive isotopic labeling study (32). No significant bands due to thymine are observed at frequencies above 1800 cm^{-1}. Very weak bands are observed below 700 cm^{-1}, too weak to determine accurate frequencies. Therefore, only vibrational bands within the 700-1800 cm^{-1} region were considered. Several bands are observed in this region of the spectrum, arising mainly from ring stretches with stretches, bends, wags and rocks of the exocyclic groups (32). Because the vibrations in this region of the spectrum arise from all of the groups of the molecule, particularly the NH and CO groups which are expected to interact strongly with solvent, this "fingerprint" region should allow a determination of the interaction sites with solvent.

To determine the sensitivity of Raman spectroscopy to specific solvent-solute interactions, and to identify the molecular sites of interaction with thymine, the Raman spectra of thymine dissolved in eight solvents with a wide range of properties were obtained. The Raman spectra of the various solvents used are presented in Figure 2.4, while the Raman spectra of thymine solutions are presented in Figure 2.5. Good quality spectra are obtained in all cases. Table 2.3 compiles the thymine peaks in the various solvents spectra in Figure 2.5. In some solvents, Raman scattering from the solvent interfered with the precise determination of the data in some regions of the spectrum. These regions have been blanked out in Figure 2.5. Examination of Figure 2.4 shows that the general pattern of the Raman spectrum is the same in all of the different solvents. To ensure that no reaction was occurring between thymine and solvent, UV-absorption spectra were taken of the thymine solutions before and after irradiation. The absorption spectra of thymine were similar, with only slight absorption maximum shifts, in all of the solvents studied. This is in agreement with ^{1}H-NMR spectra obtained of thymine in the perdeuterated form of each solvent used in the Raman experiments (33). Except for slight changes in coupling constants, expected from the different hydrogen-bonding properties of the solvents, no changes were seen in any ^{1}H-NMR spectrum of fresh

Figure 2.3 - Raman spectra of thymine in water excited at 457.9 nm. The spectra are the sum of three to nine scans and a Raman spectrum of water has been subtracted. The vibrational assignments (32) are shown above the bands. The symbols denote ν-stretch, δ-in-plane bend, γ-out-of-plane bend (wag), and r-rock. The superscripts "a" and "s" stand for asymmetric and symmetric, respectively.

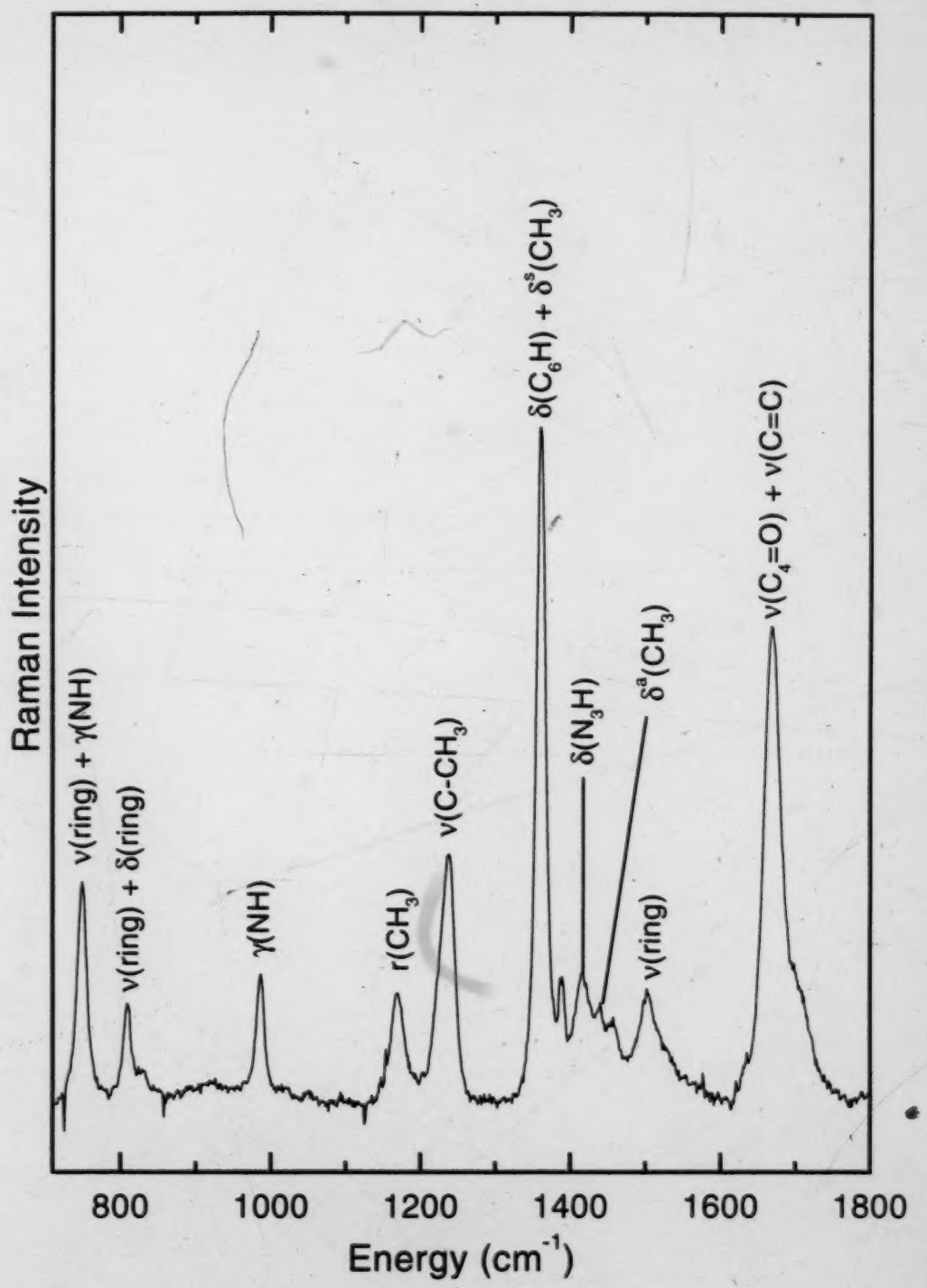
Raman Intensity
ν(ring) + γ(NH)
ν(ring) + δ(ring)
γ(NH)
r(CH3)
ν(C-CH3)
δ(C6H) + δs(CH3)
δ(N3H)
δa(CH3)
ν(ring)
ν(C4=O) + ν(C=C)
800
1000
1200
1400
1600
1800
Energy (cm-1)

Figure 2.4 - Raman spectra of various solvents used, glacial acetic acid (A), benzyl alcohol (B), N,N-dimethylformamide (C), ethanol (D), ethylene glycol (E), formamide (F), formic acid (G), pyridine (H), trifluoroacetic acid (I), and water (J). Trifluoroacetic acid has a broad peak around 1810 cm^{-1} that is only partially shown.

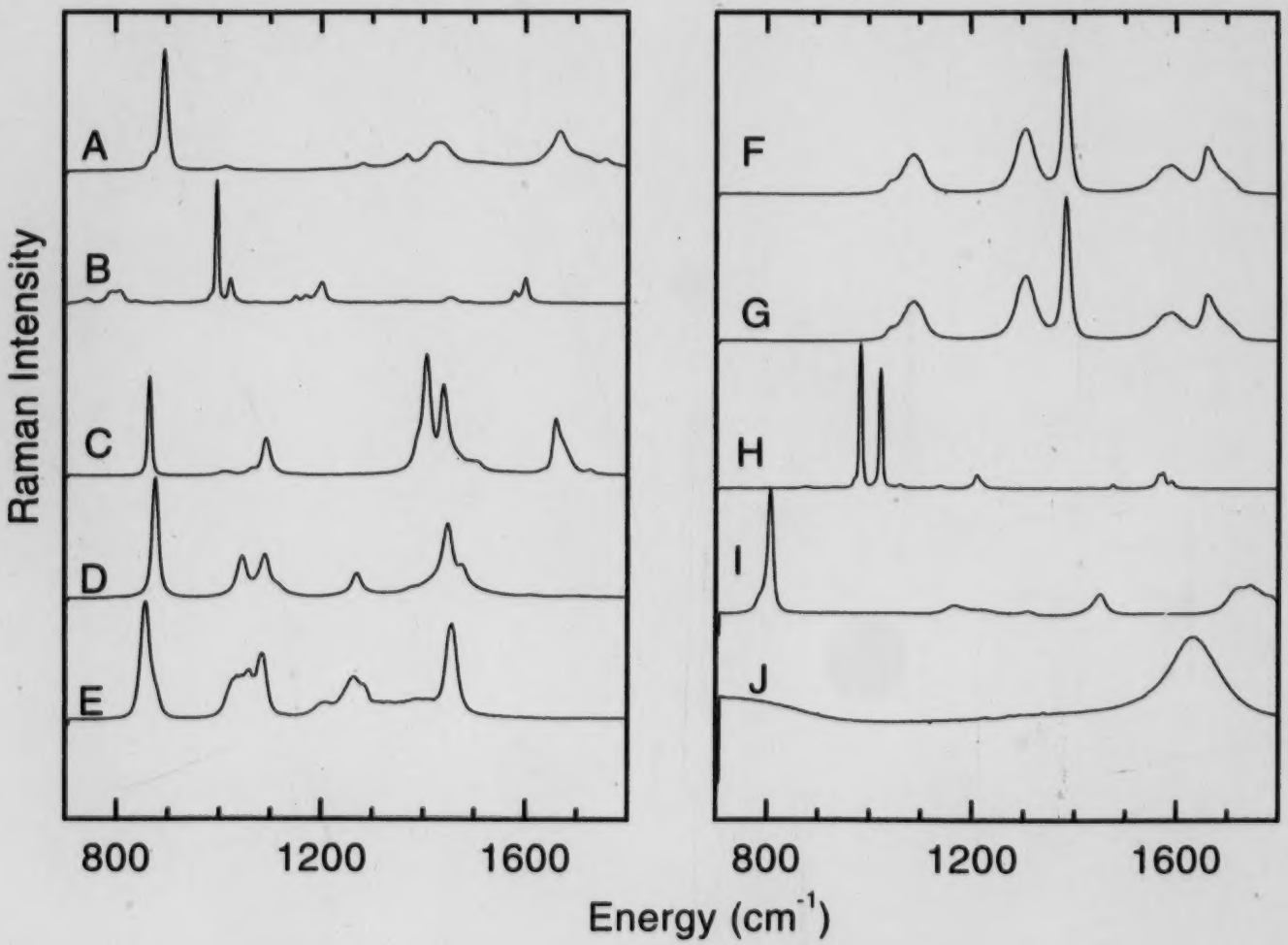
Raman Intensity
A
B
C
D
E
F
G
H
I
J
800
1200
1600
800
1200
1600
Energy (cm-1)

Figure 2.5 - Raman spectra of thymine in glacial acetic acid (A), N,N-dimethylformamide (B), ethylene glycol (C), formamide (D), formic acid (E), pyridine (F), trifluoroacetic acid (G), and water (H). Solvent spectra shown in Figure 2.4 have been subtracted from each spectrum. The portions of each spectrum where no data are reported results from strong solvent interference in those regions.

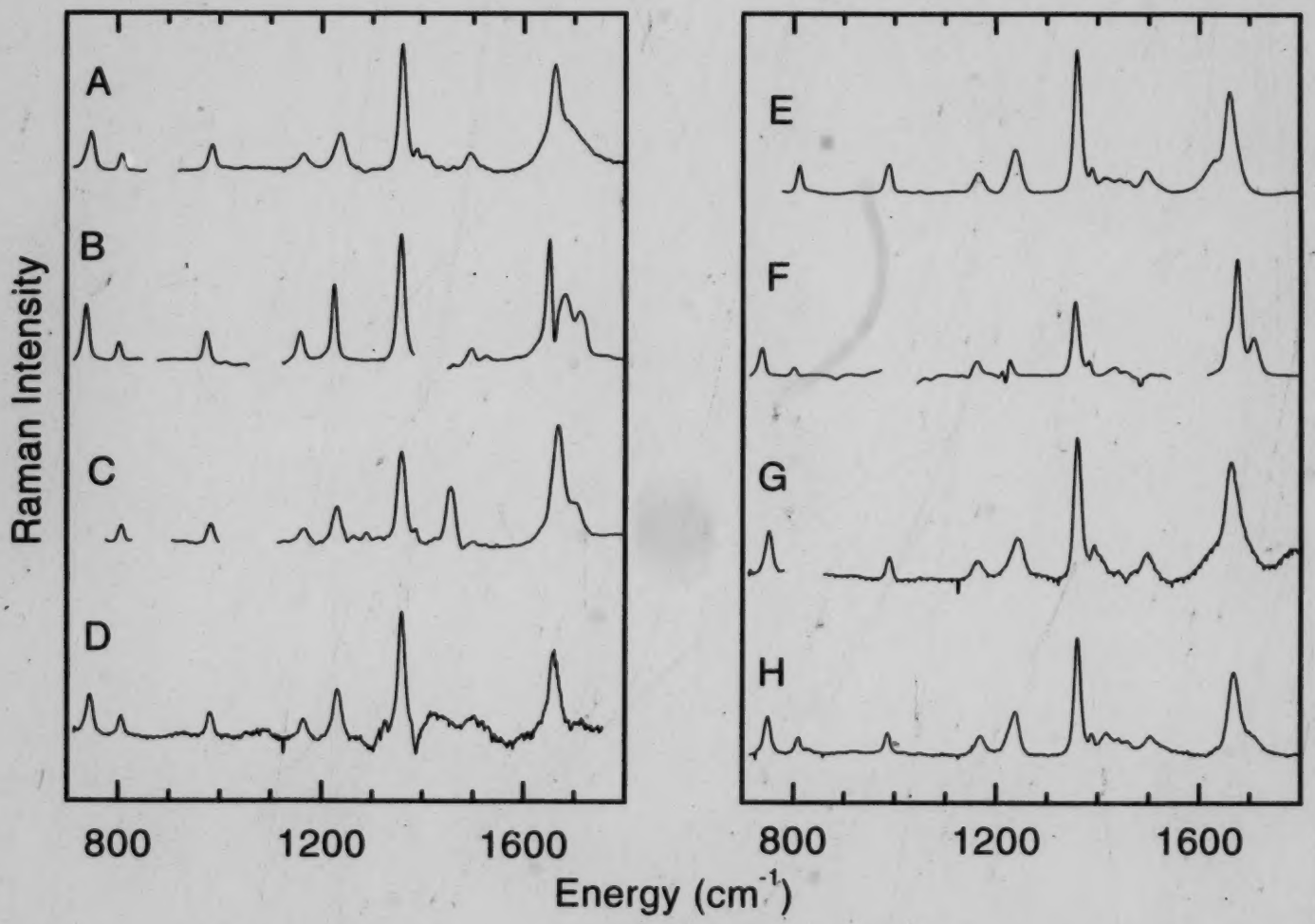
A
B
C
D
E
F
G
H
Raman Intensity
800
1200
1600
800
1200
1600
Energy (cm-1)

TABLE 2.3: Thymine Peaks in Various Solvents from Spectra in Figure 2.5

Solvent	Vibrational Band Frequency (cm^{-1})									
	740	800	980	1160	1230	1360	1390	1500	1665	1707
acetic acid	749	808	985	1163	1236	1359	1387	1493	1662	
N,N-DMF	738	802	974	1158	1224	1357		1496	1681	1711
ethylene glycol	746	806	982	1166	1230	1358	1386		1670	1707
formamide	744	806	981	1164	1231	1358			1659	
formic acid	751	810	986	1164	1238	1359		1496	1661	
pyridine	737	800		1163	1227	1356	1385		1675	1707
trifluoroacetic acid	752	806	989	1164	1242	1360	1393	1497	1663	
water	750	810	986	1169	1238	1361	1388	1502	1668	

solutions or after sitting for 3-5 days. All of these observations suggest that there is no reaction between thymine and any of the solvents used.

Although no major changes in the absorption or Raman spectra are observed, there are obvious frequency shifts and relative intensity changes in the Raman spectra as a function of the solvent environment. The frequencies of the bands at ca. 740, 980, 1230, 1360, 1390, and 1500 cm^{-1} all vary with solvent (Figure 2.5, Table 2.3). In addition to these frequency shifts, striking changes in relative intensity also appear as a function of solvent. The most dramatic of these intensity changes occur in the 1600-1800 cm^{-1} region. In some solvents, such as acetic acid, water, trifluoroacetic acid and formamide, a single peak is observed at ca. 1680 cm^{-1}. However, in other solvents one or more additional peaks are seen in this region. For example, the band at 1680 cm^{-1} exhibits a high-frequency shoulder in ethylene glycol and pyridine, exhibits a low-frequency shoulder in formic acid and pyridine, and exhibits 2 or more peaks at higher frequency in N,N-DMF. The presence of a solvent peak at 1660 cm^{-1} in N,N-DMF (Figure 2.4C) raises doubt to the assignment of these two new peaks to thymine in this region. However, in the subtraction, the three most intense solvent peaks at 865, 1406 and 1439 cm^{-1} were well subtracted, in which case any contribution from the less intense 1660 cm^{-1} peak was completely removed. Hence, we assign the three peaks to actual thymine peaks, not due to solvent subtraction artifacts. In addition to these dramatic changes, smaller changes in relative intensity also occur between the 1680 and 1360 cm^{-1} peaks in many of the solvents, in the 1230 cm^{-1} in N,N-DMF, and in the 1460 cm^{-1} peak in ethylene glycol.

The most logical interaction between solvent and thymine would be a hydrogen-bonding interaction, because of the extensive number of sites on thymine where hydrogen bonding can occur. Therefore, we also obtained the Raman spectrum of thymine at low and high pH's. These spectra in the 800-1800 cm^{-1} region are shown in Figure 2.6. The Raman spectra of thymine at neutral and acidic pH (pH~3) are essentially identical. However, significant differences between the Raman spectra at neutral and basic pH are observed. In the pH range 2-11, thymine is neutral in the acidic region and negatively charged in the alkaline region (34). Therefore at the pH used in this study (pH~11), the

Figure 2.6 - Raman spectra of thymine in acid (A), neutral (B), and basic (C) aqueous solution. A solvent spectrum has been subtracted from each spectrum. The new bands in the base spectrum are marked with asterisks (*).

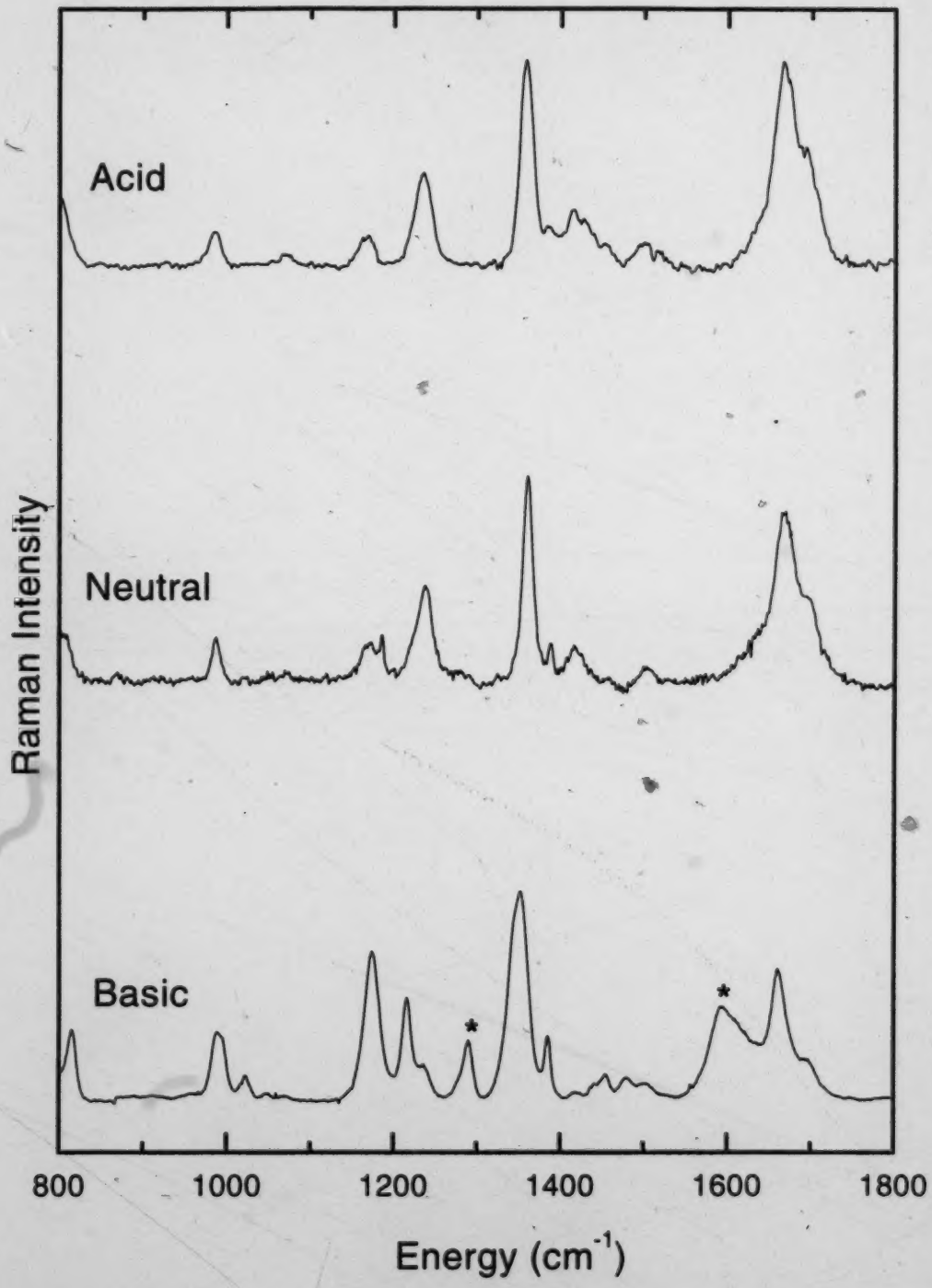
Acid
Neutral
Basic
Raman Intensity
800
1000
1200
1400
1600
1800
Energy (cm-1)

thymine probably exists mostly as the monovalent anion, since the N_3 pK_a of thymine is 10.0 (34). The Raman spectrum at pH~11 therefore represents a weighted mixture of the spectra for the monovalent anion and neutral. The largest differences between the neutral and basic thymine Raman spectra are the presence of two strong new bands at 1290 and 1593 cm^{-1} in the high pH spectrum (marked with asterisks, *). Thus, the presence of these two bands can be used as a diagnostic for the deprotonation of thymine in the solvents used in this study. Since none of the spectra in Figure 2.5 show bands at either 1290 or 1593 cm^{-1}, no deprotonation of thymine occurs in any of the solvents tested.

2.4 Discussion

To understand the significant changes in the Raman spectrum of thymine observed in Figure 2.5 as a function of solvent, correlations were obtained between the observed Raman frequencies and the solvent properties expected to be important in solvent-solute interactions, such as polarity, polarizability, and hydrogen bonding. A list of the important empirical and derived solvent properties are given in Tables 2.1 and 2.2. As a first step, the solvent-induced frequency shifts were correlated with each solvent property in Tables 2.1 and 2.2. The results are shown in Table 2.4. From the resulting table of correlation coefficients between mode-frequency and solvent property, it became rapidly clear that only a few solvent properties were well-correlated with the observed frequency shift. These two significant properties, as well as three others, which show little or no correlation with frequency shifts are presented in Table 2.5.

Close examination of Table 2.5 provides several important clues as to the nature of the interaction between thymine and solvent. Note that there is no correlation between any of the "non-specific" solvent properties, such as polarity (ε, K) and polarizability (n, L), or mixed terms (ε_p, KL) with the vibrational frequency of any mode, except for the 1500 cm^{-1} mode which correlates slightly (correlation coefficients of ca. 0.75) with ε and ε_p. However, clear correlations exist between the specific solvent property of acceptor/donor numbers and the vibrational frequency for many of the modes. The acceptor numbers are derived from ^{31}P-NMR chemical shifts of triethylphosphine oxide

Table 2.4: Correlation Coefficients between Vibrational Frequencies and Solvent Parameters for Thymine

Solvent Parameter	Vibrational Band Frequency (cm^{-1})								
	740	800	980	1160	1230	1360	1390	1500	1665
n	-0.04	-0.45	0.21	-0.24	0.11	-0.11	0.58	-0.11	0.02
ε	-0.10	-0.02	-0.19	0.03	-0.15	-0.09	-0.13	0.76	-0.43
AN	**0.90**	0.63	**0.89**	0.46	**0.94**	**0.83**	**0.99**	0.13	-0.65
DN	**-0.93**	-0.75	**-0.88**	-0.38	**-0.90**	**-0.84**	**-0.85**	0.11	0.64
π*	-0.32	0.05	-0.39	0.27	-0.44	-0.15	-0.65	0.65	0.13
π*II	0.05	0.14	-0.02	0.70	0.03	0.33	0.15	1.00	0.20
Y	-0.14	0.13	-0.38	0.16	-0.28	-0.01	-0.32	0.61	0.14
Π	-0.08	-0.48	0.18	-0.27	0.07	-0.14	0.56	-0.12	0.04
B	0.17	-0.07	0.37	-0.14	0.30	0.04	0.29	-0.62	-0.16
K	-0.17	0.08	-0.38	0.14	-0.29	-0.04	-0.30	0.62	0.15
Θ	-0.08	0.14	-0.31	0.17	-0.21	0.01	-0.27	0.64	-0.20
ε_p	-0.10	-0.02	-0.19	0.03	-0.15	-0.09	-0.14	0.75	-0.43
M'	-0.02	0.37	-0.31	0.27	-0.19	0.10	-0.51	0.45	0.06
M	-0.10	0.24	-0.37	0.21	-0.26	0.03	-0.45	0.54	0.08
L	-0.10	-0.50	0.16	-0.28	0.04	-0.18	0.52	-0.14	0.04
KL	-0.26	-0.51	-0.12	-0.25	-0.19	-0.26	0.35	0.17	0.15

The table contains correlation coefficients from the correlation of the frequency shifts in Table 2.3 with the various solvent parameters presented in Tables 2.1 and 2.2. Correlation coefficients $\geq \pm 0.80$ are in bold type.

TABLE 2.5: Selected Correlations between Observed Raman Frequencies and Solvent Properties for Thymine

Solvent Parameter	Vibrational Band Frequency (cm^{-1})							
	740	800	980	1230	1360	1390	1500	1670
n	-0.01(8)	-0.45(8)	0.21(7)	0.11(8)	-0.11(8)	0.58(5)	-0.11(5)	0.02(8)
ε	-0.10(8)	0.02(8)	-0.19(7)	-0.15(8)	-0.09(8)	-0.13(5)	0.76(5)	-0.43(8)
AN	**0.90** (6)	0.63(6)	**0.89** (5)	**0.94** (6)	**0.83** (6)	**0.99** (4)	0.13(4)	-0.65(6)
DN	**-0.93** (6)	-0.75(6)	**-0.88** (5)	**-0.90** (6)	**-0.84**(6)	**-0.85**(4)	0.11(4)	0.64(6)
ε_p	-0.10(8)	-0.02(8)	-0.19(7)	-0.15(8)	-0.09(8)	-0.14(5)	0.75(5)	-0.43(8)

The table values are the correlation coefficient (R) with the number of points in parentheses. Correlations with coefficients greater than ±0.8 and a reasonable number of points are in bold type.

(Et_3PO) (27), while the donor numbers are obtained directly from calorimetric measurements with $SbCl_5$, or inferred indirectly from ^{23}Na-NMR chemical shifts of $NaClO_4$ (27). The acceptor number (AN) is defined as a dimensionless number:

$$AN = \delta_{corr} * 100 / \delta_{corr}(Et_3PO.SbCl_5) = \delta_{corr} * 2.348 \qquad (2.1)$$

where $\delta_{corr}(Et_3PO.SbCl_5) = 42.59$ ppm. Note that the scale runs from 0 (hexane) to 100 ($SbCl_5$). The donor number (DN) is defined as the molar enthalpy value for the reaction of the donor (D) with $SbCl_5$ as a reference acceptor in 10^{-3} M solution of dichloroethane:

$$D + SbCl_5 = D.SbCl_5 \quad (-\Delta H_{D.SbCl_5} \equiv DN) \qquad (2.2)$$

These parameters are thought to be a measure of hydrogen-bonding ability of the solvent, either as an acceptor or a donator of electrons. This correlation is observed in the 740, 980, 1230, 1360 and 1390 cm^{-1} modes. This clear correlation with acceptor and donor numbers indicates the interaction between thymine and solvent is a *specific* interaction, nominally involving hydrogen bonding. The quality of the correlation is shown in Figure 2.7. Figure 2.7A shows a representative acceptable correlation, where the correlation coefficient is -0.93, while Figure 2.7B shows a representative unacceptable correlation where the correlation coefficient is -0.75.

The nature of the vibrations affected by the hydrogen-bonding properties of the solvent can be used to determine the sites of interaction between thymine and solvent. The modes at 740, 980 and 1390 cm^{-1} all contain contributions from N-H bending vibrations, either in-plane or out-of-plane (Figure 2.3). The sensitivity of these N-H vibrations to the hydrogen-bonding ability of the solvent is expected and indicates solvent interacts at the N_1 and/or N_3 nitrogens. Since both of these nitrogens are protonated and the nitrogen lone pairs are resonantly delocalized over the molecule (see Figure 2.8 below), this interaction should be donation of a lone-pair of electrons from the solvent to the hydrogens on the nitrogens. The mode at 1230 cm^{-1} is the isolated C_5-$C_\alpha H_3$ stretch and correlates very well with solvent hydrogen-bonding strength. It is difficult to imagine why this should be so. This result may indicate that this C-C stretching internal coordinate is mixed with N-H internal coordinates. Significant hydrogen-bonding

Figure 2.7 - Good (R=-0.93) and poor (R=-0.75) correlations of the Raman frequency with solvent parameter.

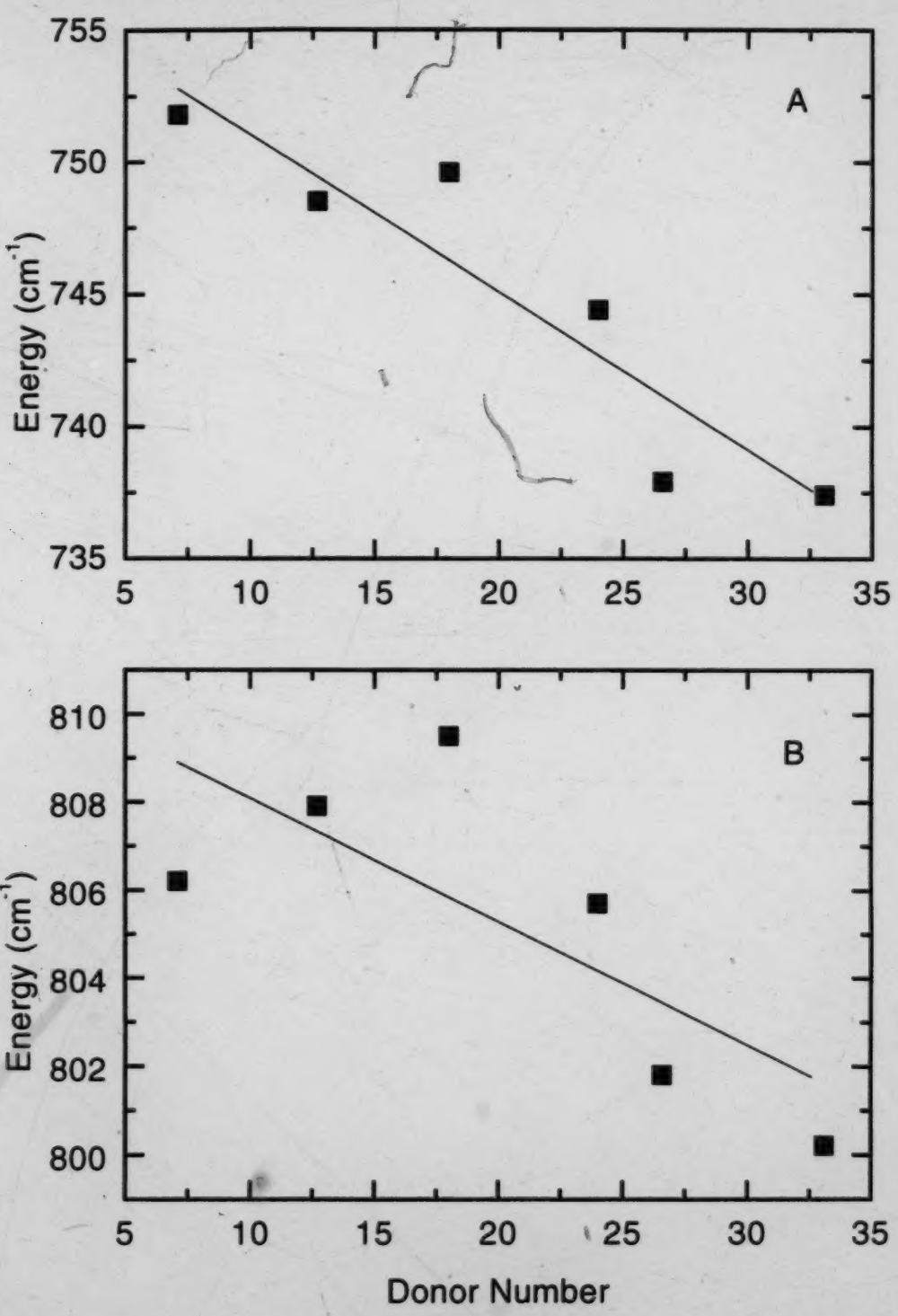
A
B
Energy (cm-1)
Energy (cm-1)
755
750
745
740
735
810
808
806
804
802
800
5
10
15
20
25
30
35
Donor Number

correlation is also observed for the 1360 cm^{-1} mode which has been assigned to $\delta(C_6H)+\delta(C_\alpha H_3)$. This could be due to the influence of the π-electrons from the $C_5=C_6$ bond, although the $C_5=C_6$ stretch itself does not appear to be solvent sensitive.

Similar arguments can be used to understand the relative intensity changes in the 1600-1800 cm^{-1} region. The two CO stretches $\nu(C_2=O)$ and $\nu(C_4=O)$, as well as the $\nu(C_5=C_6)$ bands are all expected in this region. The most intense peak in this region around 1680 cm^{-1} in all the spectra in Figure 2.5 has been assigned to $\nu(C_4=O)$ coupled with $\nu(C_5=C_6)$ (Figure 2.3) from an extensive isotopic labeling experiment (32). Spiro, et al. (18, 35) reported from UV resonance Raman experiments on thymine and its derivatives that, at higher excitation wavelengths (240-266 nm), a single broad band appears around 1665 cm^{-1}. However, with lower wavelength excitation (218, 200 nm), a narrower band is observed at 1648 cm^{-1}, with a shoulder at 1700 cm^{-1}. They interpreted the results to show that the $\nu(C_5=C_6)$ and $\nu(C_4=O)$ were coupled or degenerate in water solutions to give a single peak at 1665 cm^{-1} and the $\nu(C_2=O)$ vibration gave the band at 1700 cm^{-1}. This is an indication that the $\nu(C_4=O)$ is part of the composite band at 1665 cm^{-1}, in agreement with our assignment of the mode around 1680 cm^{-1} in our spectra to accidentally degenerate $\nu(C_4=O)$ and $\nu(C_5=C_6)$ (32). While these assignments may imply that the peaks are due to localized internal coordinates, in reality each peak should be regarded as normal modes with different contributions from each internal coordinate, with say the $\nu(C_5=C_6)$ contribution being dominant for the 1680 cm^{-1} peak. Also, the lack of correlation between the mode at 1680 cm^{-1} and any property of the solvent supports a previous assignment of this mode in the Raman spectrum primarily to the C=C vibration, which should be relatively insensitive to solvent polarity, polarizability, and/or hydrogen bonding. This suggests that the C=O contribution to this band's intensity is minimal, as it is expected to be solvent sensitive. This assignment is additionally confirmed by spectral intensity changes in this region.

There are three possible explanations for the spectral intensity changes observed in the 1600-1800 cm^{-1} region: symmetry breaking of the vibrational bands due to strong solvent-solute interactions, interaction at the C=O sites only, and/or interaction with both

the N-H and C=O sites. Myers and Johnson (36, 37) observed in resonance Raman experiments for the photodissociation of I_3 that, in addition to the allowed symmetric stretch band seen in all the solvents, the symmetry forbidden asymmetric stretch was also observed in ethanol, the most polar solvent used. This was attributed to solvent-induced symmetry breaking of the "chromophore" effectively lowering its symmetry and giving some allowed character to the nominally forbidden bands. However, in our results, a doublet appears in the less or non-polar solvents such as N,N-DMF and pyridine, while a single peak is seen in the more polar/hydrogen bonding solvents water, formamide and trifluoroacetic acid. Therefore, the intensity changes observed in our spectra cannot be due to solvent-induced symmetry-breaking, as they are inconsistent with increased symmetry breaking as the solvent polarity increases.

The second possible cause for these intensity changes is interaction of solvent with the C=O sites alone of thymine. UV resonance Raman (UVRR) experiments of nucleobase derivatives in several solvents (38), have shown that for uracil, the $\nu(C_5=C_6)$ appears at 1620-1630 cm^{-1} in all the solvents with little or no frequency shift with solvent. The $\nu(C_4=O)$ band at 1673 cm^{-1} in water was seen to shift to higher frequency, however, as the polarity of the solvents decreased, an indication of a stronger C=O bond and weaker hydrogen bonding of the solvent at the C=O sites. For thymine, only one band is observed at 1600-1800 cm^{-1} in the polar solvents water and methanol around 1665 cm^{-1} in the UVRR spectrum, assigned to overlap of the $\nu(C_4=O)$ and $\nu(C_5=C_6)$. Because the $\nu(C_5=C_6)$ is shifted to higher frequency in thymine compared to uracil (18), due to the electron donating effect of the C_5-$C_\alpha H_3$ group, it overlaps with the $\nu(C_4=O)$ in the polar solvents giving rise to a single peak. The $\nu(C_2=O)$ has a weak Raman signal which only has intensity at excitation wavelengths of 218 nm and below. However in non-H-bonded solvents such as 1,4-dioxane and chloroform, doublets are seen with the $\nu(C_5=C_6)$ well separated from the $\nu(C_4=O)$. Because of weaker or no hydrogen bonding at the C=O sites in these low polarity or non-polar solvents, the $\nu(C_4=O)$ vibration shows up well separated and at higher frequency than the unshifted $\nu(C_5=C_6)$. Although these results were obtained in UVRR experiments, we observe similar spectral features in the

1600-1800 cm^{-1} region in our Raman data. Therefore, the single peak observed in the polar solvents water, trifluoroacetic acid, formamide and formic acid in the 1600-1800 cm^{-1} region (Figure 2.5), is due to interaction of solvent with the C=O sites lowering the $\nu(C_4=O)$ and making it overlap with the $\nu(C_5=C_6)$. The doublets in pyridine, and N,N-DMF which have low H-bonding capability as shown by their lower acceptor numbers (Table 2.1), result from separation of the $\nu(C_5=C_6)$ from the $\nu(C_4=O)$ which appears at a higher frequency due to less/no interaction in these solvents. However, interaction solely at the $C_4=O$ bond does not explain the frequency shifts and sensitivity of the N-H modes with solvent. From the comparison of the spectra in Figure 2.5 to the base spectrum of thymine in Figure 2.6C, we conclude that the thymine is not deprotonated in any of the solvents. Depending on the polarity of the solvent and the extent of interaction mainly at the N_3-H site, the electronic structure of thymine may resemble a zwitterionic or neutral thymine in solution (Figure 2.8). Increased interaction at the C=O sites would be expected to stabilize structure II in Figure 2.8. Since the N-H bends are not directly affected, it is unclear how this interaction could explain the sensitivity of the N-H deformations and wags to solvent. The dramatic intensity changes cannot therefore be completely explained by H-bonding with solvent at the C=O sites only.

The only other possible explanation for the intensity changes observed is a strong interaction of solvent with the C=O and N-H sites of thymine. This explanation can best be understood by considering the resonance structures of thymine. In the polar solvents, the zwitterionic structure II is expected to dominate, lowering the $\nu(C_4=O)$ band and making it overlap with the $\nu(C_5=C_6)$. This gives rise to a single peak in these solvents. However, in the less or non-polar solvents, because of little or no electron-pair donation to the N_3-H site, the neutral thymine structure I dominates giving rise to a higher frequency $\nu(C_4=O)$ band which is well separated from the $\nu(C_5=C_6)$, and a doublet is observed in these solvents. Again this interaction only accounts for the intensity changes in the 1600-1800 cm^{-1} region, but does not explain the changes in the N-H modes with solvent observed in our results. As suggested by Zhang, et al. (32), the peaks in the 1600-1800 cm^{-1} region may not be due to localized internal coordinates or overlapping bands,

Figure 2.8 - Resonance structures of thymine. In this Figure, I is the neutral form and II is the zwitterionic form.

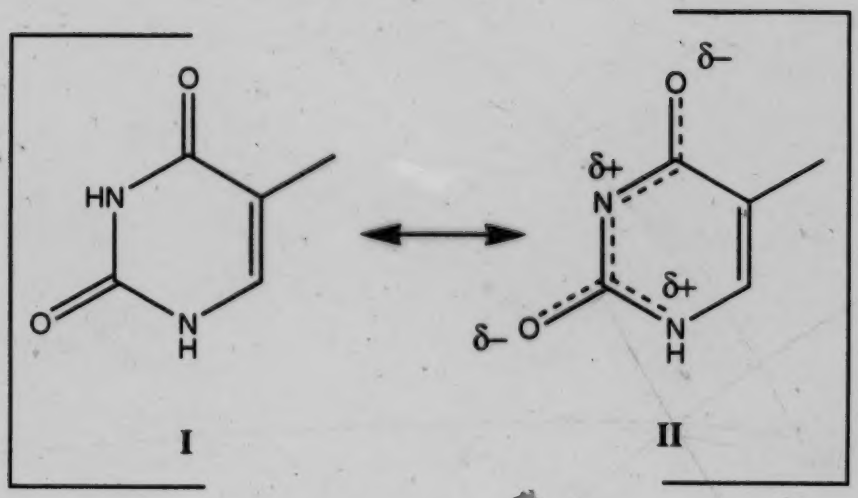
O
HN
O
NH
I
δ−
O
δ+
N
δ+
δ−
O
NH
II

but may be due to mixed/coupled vibrational modes. It is therefore also possible that the spectral changes observed are due to solvent "turning on" intensity in weak/forbidden modes, such as the $\nu(C_2{=}O)$. However, since this band has a weak Raman signal and is only strongly enhanced at lower wavelength excitation (218, 200 nm), the contribution due to this effect is minimal.

We therefore conclude that the intensity changes observed are not due to solvent-induced symmetry breaking, but rather as a result of the interaction of solvent with thymine at both the C=O and N-H sites. This leads to a weakening of the $\nu(C_4{=}O)$ frequency in the polar solvents resulting in an overlap with the $\nu(C_5{=}C_6)$ and giving rise to a single peak. However, the interaction of solvent with thymine at these sites also results in the frequency shifts and good correlation of the N-H modes with solvent as shown by the sensitivity of the N-H modes to acceptor and donor numbers (Table 2.5).

2.5 Conclusion

In this Chapter, Raman spectra of thymine in eight solvents, acid and base were obtained with visible excitation. Correlation of the observed frequency shifts of specific vibrational modes with characteristic properties of the solvent shows that a significant hydrogen-bonding interaction occurs between the N-H protons on thymine and lone pairs of electrons on the solvent molecules and between the solvent hydrogens and lone pairs on C=O sites. The solvent-dependent intensity in bands between 1500 and 1800 cm^{-1}, indicates a strong interaction between thymine and solvent at the C=O and N-H sites that leads to separation of the C=O stretches from the C=C stretch. These results suggest that Raman spectroscopy is uniquely sensitive to specific interactions of thymine with its environment and that it may be a useful technique in probing DNA binding of intercalants, proteins, and other substances.

2.6 References

1. Fisher, G. J.; Johns, H. E. In *Photochemistry and Photobiology of Nucleic Acids*; Wang, S. Y., Ed.; Academic Press: New York, 1976, Vol. 1, p.169.
2. Fisher, G. J.; Johns, H. E. In *Photochemistry and Photobiology of Nucleic Acids*; Wang, S. Y., Ed.; Academic Press: New York, 1976; Vol. 1, p. 225.
3. Patrick, M. H.; Rahn, R. O. In *Photochemistry and Photobiology of Nucleic Acids*; Wang, S. Y., Ed.; Academic Press: New York, 1976; Vol. 2, p. 35.
4. Park, H.-W.; Kim, S.-T.; Sancar, A.; Deisenhofer, *J. Science* **1995**, *268*, 1866.
5. Rupert, C. S.; Goodgal, S. H.; Herriott, R. M. *J. Gen. Physiol.* **1958**, *41*, 451.
6. Kim, S.-T.; Sancar, A. *Photochem. Photobiol.* **1993**, *57*, 895.
7. Sancar, A. *Biochemistry* **1994**, *33*, 2.
8. Morikawa, K. et al. *Science* **1992**, *256*, 523.
9. Ishida, M.; Kanamori, Y.; Hori, N.; Inaoka, T.; Ohtsuka, E. *Biochemistry* **1990**, *29*, 3817.
10. Lee, B, J.; Sakashita, H.; Ohkubo, T.; Ikehara, M.; Doi, T. et al. *Biochemistry* **1994**, *33*, 57.
11. Sealey, P. G.; Southern, E. M. In *Gel Electrophoresis of Nucleic Acids: A Practical Approach*; Rickwood, D.; Hames, B. D.; Ed.; IRL Press Ltd.: Oxford, 1982, p. 39.
12. Fangman, W. L. *Nucleic Acid Res.* **1978**, *5*, 653.
13. Jovin, T. M. In *Methods in Enzymology*; Grossman, L.; Moldave, K., Eds.; Academic Press Inc.: London, 1971; Vol. 21, p. 179.
14. Nakamoto, K.; Ferraro, J. R. *Introductory Raman Spectroscopy*; Academic Press Inc.: San Diego, 1994, p. 1.
15. McHale, J. L. *Molecular Spectroscopy*; Prentice Hall: New Jersey, 1999, p.364.
16. Tsuboi, M.; Takahushi, S.; Harada, I. In *Physico-chemical Properties of Nucleic Acids*; Duchesne, J., Ed.; Academic Press: New York, 1973; Vol. 2, p. 91.
17. Hartman, K. A.; Lord, R. C.; Thomas, G. J., Jr. In *Physico-chemical Properties of Nucleic Acids*; Duchesne, J., Ed.; Academic Press: New York,1973; Vol. 2, p. 1.
18. Fodor, S. P. A.; Rava, R. P.; Hays, T. R.; Spiro, T. G. *J. Am. Chem. Soc.* **1985**, *107*,

1520.

19. Tsuboi, M.; Nishimura, Y.; Hirakawa, A. Y. In *Biological Applications of Raman Spectroscopy*; Spiro, T. G., Ed.; Wiley-Interscience: New York, 1987; Vol. 2, p.109.
20. Peticolas, W. L.; Thomas, G. A.; Tsuboi, M. *In Biological Applications of Raman Spectroscopy*; Spiro, T. G., Ed.; Wiley-Interscience: New York, 1987; Vol. 1, p. 81.
21. See: Carey, P. R. "*Biochemical Applications of Raman and Resonance Raman Spectroscopies*"; Academic Press: New York, 1982.
22. Fodor, S. P. A.; Spiro, T. G. J. *Am. Chem. Soc.* **1986**, *108*, 3198.
23. Mitambo, M. M.; Loppnow, G. R. *Chem. Phys. Lett.* **1996**, *261*, 691.
24. Webb, M. A.; Fraga, E.; Loppnow, G. R. *J. Phys. Chem.* **1996**, *100*, 3278.
25. CRC *Handbook of Chemistry and Physics*, 54th ed.; Weast, R. C., Ed.; CRC Press: Cleveland, OH, 1974.
26. Riddle, F. L. Jr.; Fowkes, F. M. *J. Am. Chem. Soc.* **1990**, *112*, 3259.
27. Gutmann, V. *The Donor-Acceptor Approach to Molecular Interactions*; Plenum: New York, 1978, p.17
28. Kamlet, M. J.; Abboud, J-L. M.; Taft, R. W. *J. Am. Chem. Soc.* **1977**, *99*, 6027.
29. Fawcett, W. R.; Kloss, A. A. *J. Phys. Chem.* **1996**, *100*, 2019.
30. Kamlet, M. J.; Abboud, J-L. M.; Abraham, M. H.; Taft, R. W. *J. Org. Chem.* **1983**, *48*, 2877.
31. Kolling, O. W. *J. Phys. Chem.*, **1996**, *100*, 16087.
32. Zhang, S. L.; Michaelian, K. H.; Loppnow, G. R. *J. Phys. Chem.* **1998**, *102*, 461.
33. Arboleda, P.; Loppnow, G. R. Unpublished work.
34. Ts'o, P. O. P. In *Basic Principles in Nucleic Acid Chemistry*; Ts'o, P. O. P., Ed.; Academic Press: New York, 1974; Vol. 1, p. 453.
35. Grygon, C. A.; Spiro, T. G. *Biopolymers*, **1990**, *29*, 707.
36. Johnson, A. E.; Myers, A. B. *J. Phys. Chem.* **1996**, *100*, 7778.
37. Johnson, A. E.; Myers, A. B. *J. Chem. Phys.* **1995**, *102*, 3519.
38. Toyama, A.; Takeuchi, H.; Harada, I. *J. Mol. Struct.* **1991**, *242*, 87.

Chapter 3 - Solvent-Dependence of Thymidine Raman Spectrum

3.1 Introduction

Thymidine (1-[2'-deoxy-β-ribofuranosyl]-5-methyluracil; see Figure 2.1), one of the four nucleoside constituents of DNA, is of fundamental importance in molecular biology (1). It consists of a sugar (2'-deoxyribose) attached to the pyrimidine base thymine, one of the four nucleobases found in DNA. The pyrimidine nucleosides are more photochemically active than their purine counterparts, with thymidine and its derivatives being the most photochemically active (2). Exposure of the human skin to solar ultraviolet radiation leads to DNA damage, such as formation of photoproducts, strand breaks, lesions and cross-links (2-9). Much of this damage can be repaired by indigenous repair enzymes such as DNA photolyase (10-12) and T4 endonuclease (10, 13, 14), although incomplete repair of this damage can eventually lead to skin cancer (15, 16).

Many aspects of the photophysical, photochemical and photobiological properties of DNA and related compounds have been intensively studied (3, 13-16), resulting in a large body of information of the various structural features of the photoproducts (17). The most important/stable photoproducts include pyrimidine (mainly thymidine) dimers, 6-4 adducts and photohydrates, as well as strand breaks due to reaction of singlet molecular oxygen with DNA (3-5, 7-9, 18). The rate of repair of the 6-4 adducts and photohydrates is thought to be 10-20 times faster than for the thymidine dimers (19). This results in the accumulation of thymidine dimers which may be responsible for inducing skin cancer (15, 16, 19). Most methods for detecting and quantifying DNA photodamage and repair, such as chromatography, gel electrophoresis and immunological approaches, (16, 20-22) are invasive and destructive. The aim of this work is to probe DNA structure and dynamics using Raman spectroscopy, a non-invasive method.

Vibrational spectroscopy has been applied to numerous problems in nucleic acid structure. It therefore serves as a convenient and effective probe of thymine and thymidine structure, dynamics, and interaction with solvent. Much effort has been devoted to the application of infrared spectroscopy, an absorption process, on nucleic acids and constituents. These studies have led to vibrational assignments of various IR-

allowed modes observed in uracil and thymine (23-26). Raman spectroscopy is a scattering process in which light is inelastically scattered off a molecule yielding vibrational information (27-29). As discussed in Chapter 1, Raman spectroscopy has several advantages over IR, and complements the IR technique. Conventional Raman spectroscopy has also proven to be a useful tool for probing nucleic acid structure (26, 30-34), and many of the observed Raman modes in thymine have been assigned. Raman spectroscopic studies of thymidine-containing molecules have also been performed leading to the preliminary assignment of thymidine vibrational Raman bands (1, 35-37). Advantage has also been taken of the more selective and sensitive method of resonance/UV–resonance Raman spectroscopy to probe nucleic acids and constituents, DNA and related molecules (38-40). However, these studies have focused on the structure of nucleic acids, and few studies have explored the applicability of using Raman spectroscopy to probe nucleic acids interactions with different chemical environments and other molecules.

Since thymidine has both proton-accepting and proton-donating sites, spectral changes are expected due to its interaction with proton-acceptor and acceptor/donor solvents (41). Mitambo and Loppnow (42) observed significant changes in the Raman spectra of ethyl 4-(dimethylamino)benzoate (DMABEE) in different solvents. Similar results were also reported with thymine, described in Chapter 2. In this work, we report the effects of solvents on the Raman vibrational modes of thymidine in nine solvents of varying properties. Our results provide an important foundation for analyzing the spectra of nucleic acids in different chemical environments, which will eventually lead to developing Raman spectroscopy as a better probe of the DNA damage and repair mechanism. Also, a better understanding of the interaction of nucleic acids with various proteins and intercalants, the long-range goal of this work, will be achieved.

3.2 Experimental

Thymidine (99%) was obtained from Sigma Chemical Company (St. Louis, MO) and used as received. Acetic acid, benzyl alcohol, N,N-dimethylformamide, ethanol, ethylene glycol, formamide, formic acid, pyridine, and water (deionized, 18 MΩ) were of analytical grade and used as received. The important solvent parameters are listed in Tables 2.1 and 2.2.

Room-temperature Raman spectra of freshly prepared saturated solutions of thymidine in the solvents listed above were obtained on 300 μL samples. Typical concentrations were in the range of 0.40 M in ethanol to 4.00 M in formic acid. Raman scattering was excited by spherically focusing the laser onto a spinning 5-mm diameter (o.d.) NMR tube containing the sample in a 135^0 backscattering geometry (42-44, see Figure 2.2). Laser excitation was obtained with an Argon ion (Ar^+) laser (Coherent, Santa Clara, CA), at 457.9 nm. The laser power at the sample was 250 mW. Multichannel detection of the Raman scattering was obtained with a liquid nitrogen–cooled, charged-coupled device (CCD) detector (Princeton Instruments, Trenton, NJ) coupled to the first half of a double monochromator (Spex Industries, Metuchen, NJ), (42-44). Spectral resolution was 5 cm^{-1} and the spectral acquisition time was 1 hour. UV-visible absorption spectra of the samples were measured using a diode array spectrophotometer (Hewlett-Packard, Sunnyvale, CA) before and after irradiation.

Raman spectra were analyzed using a 486 DX2-66V computer (Gateway Computers, North Sioux City, SD). A solvent spectrum was subtracted from each solution Raman spectrum, and the resulting spectrum was frequency calibrated by measuring the Raman scattering of solvents with known frequencies (acetone, benzene, carbon tetrachloride and chloroform). The baselines were leveled by subtraction of multiple joined line segments. Reported frequencies are accurate to ±1.5 cm^{-1}. Raman spectra were also obtained of freshly prepared saturated solutions of thymidine in acid (2.0 M, H_2O at pH~3) and base (4.0 M, H_2O at pH~11).

3.3 Results

The Raman spectrum and vibrational assignments of thymidine in water in the 700-1800 cm^{-1} region are presented in Figure 3.1. The 700-800 cm^{-1} region is dominated by bands assigned to ring breathing modes of the thymine base (35). In the 800-1200 cm^{-1} region are normal modes localized on the 2'-deoxyribose sugar ring, while in the 1200-1600 cm^{-1} region we expect modes resulting from the coupling of the vibrational coordinates of the thymine base and the sugar ring. The C=C and C=O double bond stretches appear in the 1600-1800 cm^{-1} region. The assignment of the 740, 787, 1180, 1235, 1372, and 1660 cm^{-1} modes to the thymine base are from an extensive isotopic labeling study of Zhang, et al. (34). Modes assigned to the 2'-deoxyribose sugar ring only and vibrations due to coupling of the base and sugar ring are based on Raman studies of thymidine (1, 35-37). The results in these studies agree closely with the modes assigned to the base by Zhang, et al. The mode at 787 cm^{-1} contains significant contributions from the sugar ring. The $C_2'H_2$ rocking, twisting, wagging and scissoring modes are expected around 900, 1070, 1170 and 1400 respectively cm^{-1} (1). The 868 cm^{-1} mode assigned to the deoxyribose ring contains strong contribution from the $C_2'H_2$ rocking vibration. The 1100 and 1180 cm^{-1} modes are most probably due to the $C_2'H_2$ twisting and wagging modes respectively, while the mode around 1415 cm^{-1} could be due to the $C_2'H_2$ scissoring (1).

Since thymidine has multiple proton-accepting and proton-donating sites on both the base and sugar, its vibrations are expected to be sensitive to solvent interaction. To determine the sensitivity of Raman spectroscopy to specific solvent-solute interaction, Raman spectra were obtained of saturated solutions of thymidine in nine different solvents whose solvent parameters are given in Tables 2.1 and 2.2. The Raman spectra of the solvents used in this study are presented in Figure 2.4, while Figure 3.2 shows the Raman spectra of the thymidine solutions. Good quality Raman spectra were obtained in each case. Table 3.1 compiles the thymidine Raman peak shifts from the spectra in Figure 3.2. The gaps in some of the spectra are regions where the solvent Raman scattering was found to interfere with accurate determination of the thymidine data.

Figure 3.1 - Raman spectra of thymidine in water excited at 457.9 nm. The spectra are the sum of three to nine scans and a Raman spectrum of water has been subtracted. Vibrational assignments, after refs. 1, 34-37, are shown above the bands. The symbols denote ν-stretch, δ-in-plane bend, γ-out-of-plane bend (wag), and r-rock. The superscripts "a" and "s" stand for asymmetric and symmetric, respectively.

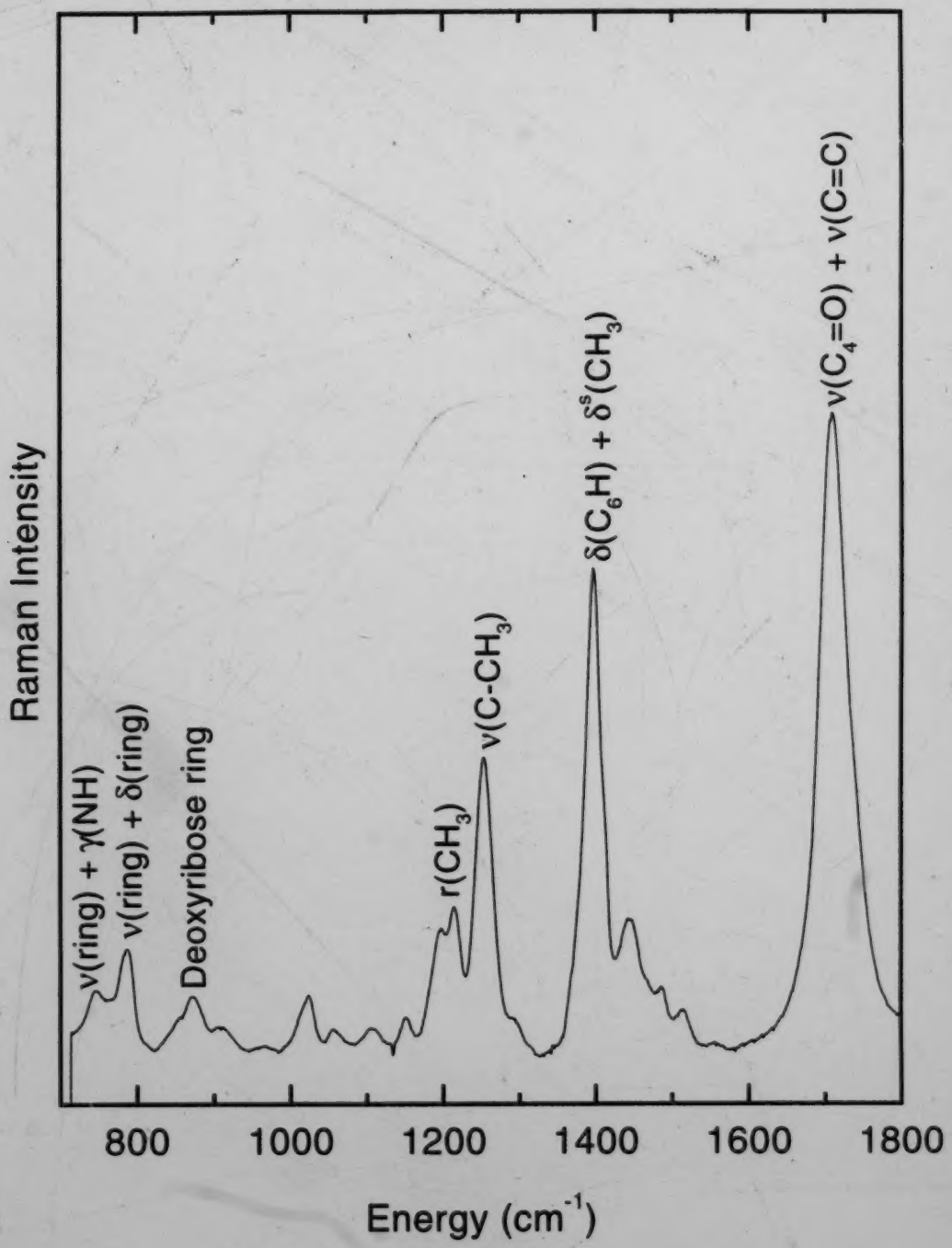
Raman Intensity
ν(ring) + γ(NH)
ν(ring) + δ(ring)
Deoxyribose ring
r(CH3)
ν(C-CH3)
δ(C6H) + δs(CH3)
ν(C4=O) + ν(C=C)
800
1000
1200
1400
1600
1800
Energy (cm-1)

Figure 3.2 - Raman spectra of thymidine in glacial acetic acid (A), benzyl alcohol (B), N,N-dimethylformamide (C), ethanol (D), ethylene glycol (E), formamide (F), formic acid (G), pyridine (H), and water (I). Solvent spectra, shown in Figure 2.4, have been subtracted from each spectrum. The portions of each spectra where no data are reported results from strong solvent interference in those regions.

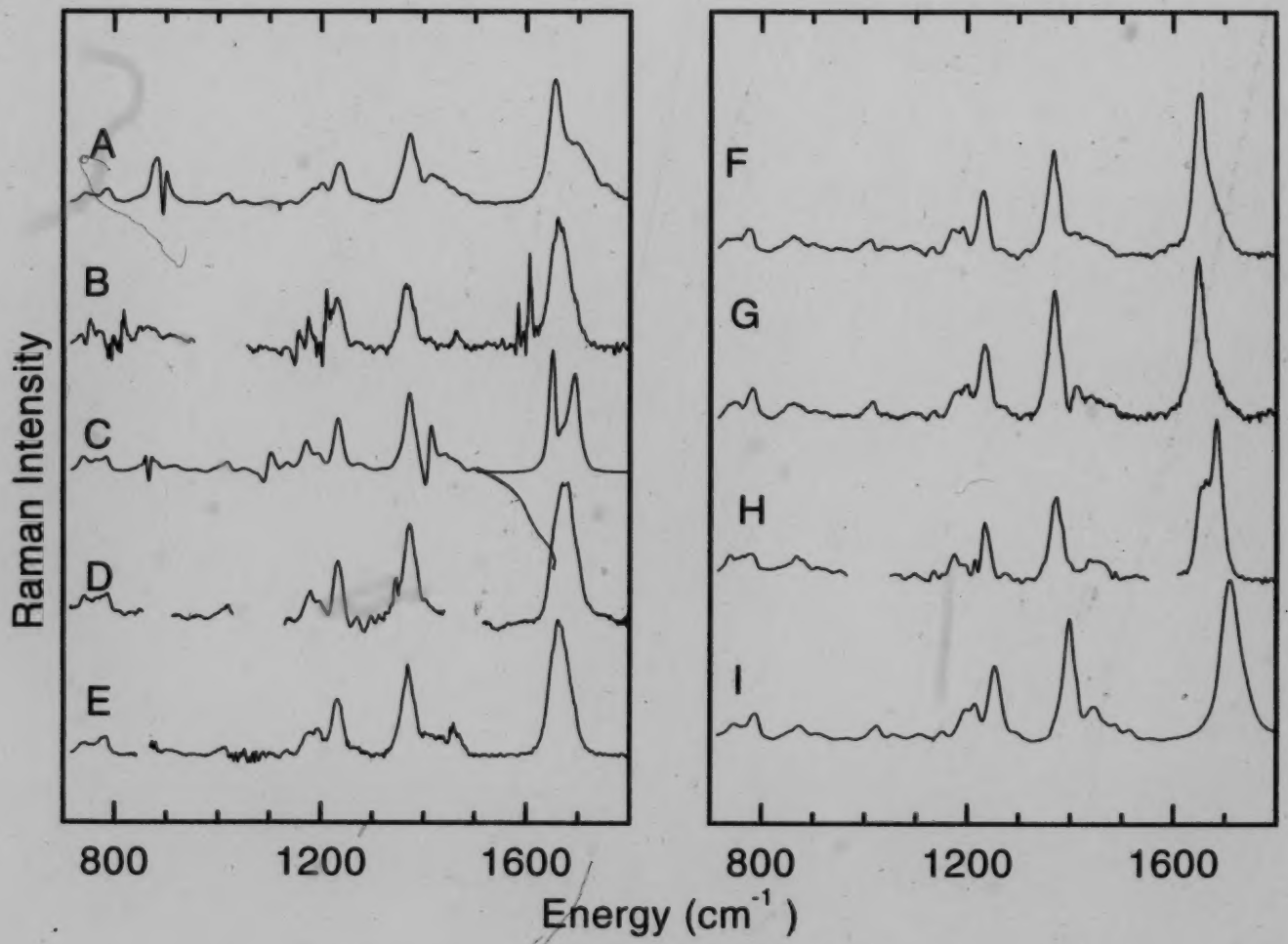
A
B
C
D
E
F
G
H
I
Raman Intensity
800
1200
1600
800
1200
1600
Energy (cm-1)

Table 3.1: Thymidine Peaks in Various Solvents from the Spectra in Figure 3.2

Solvent	Vibrational Band Frequency (cm^{-1})													
	740	787	868	1019	1100	1140	1180	1200	1235	1372	1415	1450	1660	1690
acetic acid	745	785	882	1018	1101	1140		1201	1235	1371	1415		1654	1698
benzyl alcohol			868			1159	1179		1235	1369		1465	1664	
N,N-DMF	739	783		1018	1104	1135	1172	1195	1234	1371	1415	1442	1650	1693
ethanol	741	787		1019			1180	1198	1233	1372			1674	
ethylene glycol	743	784		1013		1139	1182	1198	1237	1372		1462	1666	
formamide	740	782	868	1017	1095		1178	1198	1238	1374	1417		1658	
formic acid	750	787	866	1019			1185	1202	1238	1372	1415	1444	1652	
pyridine	739	777	868		1096	1135	1175		1235	1372		1437	1663	1684
water	746	787	872	1024	1106	1151	1197	1215	1253	1397	1445	1487		1709

Similar spectral features are seen in Figure 3.2 for all the solvents, with the most intense peaks occurring in the 1200-1800 cm^{-1} region. UV-visible absorption spectra of the samples before and after irradiation showed no changes, indicating that no photodecomposition or chemical reaction occurred. Although there are no obvious major changes in the Raman spectra in Figure 3.2, some frequency shifts and slight intensity changes are observed. The frequencies of the bands at ca. 740, 787, 1140, 1180, 1450, and 1690 cm^{-1} all shift significantly with solvent, while slight shifts occur for the modes at 867, 1100 and 1200 cm^{-1}. Some slight intensity changes are also evident, especially in the 1600-1800 cm^{-1} region. While a single peak appears around 1660 cm^{-1} in all the other solvents, two peaks appear in N,N-DMF. The presence of a solvent peak at 1660 cm^{-1} in N,N-DMF (Figure 2.4C) raises doubt to the two peaks assigned to thymidine in this region. However, in the subtraction, the three most intense solvent peaks at 865, 1406 and 1439 cm^{-1} were well subtracted, in which case any contribution from the less intense 1660 cm^{-1} peak was completely removed. Hence, we assign the two peaks to thymidine, and not to solvent subtraction artifacts. In pyridine, a low-frequency shoulder is seen, while for acetic acid a high-frequency shoulder is observed. However, there is very little change in the relative intensities of the 1660 cm^{-1} peak to the 1240 and/or the 1450 cm^{-1} peaks.

Since the most logical interaction between thymidine and solvent will be a hydrogen-bonding interaction, Raman spectra were also obtained of thymidine at low and high pH's. These spectra in the 800-1800 cm^{-1} region are presented in Figure 3.3. A comparison of the acid and base spectra of thymidine to those of thymine (Figure 2.6) shows great similarities. This is expected, since thymine is the main contributor to the Raman spectrum of thymidine. It can be seen from Figure 3.3 that while the spectra at neutral and acidic pH (pH~3) are essentially identical, significant differences between the neutral and basic pH (pH~11) are observed. Three new strong bands are seen at 1136, 1303, and 1594 cm^{-1} in the basic spectrum which are not present in the neutral spectrum (marked with asterisks, *). A number of bands also experience relative intensity changes such as the bands at 1100 and 1450 cm^{-1}. Because thymidine can be deprotonated/protonated at the N_3-H site, which has a pK_a of 9.93 (45, 46), thymidine

Figure 3.3 - Raman spectra of thymidine in acid (A), neutral (B), and basic (C) aqueous solution. A solvent spectrum has been subtracted from each spectrum. The three new bands in the base spectrum are marked with asterisks (*).

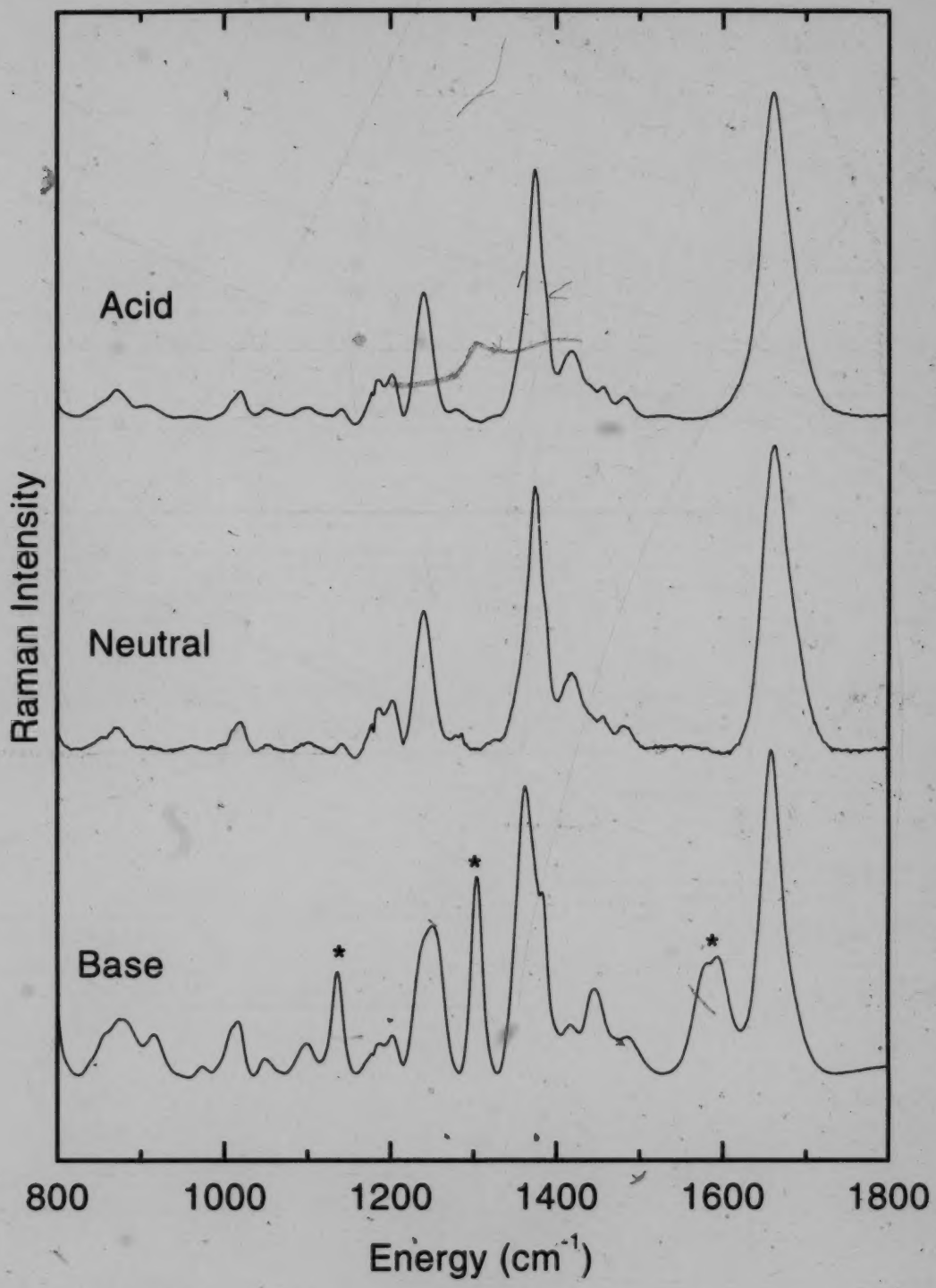
Acid
Neutral
Base
Raman Intensity
800
1000
1200
1400
1600
1800
Energy (cm-1)

probably exists mostly as the monovalent anion at the pH~11 used for this study. Thus, the presence of these three new bands in the basic pH spectrum can be used as a diagnostic for the deprotonation of the thymidine in the other solvents used for this study. Since the 1136, 1303 and 1594 cm^{-1} bands are not observed in any of the spectra in Figure 3.2, we conclude that no deprotonation of thymidine occurred in any of the solvents used for the study.

3.4 Discussion

The thymidine molecule has 31 atoms and 87 normal modes of vibration. These include 14 C-H, O-H, and N-H stretching vibrations expected to have frequencies above 2800 cm^{-1}. The remaining 73 vibrations are expected with frequencies below 1800 cm^{-1} (1). The results obtained in this work agree closely with other Raman data obtained for thymidine (1, 35-37). It is evident from the spectra in Figure 3.2 that the Raman modes due to the sugar ring are very weak, the most intense peaks being those due to coupled vibrations of the base and sugar, and those due to the base only, with the mode assigned to the C=C and C=O double bond stretches of the base being the most intense. Also, some of the base modes show up at the same frequencies as for thymine (see Chapter 2). For example, for pyridine and N,N-DMF (the least polar solvents used), the 740 cm^{-1} mode appears at the same frequency in both thymine (Table 2.3) and thymidine (Table 3.1), and very close for acetic acid and water (the most polar solvents used). The contribution of the sugar ring to the 800 cm^{-1} mode of thymine lowers this mode significantly in thymidine to 787 cm^{-1}. The 1235 cm^{-1} mode appears at a lower frequency of 1227 and 1224 cm^{-1} respectively for pyridine and N,N-DMF in thymine, compared to around 1235 cm^{-1} for both solvents in thymidine. However, the mode shows up at the same frequency in acetic acid for both thymine and thymidine, but appears at a higher frequency of 1253 cm^{-1} in thymidine, as opposed to 1238 cm^{-1} in thymine for water. Also, the 1360 cm^{-1} mode of thymine appears at a higher frequency of 1372 cm^{-1} in thymidine. While the 1415 cm^{-1} mode in thymidine is closer to the N-H mode of thymine at 1390 cm^{-1}, the lack of sensitivity of the mode to solvent, and the

sensitivity of the 1450 cm^{-1} mode to solvent suggests that this mode contains significant contribution from the N-H vibrations. The 1660 cm^{-1} mode also shows up at a lower frequency in all the solvents for thymidine compared to thymine, except in water. Finally, although the mode at 1019 cm^{-1} in thymidine is close to the 985 cm^{-1} mode of thymine assigned to γ(NH), the lack of sensitivity of this mode to solvent shows that it has very little or no NH contribution.

As observed in Figure 3.2 and Table 3.1, there are some significant frequency shifts with solvent. To understand these significant changes in the Raman spectra of thymidine with solvent, correlations were obtained between the observed Raman frequencies and solvent properties (Tables 2.1 and 2.2) which are expected to be important in solvent-solute interactions such as polarity, polarizability and hydrogen bonding. Presented in Table 3.2 are the correlation coefficients obtained from the correlation of the various thymidine peak frequencies in Table 3.1, with each solvent property in Tables 2.1 and 2.2. It is clear from Table 3.2 that only a few solvent properties correlate well with the observed frequency shift. These factors are collected in Table 3.3. It can be seen from Table 3.3 that the modes at 740, 787, 1450, and 1690 cm^{-1} all correlate very well with the acceptor and/or donor numbers. The acceptor numbers are derived from ^{31}P NMR chemical shifts in triethylphosphine oxide (Et_3PO) (47), while the donor numbers are obtained directly from calorimetric measurements with $SbCl_5$, or inferred indirectly from ^{23}Na-NMR chemical shifts of $NaClO_4$ (47), (see Chapter 2 for definitions and relevant equations). These parameters are thought to be a measure of hydrogen-bonding ability, either as an acceptor or a donator of electrons. These modes are due to vibrations of the thymine base only or to coupling of the base and sugar ring. However, none of the sugar ring modes correlates well with the solvent property of hydrogen bonding, although the 1180 cm^{-1} mode correlates well with acceptor number only. This is an indication that the proton-accepting/donating sites of the molecule localized on the thymine base are more solvent-sensitive than those on the sugar ring. There is also significant correlation between several modes and "non-specific" solvent properties such as the 787, 1100, 1200 and 1690 cm^{-1} modes with polarizability (n, L, Π), the 1180 and 1450 cm^{-1} modes with dipolarity ($\pi^*/\pi^*\Pi$), and the 1140 cm^{-1} mode

Table 3.2: Correlation Coefficients between Vibrational Frequencies and Solvent Parameters for Thymidine

Solvent Parameter	Vibrational Band Frequency (cm^{-1})													
	740	787	868	1019	1100	1140	1180	1200	1235	1372	1415	1450	1660	1690
n	-0.65	**-0.88**	-0.44	-0.71	-0.78	0.14	-0.66	-0.71	-0.47	-0.52	-0.66	-0.30	0.06	**-0.97**
ε	-0.29	-0.23	-0.20	-0.12	-0.59	0.13	-0.16	-0.20	0.04	-0.03	-0.18	0.47	-0.07	0.76
AN	**0.92**	0.75	0.65	0.54	0.34	0.50	**0.87**	0.74	0.58	0.51	---	**0.99**	0.24	**0.86**
DN	**-0.85**	**-0.86**	-0.64	-0.32	-0.48	-0.62	-0.57	-0.48	-0.22	-0.14	---	-0.75	-0.22	-0.77
π*	0.06	-0.22	-0.73	0.11	-0.04	0.57	0.32	0.36	0.57	0.43	---	**0.98**	-0.34	0.45
π*II	0.03	0.10	-0.72	0.33	0.22	0.63	**0.92**	0.51	0.72	0.69	---	**0.99**	0.68	0.42
Y	0.17	0.29	-0.68	0.10	0.09	0.05	0.50	0.14	0.42	0.35	0.27	0.20	0.04	0.35
Π	-0.65	**-0.87**	-0.44	-0.71	-0.78	0.12	-0.67	-0.72	-0.47	-0.53	-0.66	-0.32	0.05	**-0.97**
B	-0.09	-0.21	0.74	-0.07	-0.03	-0.07	-0.45	-0.09	-0.37	-0.31	-0.25	-0.19	-0.09	-0.26
K	0.11	0.19	-0.67	0.07	0.03	-0.06	0.42	0.12	0.41	0.35	0.25	0.11	-0.02	0.27
Θ	-0.08	0.20	-0.56	0.08	-0.25	**0.84**	-0.02	-0.05	0.04	-0.06	0.09	0.36	0.38	0.48
ε_p	-0.29	-0.23	-0.20	-0.12	-0.59	0.13	-0.16	-0.20	0.04	-0.03	-0.18	0.47	-0.07	0.76
M'	0.46	0.68	-0.23	0.48	0.48	0.00	0.65	0.51	0.57	0.56	0.58	0.29	0.05	0.78
M	0.28	0.44	-0.50	0.23	0.20	0.02	0.57	0.26	0.50	0.45	0.36	0.25	0.04	0.55
L	-0.77	-0.67	-0.36	-0.58	-0.79	0.53	-0.48	-0.79	-0.45	-0.48	-0.67	-0.04	0.40	**-0.98**
KL	-0.44	-0.04	-0.55	-0.15	-0.57	0.60	-0.37	-0.39	-0.40	-0.37	-0.23	0.02	0.71	-0.66

The table contains correlation coefficients from the correlation of the frequency shifts in Table 3.1 with the various solvent parameters presented in Tables 2.1 and 2.2. Correlation coefficients $\geq \pm 0.80$ are in bold type.

TABLE 3.3: Selected Correlations between Observed Raman Frequencies and Solvent Properties for Thymidine

Solvent Parameter	Vibrational Band Frequency (cm^{-1})									
	740	787	868	1100	1140	1180	1200	1450	1660	1690
n	-0.65(9)	**-0.88(9)**	-0.44(6)	-0.78(6)	0.14(7)	-0.66(9)	-0.71(8)	-0.30(6)	0.06(9)	**-0.97(4)**
AN	**0.92(6)**	0.75(6)	0.65(4)	0.34(5)	0.50(6)	**0.87(6)**	0.74(5)	**0.99(4)**	0.24(6)	**0.86(4)**
DN	**-0.85(6)**	**-0.86(6)**	-0.64(4)	-0.48(5)	-0.62(6)	-0.57(6)	-0.48(5)	-0.75(4)	-0.22(6)	-0.77(4)
π^*	0.06(7)	-0.22(7)	-0.73(5)	-0.04(5)	0.57(6)	0.32(7)	0.36(7)	**0.98(5)**	-0.34(7)	0.45(4)
$\pi^*\Pi$	0.03(6)	0.10(6)	-0.72(4)	0.22(5)	0.63(5)	**0.92(5)**	0.51(5)	**0.99(4)**	0.68(5)	0.42(4)
Π	-0.65(9)	**-0.87(9)**	-0.44(6)	-0.78(6)	0.12(7)	-0.67(9)	-0.72(8)	-0.32(6)	0.05(9)	**-0.97(4)**
Θ	-0.08(9)	0.20(9)	-0.56(6)	-0.25(6)	**0.84(7)**	-0.02(9)	-0.05(8)	0.36(6)	0.38(9)	0.48(4)
M'	0.46(9)	0.68(9)	-0.23(6)	0.48(6)	0.00(7)	0.65(9)	0.51(8)	0.29(6)	0.05(9)	0.78(4)
L	-0.77(9)	-0.67(9)	-0.36(6)	-0.79(6)	0.53(7)	-0.48(9)	-0.79(8)	-0.04(6)	0.40(9)	**-0.98(4)**

The table values are the correlation coefficient (R) with the number of points in parentheses. Correlations with coefficients greater than ±0.8 and a reasonable number of points are in bold type.

with polarity (Θ). From Table 3.3, we note that good correlation of the modes with these solvent parameters is not due to a few number of data points, since even with the lowest number of points (e.g., 4 for the 1450 and 1690 cm^{-1} modes), they show only good correlation with these solvent parameters and not with the others.

Therefore, unlike in thymine where good correlation is only observed between certain modes and the specific solvent property of hydrogen-bonding, good correlation of the observed frequency shifts with a few "non-specific" solvent properties such as polarity and polarizability exists for thymidine. We attribute this difference in good correlation with "non-specific" solvent properties between thymine and thymidine as being due to the larger size of the thymidine molecule compared to the smaller thymine molecule. As the molecule becomes larger, bulk properties of the solvent should become more important than specific solvent properties, such as hydrogen bonding.

While it is difficult to explain all these varied correlations of several modes with numerous and diverse solvent properties, it is clear that the modes that correlate very well with acceptor and donor numbers, ca. 740, 787, 1180, 1450 and 1690 cm^{-1} are due mainly to the N_3-H and C=O sites or contain contributions from these sites. These results are similar to those obtained for thymine in Chapter 2, where all the modes with N-H contributions, ca. 740, 980, and 1390 cm^{-1} showed good correlation with acceptor and donor numbers. This clear correlation suggests that the major interaction between thymidine and solvent is a specific interaction involving hydrogen bonding. The quality of correlation is shown in Figure 3.4. In Figure 3.4A we have a representative acceptable correlation with a correlation coefficient of -0.86, while Figure 3.4B shows an unacceptable correlation with a correlation coefficient of -0.62.

Some intensity changes as a function of solvent environment are observed mainly in the 1600-1800 cm^{-1} region. As in thymine, a peak appears around 1660 cm^{-1} in all the spectra in Figure 3.2, assigned to the $\nu(C_4=O)$ coupled with the $\nu(C_5=C_6)$ (1, 34), in agreement with the results of Spiro, et al. (38, 40) from ultraviolet resonance Raman (UVRR) experiments on thymine and its derivatives. Again, we note that these assignments do not refer to localized internal coordinates, but to normal modes with different contributions from each internal coordinate. Hence, the contribution of the

Figure 3.4 - Good (R=-0.86) and poor (R=-0.62) correlations of the Raman frequency with solvent parameter.

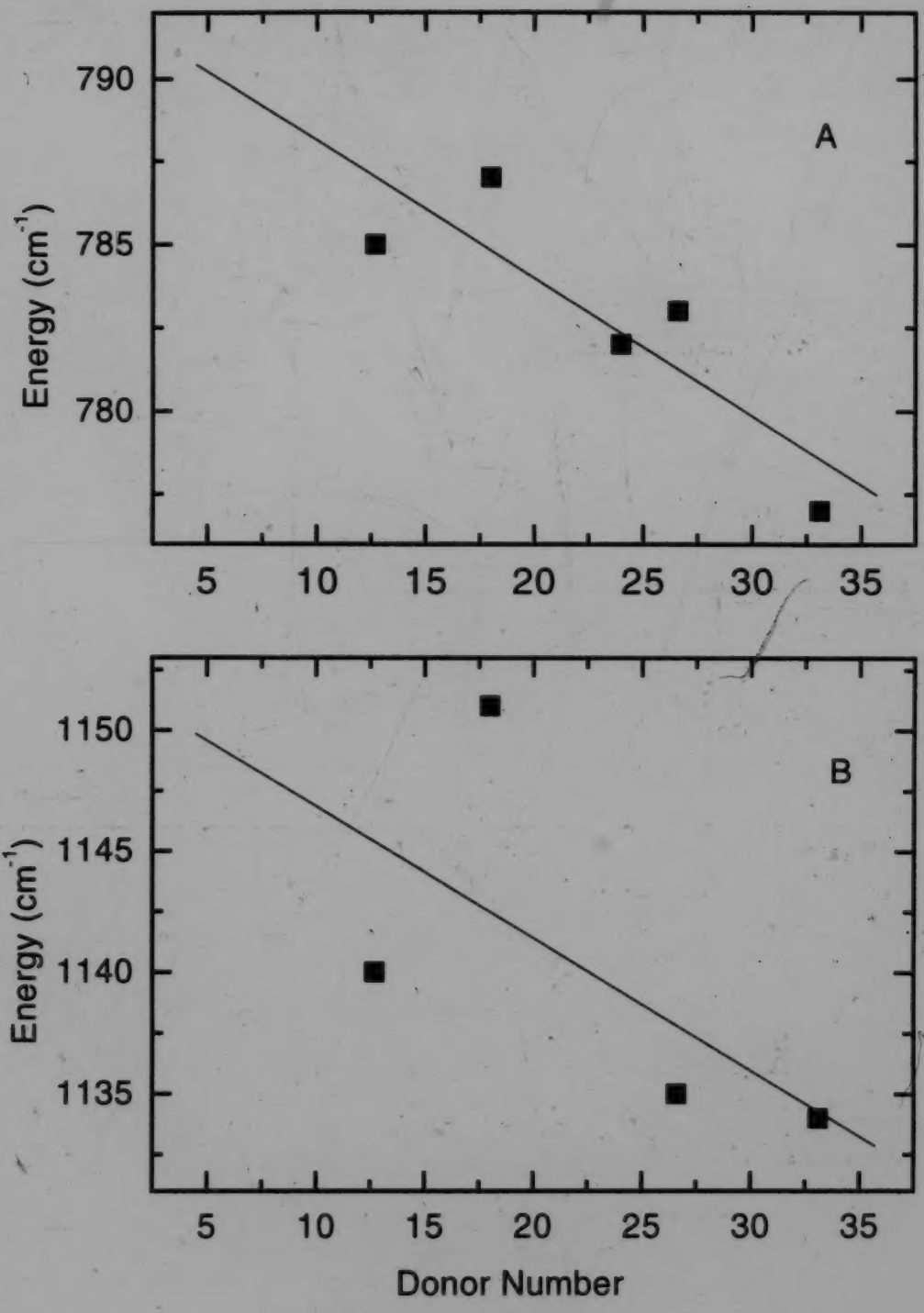
790
785
780
Energy (cm-1)
A
5
10
15
20
25
30
35
1150
1145
1140
1135
Energy (cm-1)
B
5
10
15
20
25
30
35
Donor Number

$\nu(C_5=C_6)$ internal coordinate is dominant for the 1660 cm^{-1} mode, with the $\nu(C_4=O)$ contribution to the intensity of this band being minimal as shown by the lack of correlation of this band with any solvent property, and the $\nu(C_2=O)$ contribution being negligible, since it has a weak Raman signal which only has intensity at excitation wavelengths of 218 nm and below. While a single peak is observed in the more polar/hydrogen bonding solvents such as water, formamide, formic acid and the alcoholic solvents, a doublet appears in the less or non-polar solvents pyridine and N,N-DMF. However, it is not clear why a doublet appears in acetic acid, a very polar solvent. Acetic acid is known to associate in solution forming dimers and to a smaller extent higher polymers (48-51). The dimerization is due to the formation of hydrogen bonds between two or more monomers of acetic acid. In fact, infrared spectra have been reported (50, 51) for acetic acid solutions in carbon tetrachloride where absorption bands for monomers and dimers were observed. Hence, acetic acid dimer formation may make it interact to a lesser extent with the thymidine, as is the case for the non-polar solvents, resulting in the doublet/higher shoulder peak. As in the case of thymine, based on UVRR experiments of nucleobase derivatives in several solvents (41), these intensity changes are due partly to the interaction of solvent with thymidine at the C=O sites. This interaction weakens the C=O bond strength leading to a lowering of the $\nu(C_4=O)$ frequency in the polar solvents, causing it to overlap with the $\nu(C_5=C_6)$, giving rise to a single peak. In the less polar solvents, due to less or no interaction of solvent with thymidine, the $\nu(C_4=O)$ appears at a higher frequency, well separated from the $\nu(C_5=C_6)$, and gives rise to a doublet in these solvents. However, interaction of solvent solely at the $(C_4=O)$ site cannot explain the dramatic intensity changes observed, neither does it account for the sensitivity of the N_3-H modes to solvent. A comparison of the spectra in Figure 3.2 to the base spectrum in Figure 3.3 shows that the thymidine is not deprotonated in any of the solvents. Again, as in thymine, depending on the polarity of the solvent, there is electron pair donation to the proton at the N_3 site leading to a change in the balance of resonance structures between a zwitterionic and neutral thymine species in solution (Figure 2.8). Increased interaction at the C=O sites would be expected to stabilize structure II, weakening the $(C_4=O)$ bond strength, making it appear at a lower frequency and thus overlapping with the $\nu(C_5=C_6)$

in the polar solvents. These observed intensity changes can only be explained by interaction of solvent with thymidine at both the C=O and N_3-H sites. Since the zwitterionic species II, is a better representation of thymine in the more polar solvents, the $\nu(C_4{=}O)$ stretch with its weaker ($C_4{=}O$) bond, appears at a lower frequency and overlaps with the $\nu(C_5{=}C_6)$ stretch. Hence, the single peak in these solvents. However, in the less polar solvents, due to less or no interaction of solvent with thymidine, the neutral species I predominates. Therefore, the $\nu(C_4{=}O)$ stretch with its stronger ($C_4{=}O$) bond, appears at higher frequency, well separated from the $\nu(C_5{=}C_6)$.

We therefore conclude that the interaction of thymidine with solvent results in frequency shifts and slight intensity changes. The major interaction is at the proton accepting/donating sites of the thymine base, i.e. at both the N_3-H and C=O sites, with little or no apparent interaction with the proton-accepting/donating sites of the sugar ring.

3.5 Conclusions

The Raman spectra of thymidine in nine different solvents with varied solvent parameters, acid and base are presented in this Chapter. Frequency shifts are observed in several modes as well as slight intensity changes. A correlation of the observed frequency shifts of specific vibrational modes with solvent properties shows good correlation with specific solvent property, as well as with a few "non-specific" solvent properties. However, the most significant correlation was observed between the specific solvent property of hydrogen bonding and the modes localized at C=O and N_3-H sites. Slight intensity changes in the 1600-1800 cm^{-1} spectral region are also observed due to interaction of solvent with these sites. This shows that the major interaction of solvent with thymidine is at the proton-accepting/donating sites of the thymine base with little or no apparent interaction with the sugar ring. These results suggest that Raman spectroscopy is a sensitive technique that can be used to probe thymidine-solvent interaction leading to a better understanding of DNA structure and dynamics in future.

3.6 References

1. Tsuboi, M et al. *J. Am. Chem. Soc.* **1997**, *119*, 2025.
2. Patrick, M. H.; Rahn, R. O. In *Photochemistry and Photobiology of Nucleic Acids*; Wang, S. Y., Ed.; Academic Press: New York, 1976; Vol. 2, p. 35.
3. Görner, H. J. Photochem. *Photobiol. B: Biol.* **1994**, *26*, 117.
4. Fisher, G. J.; Johns, H. E. In *Photochemistry and Photobiology of Nucleic Acids*; Wang, S. Y., Ed.; Academic Press: New York, 1976; Vol. 1, p.169.
5. Fisher, G. J.; Johns, H. E. In *Photochemistry and Photobiology of Nucleic Acids*; Wang, S. Y., Ed.; Academic Press: New York, 1976; Vol. 1, p. 225.
6. Jagger, J. In *Photochemistry and Photobiology of Nucleic Acids*; Wang, S. Y., Ed.; Academic Press: New York, 1976; Vol. 2, p. 147.
7. Hussian, I.; Griffith, J.; Sancar, A. *Proc. Natl. Acad. Sc. U.S.A.* **1988**, *85*, 2558.
8. Begley, T. P. *Acc. Chem. Res.* **1994**, *27*, 394.
9. Hussian, I.; Sancar, A. *Nucleic Acids Res.* **1987**, *15*, 1109.
10. Park, H.-W.; Kim, S.-T.; Sancar, A.; Deisenhofer, *J. Science* **1995**, *268*, 1866.
11. Rupert, C. S.; Goodgal, S. H.; Herriott, R. M. *J. Gen. Physiol.* **1958**, *41*, 451.
12. Kim, S.-T.; Sancar, A. *Photochem. Photobiol.* **1993**, *57*, 895.
13. Morikawa, K. et al. *Science* **1992**, *256*, 523.
14. Ishida, M.; Kanamori, Y.; Hori, N.; Inaoka, T.; Ohtsuka, E. *Biochemistry* **1990**, *29*, 3817.
15. Kripke, M. L. In *Dermatology in General Medicine*, 4th ed.; Fitzpatrick, T. B., Eisen, A. Z., Wolff, K., Freedberg, I. M., Austen, K. F., Eds.; McGraw-Hill: NewYork, 1993, p. 797.
16. Mitchell, D. L.; Karentz, D. In *Environmental UV Photobiology*; Young, A. R., et al., Eds.; Plenum Press: New York, 1993, p. 345.
17. Cadet, J.; Vigny, P. In *Bioinorganic Photochemistry, vol. 1: The Photochemistry and the Nucleic Acids*, Morrison, H., Ed.; Wiley Interscience: New York, 1990, p.1.
18. Kim, S.-T.; Sancar, A. *Biochemistry*, **1991**, *30*, 8623.

19. Reardon, J. T. *Photochem. Photobiol.* **1996**, *63*, 85S,

20. Sealey, P. G.; Southern, E. M. In *Gel Electrophoresis of Nucleic Acids: A Practical Approach*; Rickwood, D., Hames, B. D., Eds.; IRL Press Ltd.: Oxford, 1982, p. 39.

21. Fangman, W. L. *Nucleic Acid Res.* **1978**, *5*, 653.

22. Jovin, T. M. In *Methods in Enzymology*; Grossman, L., Moldave, K., Eds.; Academic Press Inc.: London, 1971; Vol. 21, p. 179.

23. ANDRZEJ, L. et al. *Spectrochimica Acta* **1992**, *48A*, 1385.

24. Colarusso, P. et al. *Chemical Physics Letters* **1997**, *269*, 39.

25. Ivanov, A. Y. et al. *J. Mol. Struct.* **1995**, *372*, 91.

26. Tsuboi, M. In *Basic Principles in Nucleic Acid Chemistry*; Ts'o, P. O. P., Ed., Academic Press: New York, 1974, vol. 1, p. 399.

27. Nakamoto, K.; Ferraro, J. R. *Introductory Raman Spectroscopy*; Academic Press Inc.: San Diego, 1994, p. 1.

28. McHale, J. L. *Molecular Spectroscopy*; Prentice Hall: New Jersey, 1999, p.364

29. Carey, P. R. "*Biochemical Applications of Raman and Resonance Raman Spectroscopies*"; Academic Press: New York, 1982.

30. Tsuboi, M.; Takahushi, S.; Harada, I. In *Physico-chemical Properties of Nucleic Acids*; Duchesne, J., Ed.; Academic Press: New York, 1973; Vol. 2, p. 91.

31. Hartman, K. A.; Lord, R. C.; Thomas, G. J., Jr. In *Physico-chemical Properties of NucleicAcids*; Duchesne, J., Ed.; Academic Press: New York, 1973; Vol. 2, p. 1.

32. Tsuboi, M.; Nishimura, Y.; Hirakawa, A. Y. In *Biological Applications of Raman Spectroscopy*; Spiro, T. G., Ed.; Wiley-Interscience: New York, 1987; Vol. 2, p. 109.

33. Peticolas, W. L.; Kubase, W. L.; Thomas, G. A.; Tsuboi, M. In *Biological Applications of Raman Spectroscopy*; Spiro, T. G., Ed.; Wiley-Interscience: New York, 1987; Vol. 2, p. 109.

34. Zhang, S. L.; Michaelian, K. H.; Loppnow, G. R. *J. Phys. Chem.* **1998**, *102*, 461.

35. Bell, A. F. et al. *J. Chem. Soc., Faraday Trans.*, **1997**, *93*, 553.

36. Escobar, R. et al. *Analyst*, **1996**, *121*, 105.

37. Ushizawa, K. et al. *J. Mol. Struct.*, **1997**, *412*, 169.

38. Fodor, S. P. A.; Rava, R. P.; Hays, T. R.; Spiro, T. G. *J. Am. Chem. Soc.* **1985**, *107*, 1520.

39. Carey, P. R. *Biochemical Applications of Raman and Resonance Raman Spectroscopies*; Academic Press: New York, 1982.

40. Fodor, S. P. A.; Spiro, T. G. *J. Am. Chem. Soc.* **1986**, *108*, 3198.

41. Toyama, A.; Takeuchi, H.; Harada, I. *J. Mol. Struct.* **1991**, *242*, 87.

42. Mitambo, M. M.; Loppnow, G. R. *Chem. Phys. Lett.* **1996**, *261*, 691.

43. Webb, M. A.; Fraga, E.; Loppnow, G. R. *J. Phys. Chem.* **1996**, *100*, 3278.

44. Fraga, E.; Loppnow, G. R. *J. Phys. Chem. B* **1998**, *102*, 7659.

45. Ts'o, P. O. P. In *Basic Principles in Nucleic Acid Chemistry*; Ts'o, P. O. P., Ed., Academic Press: New York, 1974; Vol. 1, p. 453.

46. Saenger, W. In *Principles of Nucleic Acid Structure*; Cantor, C. R., Ed.; Springer Verlag: New York, 1984, p. 105.

47. Gutmann, V. The Donor-Acceptor Approach to Molecular Interactions, Plenum, New York: 1978, p.17

48. Shiah, I. M., Tseng, H.C. *Fluid Phase Equilibria*, **1996**, *124*, 1.

49. Shiah, I. M., Tseng, H.C. *Fluid Phase Equilibria*, **1954**, *19*, 1074.

50. Malijevskha, I., Polasek, M. *Collect. Czech. Chem. Commun.*, **1995**, *60*, 1094.

51. Bolmer, J. T., Shurvell, H. F. *J. Phys. Chem.*, **1973**, *77*, 256.

Chapter 4. DNA-Sunscreen Interactions from Raman Spectroscopy

4.1 Introduction

Sunlight radiation reaching the terrestrial surface comprises of ultraviolet (UV), visible and infrared (IR) radiation (1). As already discussed extensively in Chapters 2 and 3, exposure of the human skin to solar UV radiation (200-400 nm) is known to induce damage in DNA, resulting in the formation of a variety of photoproducts such as cyclobutane photodimers, 6-4 adducts, and photohydrates, as well as strand breaks, lesions and cross linkages. Light in the UVB (290-320 nm) and UVA (320-400 nm) regions appear to induce the most damaging effects. The pyrimidine cyclobutane dimers occur with the greatest frequency, and are only partially repaired by indigenous repair enzymes such as DNA photolyase and T4 endonuclease. This partial repair may eventually result in skin cancer.

To protect the human skin from such damage, a variety of sunscreen lotions have been formulated and commercialized. Sunscreen preparations employ a variety of active ingredients which are typically very strong absorbers, reflectors or scatterers of UV solar radiation (1). Thus, when applied to the surface of the skin, they are effective at attenuating the transmission of the most energetic solar photons that reach the earth's surface, thereby reducing skin damage from this radiation. It has also been speculated that sunscreen active ingredients may exert protective effects by rapid reaction with toxic oxidant species and by quenching excited state triplets of other molecules (2, 3). Active sunscreen constituents are of two basic types (4, 5), physical blockers that act as a protective barrier by either reflecting or scattering the UV radiation and chemical agents that absorb the UV radiation. The most common physical blockers are zinc oxide (ZnO) and titanium dioxide (TiO_2). The more common chemical absorbers include para-aminobenzoic acid (PABA) derivatives, cinnamates, benzophenones, salicylates and dibenzoyl methanes. These are mainly aromatic compounds, conjugated to a carbonyl group (C=O), and have an electron-donating group (amine or methoxyl) substituted in the ortho or para position on the aromatic ring in most cases. This high degree of conjugation results in electronic transitions associated with the UVB region for the PABA derivatives,

cinnamates and salicylates, and the UVA region for the benzophenones and dibenzoyl methanes (6, 7).

Several researchers (8-12) have reported the protective effects against damage by UVB/A radiation of these sunscreens on human and mouse skin. The physical blockers are chemically inert and hence do not cause irritation, sensitization, phototoxicity or photoallergy. However, the chemical UV absorbers can elicit such adverse reactions (4). There have been numerous reports of the adverse effects of chemical absorbers. Since the chemical absorbers function by absorbing short-wavelength (high energy) UV radiation, which they cannot destroy, the excess energy must be released somehow. Ideally, this energy should be dissipated by such harmless photophysical processes as fluorescence and phosphorescence (radiative processes), or internal conversion and vibrational relaxation (non-radiative processes). However, some of the excess energy may also be dissipated by photochemical processes such as photofragmentation, photoisomerization, direct reaction and energy transfer, all undesirable processes which result in the formation of photoproducts and reactive species which have toxic effects and eventually contribute to DNA damage (7). Photofragmentation leads to the formation of free radicals and other short-lived reactive intermediates which by themselves are toxic, or further react to produce toxic oxidants such as singlet molecular oxygen ($^1O_2$), which eventually cause DNA damage. Formation of $^1O_2$, other free radicals and short-lived reactive intermediates in illuminated aqueous sunscreen solutions have been reported (3, 13, 14), and their toxic and damaging effects have also been established (15). Also, the photoproducts formed by some of these chemical absorbers have been isolated and characterized (16-20). Some of these photoproducts may also be toxic. Direct reaction of the sunscreens with other biomolecules may also occur, if the sunscreens penetrate the skin, causing oxidative damage and forming potentially harmful sunscreen-DNA photoadducts (7). Gasparro and Battista (21), reported that PABA covalently binds to DNA bases and DNA itself, while Shaw, et al. (22), more recently isolated and characterized thymine-PABA and thymidine-PABA photoadducts. There have also been reports (23, 24) that cinnamates may be able to photobind to DNA and that binding occurs through a [2+2] cyclobutane adduct formation. The cinnamates are also subject to

both *trans-cis* photoisomerization and dimerization via a [2+2] cycloaddition across the ethylenic double bond (13, 25-27). The dibenzoyl methanes exhibit keto-enol tautomerism (27, 28), which causes a significant loss in their absorbance and protective power. The chemical absorbers can also photosensitize, an energy transfer process leading to the formation of $^1O_2$ a potentially toxic oxidant. Allen, et al. (3, 14), have reported the formation of $^1O_2$ and other reactive free radical intermediates in illuminated sunscreen solutions and there is now evidence that the chemical absorbers act as photosensitizers and induce DNA damage by dimer formation (29-33). Therefore, in spite of the beneficial uses of sunscreens, recent evidence suggest that they can potentially photosensitize and damage DNA. The mechanism of action seems to be formation of thymidine dimers, and strand breaks as a result of triplet-sensitized photoaddition and generation of singlet molecular oxygen via triplet-triplet annihilation, respectively. However, no direct observation of sunscreen-mediated DNA damage has been made *in vivo*, and the issue is controversial.

To address this controversy, a better understanding of the interaction of sunscreens with DNA and DNA model compounds is required. Sunscreens have been analyzed by various spectroscopic methods such as UV-absorption, infrared (IR), nuclear magnetic resonance (NMR) and mass spectroscopy (MS), resulting in a substantial amount of spectroscopic, chemical, and physical data on sunscreen chemicals (34, 35) available in literature. Dubois, et al. (36), reported solvent effects on the UV-absorption maxima of ketones with varied substituents in 23 different solvents. The structures of the chemical absorbers suggest similar effects and indeed, solvent effects on the UV-absorption spectra of sunscreen active ingredients have been reported (6, 37, 38).

Vibrational spectroscopy is rapidly becoming a convenient and effective tool for probing solvent-solute interactions. Several studies (39-43) have reported a significant solvent-induced frequency shift of the C=O mode in the infrared (IR) spectra of aldehydes, ketones, esters and carboxylic acids, as well as in the S=O stretching mode of dimethyl sulfoxide (44) in numerous solvents of varied properties. Raman spectroscopy, another vibrational technique which involves the inelastic scattering of light from a molecule, has been applied by a number of groups in an effort to understand solvent-

solute interaction and dynamics. Yamaguchi et al. (45), reported spectral shifts in the C=N Raman stretching modes of phenol blue in different solvents. Mitambo and Loppnow (46) have reported the shift in some Raman modes of ethyl 4-(dimethylamino)benzoate (DMABEE) in different solvents. Solvent effects on the Raman modes of thymine and thymidine (47) have also been observed. In spite of the similarity of the sunscreen active ingredients to the carbonyl compounds and DMABEE, there is no report in the literature for the solvent effects on the IR and Raman modes of the sunscreen active ingredients. In fact, only Schallreuter, et al. (20), have reported the Raman spectrum of oxybenzone. The psoralens, which are used for the treatment of skin diseases as well as in sunscreen preparations, have also been a subject of research and their photoadducts formed with DNA have been studied (48-51). However, there have been no reports of vibrational studies of these adducts and recent attempts in our lab to obtain Raman spectra of these photoadducts have not been successful (52). Also, while there have been several Raman/UVRR studies of the interaction of DNA and anticancer drugs (53-56), no such reports are available for DNA-sunscreens interaction.

In this Chapter, we present the UV-absorption spectra and the Raman spectra of sunscreen active ingredients in ten solvents. Shifts in the absorption maxima are observed for some of the sunscreens, as well as frequency shifts in the C=O Raman modes. We also report the Raman spectra for DNA-sunscreen interactions. There were no shifts observed in the frequency of the C=O marker band of the sunscreens in the presence of DNA. This is the first detailed report of solvent effects on the Raman spectra of sunscreens and DNA-sunscreen interaction.

4.2 Experimental

Sunscreen active ingredients (Figure 4.1) octyl N,N-dimethyl para-aminobenzoic acid (Escalol 507, Padimate O, ODPABA), octyl p-methoxycinnamate (Escalol 557, OMC), oxybenzone (Escalol 567, Benzophenone-3, BZ3), and octyl salicylate (Escalol 587, OCS), were generously donated by ISP Van Dyk Inc. (Main and Williams streets, Belleville, NJ 07109). Dibenzoyl methane (DBM) (98%) was obtained from Aldrich

Figure 4.1 - Structures of sunscreen active ingredients: octyl N,N-dimethyl para-aminobenzoic acid (ODPABA), octyl p-methoxycinnamate (OMC), oxybenzone (BZ3), octyl salicylate (OCS), and dibenzoyl methane (DBM).

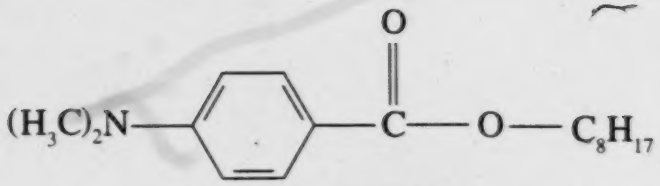

ODPABA

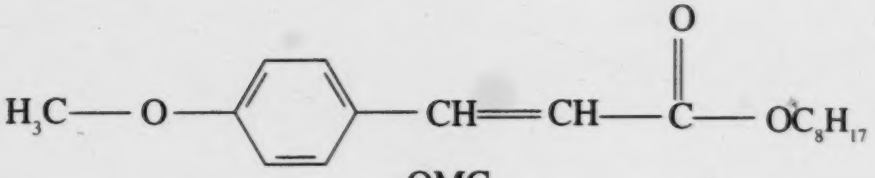

OMC

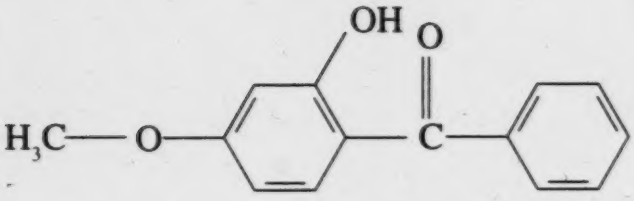

BZ3

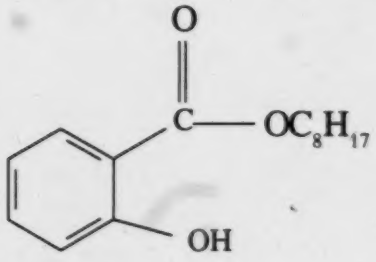

OCS

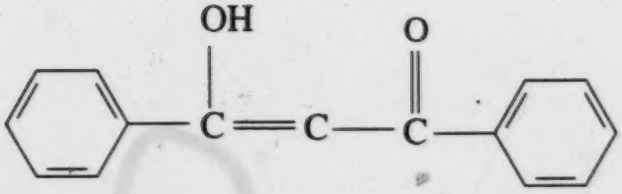

DBM

Chemical Company (Milwawkee, W1 53233, U.S.A.). All sunscreen active ingredients were used as received. Spectral analysis was performed on the samples (IR, NMR, Mass Spec., UV-Visible absorbances, elemental analysis) to check their purity. Calf thymus DNA (either Type 1:sodium salt, "Highly Polymerized" or Activated type XV from Sigma Biosciences, St. Louis, MO., U.S.A.) was also used as received. Acetone, acetonitrile, benzene, dichloromethane, diethyl ether, N,N-dimethylformamide, 1,4-dioxane, hexane, methanol, tetrahydrofuran and water (deionized, 18 MΩ) solvents were reagent grade or better from freshly-opened bottles and were used without further purification. The important solvent parameters are listed in Table 4.1.

Room-temperature Raman spectra were obtained of freshly prepared sunscreen solutions in the various solvents. Due to the differences in solubility of each sunscreen in the various solvents used, the concentration varied for each sunscreen in the various solvents. However, for each sunscreen, in each solvent, a concentration was used at which the ratio of the most intense solvent peak to that of any of the most intense sunscreen peaks was ~1:1. This was in the concentration range of 0.025-1.00 M in all cases. Raman spectra were excited by 50-70 mW of 406.7-nm light from a Kr^+ ion laser (Coherent, Santa Clara, CA) spherically-focused onto a spinning 5-mm diameter (o.d.) NMR tube containing the solution in a 135° backscattering geometry (see Figure 2.2). Multichannel detection of the resulting Raman scattering was accomplished with a liquid nitrogen-cooled charge-coupled device (CCD) detector (Princeton Instruments, Trenton, NJ) coupled to the first half of a double monochromator (Spex, Metuchen, NJ). Spectral slitwidths were 5-7 cm^{-1}, with a spectral acquisition time of 10-20 minutes. A solvent spectrum has been subtracted from the spectrum of each solution, and the resulting spectrum frequency calibrated by measuring the Raman scattering of solvents with known frequencies (acetone, benzene, carbon tetrachloride and chloroform). The reported frequencies are accurate to ±1.5 cm^{-1}. The baselines have been leveled by subtraction of multiple joined line segments.

DNA-sunscreen interaction experiments were performed with calf thymus DNA and two sunscreens, ODPABA and OMC. Since the sunscreens are insoluble in water but soluble in alcohols, rough phase diagram studies were performed to determine the ratio of

TABLE 4.1: Selected Empirical Parameters for the Solvents Used in this Study[a]

Solvent	n	ε	AN	DN	π*/π*II
hexane	1.375	1.89^{20}	0.0	-	-0.08
diethyl ether	1.3542	4.33	3.9	19.2	0.273
benzene	1.5011	2.28	8.2	0.1	0.588
THF	1.4070	-	8.0	20	0.576
1,4-dioxane	1.4232	2.209^{25}	10.8	14.8	.553
acetone	1.3588	21.24^{20}	12.5	17.0	0.683/0.71
N,N-DMF	1.4319	36.5^{16}	16.0	26.6	0.875
acetonitrile	1.3441	37.45^{0}	18.9	14.1	0.713
dichloromethane	1.4244	9.08^{25}	20.4	1.0	-
methanol	1.3288	33.62^{20}	41.5	19.0	0.586

[a] n (refractive index), and ε (dielectric constant, superscripts represent temperature in °C) data from ref. 57. AN (acceptor number) data from ref. 58. DN (donor number) from ref. 59. π*/π*II (Kamlet-Taft dipolarity numbers) data from ref. 60 and 61.

water/alcohol/sunscreen mixture that would dissolve as much sunscreen and DNA for maximal DNA-sunscreen interaction. Also, concentration dependence studies were performed to determine the maximal concentration of water/alcohol/sunscreen mixtures to give quality spectra. Power dependence studies were also done to determine the power at the sample that gave the best signal-to-noise ratio data for the concentrations determined above. Based on all these studies, room-temperature Raman spectra were obtained for 200, 100 and 50 µl, respectively of 10 mM sunscreen active ingredient in methanol mixed with 1 ml of water. Raman spectra were also obtained for 200 µl of 10 mM sunscreen active ingredient in methanol mixed with 1 ml of 1, 2 and 5 mM (base pairs) calf thymus DNA in water to give a sunscreen to DNA base pair concentration ratio of 2:1, 1:1 and 1:2.5, respectively; as well as for 100 and 50 µl of 10 mM sunscreen mixed with 1 ml of 5 mM DNA to give sunscreen to DNA base pair concentration ratio of 1:5 and 1:10, respectively. The experimental conditions were the same as above (see Figure 2.2), except Raman spectra were excited by 200 mW of 514-nm light from an Ar^+ ion laser (Coherent, Santa Clara, CA). A 514 nm holographic filter (Kaiser) was used to remove Rayleigh scattering and minimize stray light. A Raman spectrum of 50 or 20 µl of 2% milk in 1 ml water taken under identical conditions was subtracted from all spectra to correct for residual stray light. Spectra were also taken of the sample solutions after sitting for 1 day to 1 week periods in the dark at 4°C.

4.3 Results

UV absorption spectra were obtained of the sunscreens in the solvents whose parameters are listed in Table 4.1. Figure 4.2 shows the UV absorption spectra of ODPABA, OMC, BZ3, DBM, and OCS respectively in the 205-400 nm region in methanol. The highest wavelength absorption peak for ODPABA, OMC, and OCS occur around 300-310 nm, i.e., in the UVB region, while it is around 320-340 nm, for BZ3 and DBM, in the UVA region. Table 4.2 compiles the highest wavelength absorption peaks (λ_{max}) in the absorption spectra of each sunscreen in the various solvents. From Table

Figure 4.2 - UV absorption spectra of sunscreen active ingredients: octyl N,N-dimethyl para-aminobenzoic acid (ODPABA), octyl p-methoxycinnamate (OMC), oxybenzone (BZ3), dibenzoyl methane (DBM), and octyl salicylate (OCS) in methanol.

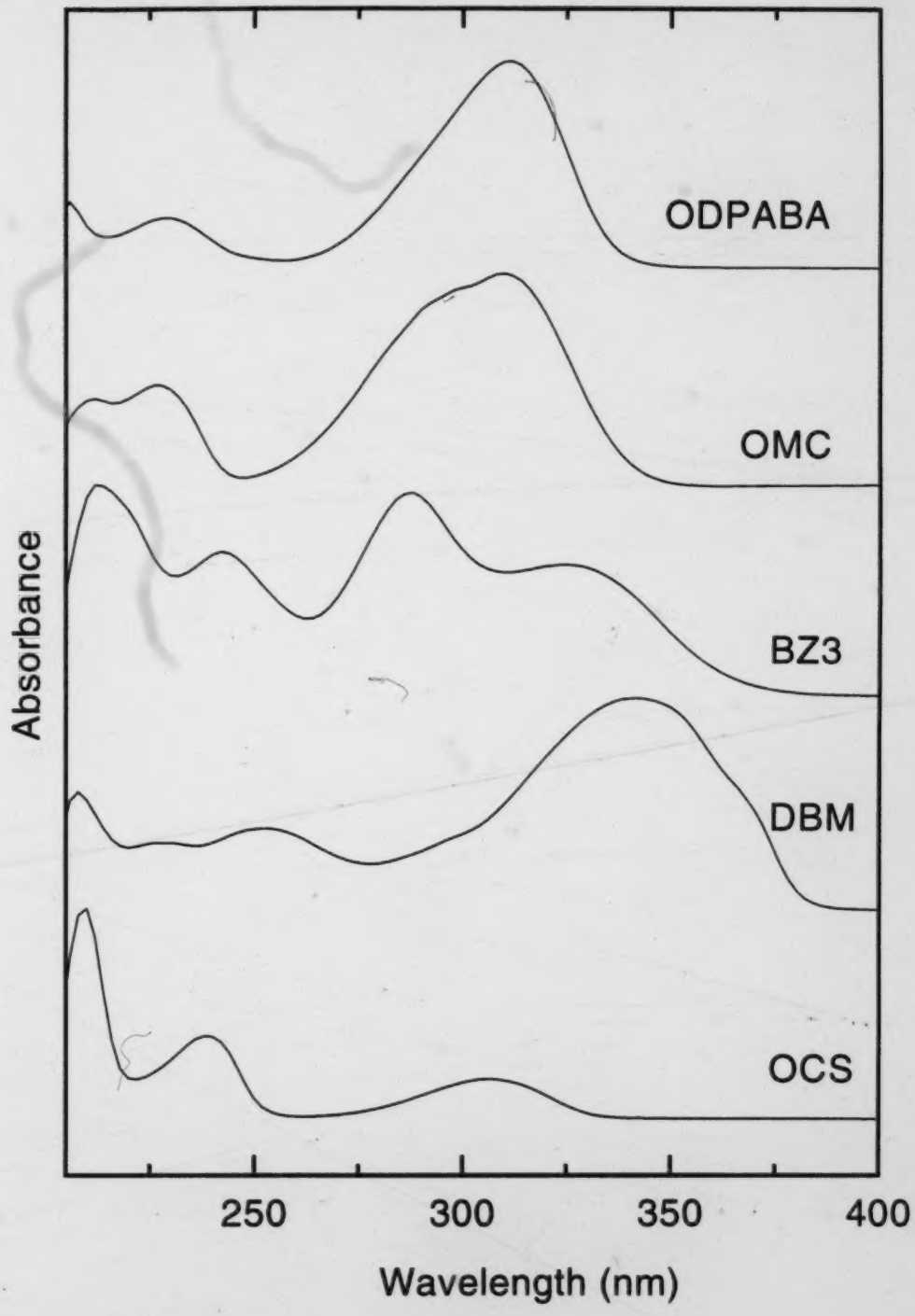
ODPABA
OMC
BZ3
DBM
OCS
Absorbance
250
300
350
400
Wavelength (nm)

Table 4.2: UV-absorption Peaks of Sunscreens from the Spectra in Figure 4.2

Solvent [a]	Wavelength (nm)					
	ODPABA	OMC	DBM	OCS	BZ3 [b]	
hexane	301	290	336	308	283	328
diethyl ether	304	292	338	308	286	326
benzene	--	--	--	--	288	328
THF	308	308	--	308	--	326
1,4-dioxane	307	308	342	306	286	326
acetone	--	--	--	--	--	--
N,N-DMF	312	310	--	--	290	--
acetonitrile	309	308	341	304	287	324
dichloromethane	310	310	342	307	288	326
methanol	312	310	342	306	288	325

[a]In order of increasing polarity/hydrogen bonding strength. [b]BZ3 has two absorption maxima around 288 and 326 nm.

4.2, we observe a shift in λ_{max} of the absorption bands from shorter to longer wavelength (a bathochromic or red shift) with increasing solvent polarity (i.e. from hexane to methanol) for ODPABA, OMC, and to a lesser extent, DBM. However, for BZ3 which has two absorption maxima at 288 and 326 nm, there is a bathochromic shift for the 288 nm band, while we observe very little change or a slight shift towards shorter wavelength (hypsochromic or blue shift) for the 326 nm band with increasing solvent polarity. For OCS, there is no significant change in λ_{max} of the absorption bands with increasing solvent polarity.

To determine the sensitivity of Raman spectroscopy to specific solvent-solute interactions, the Raman spectra were obtained of the pure liquid samples of OCS, OMC, and ODPABA. These are shown in Figure 4.3. The most intense peaks occur in the 1100-1800 cm^{-1} region in all the spectra. These peaks are assigned to individual modes below. Vibrational assignments of some of the modes are based on the Raman assignments of Forster and Hester for ethyl 4-(dimethylamino)benzoate (DMABEE, 62), IR assignments of these sunscreens (34) and IR/Raman assignments of related compounds (63).

For OCS (Figure 4.3A), five intense peaks appear at 1033, 1249, 1325, 1466, and 1674 cm^{-1}, as well as other medium and weak intensity peaks. From the IR assignments of OCS (34), the peak at 1674 cm^{-1} is the C=O stretch and the ring vibrations can be assigned to the bands at 1466, 1584 and 1614 cm^{-1}. All salicylate esters have a characteristic complex pattern of bands in the 1000-1300 cm^{-1} region resulting from mixing of the ester C-O stretch, phenolic hydroxyl bend and other motions (34). Based on the Raman assignments for DMABEE (62), the moderate peak at 815 cm^{-1} may be due to the O-C-O bend of the ester group. The spectrum of neat OMC (Figure 4.3B), shows three strong peaks at 1170, 1604, and 1634 cm^{-1}, with a medium intensity band at 1707 cm^{-1}, in addition to other weak- to moderate-intensity peaks. Based on the IR assignments of OMC (34), the peaks at 1707 and 1634 cm^{-1} are assigned to the conjugated ester C=O stretch and the conjugated exocyclic C=C stretch, respectively. Also, the modes at 1604 and 1576 cm^{-1} are assigned to aromatic ring vibrations. The aliphatic C-O stretch of the ester and the C-O stretch of the p-methoxy group appear as a

Figure 4.3 - Raman spectra of neat liquid sunscreen active ingredients: octyl salicylate (OCS, A), octyl p-methoxycinnamate (OMC, B), and octyl N,N-dimethyl para-aminobenzoic acid (ODPABA, C).

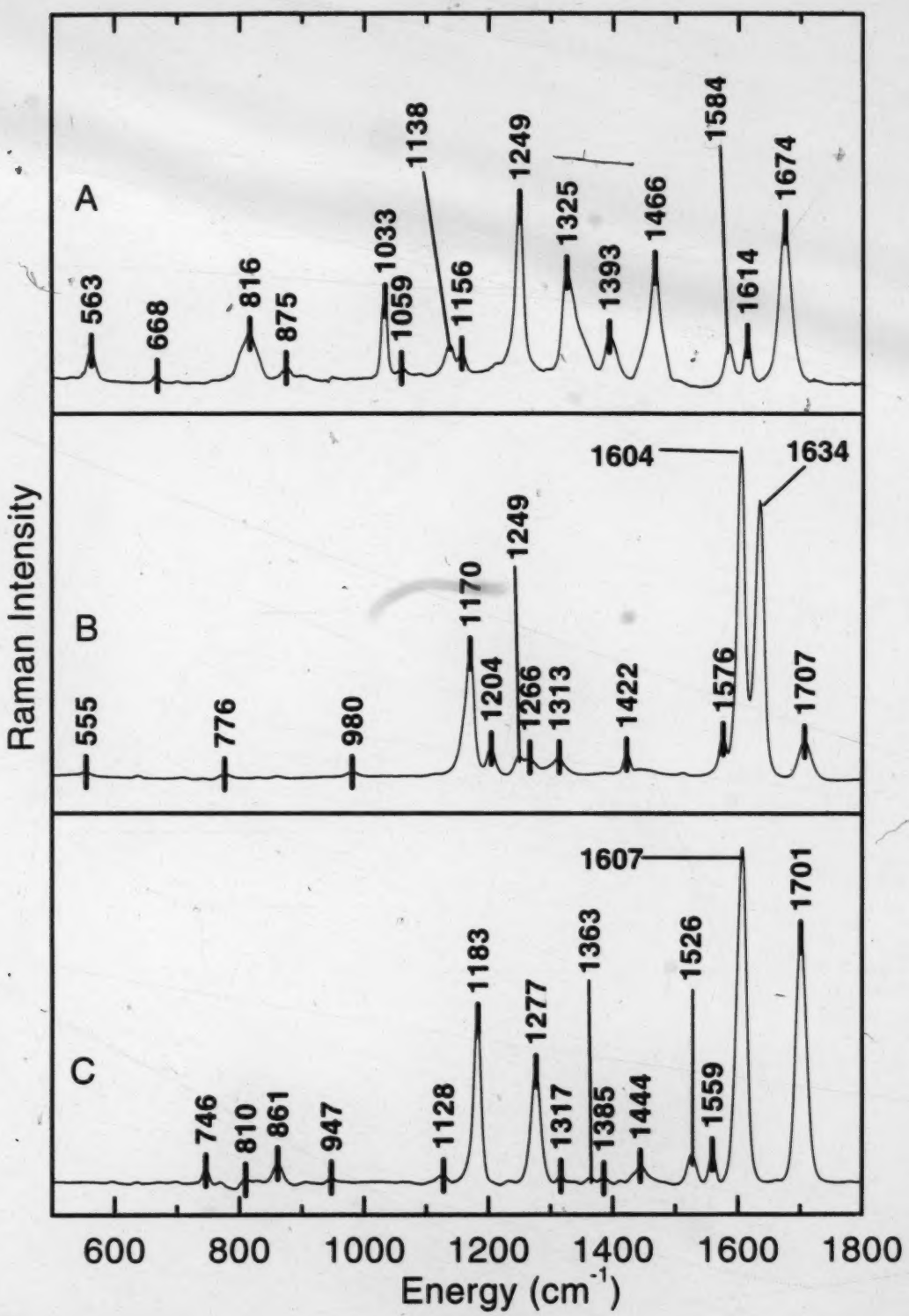
A
563
668
816
875
1033
1059
1138
1156
1249
1325
1393
1466
1584
1614
1674
B
555
776
980
1170
1204
1249
1266
1313
1422
1576
1604
1634
1707
C
746
810
861
947
1128
1183
1277
1317
1363
1385
1444
1526
1559
1607
1701
Raman Intensity
600
800
1000
1200
1400
1600
1800
Energy (cm-1)

doublet at 1249/1266 cm^{-1}, while the mode at 1204 cm^{-1} may be the C-O-C bend of the p-methoxy group. From Raman work on DMABEE (62), the peak at 1170 cm^{-1} is assigned to the C-H bend, while the expected O-C-O bend ca. 850 cm^{-1} is not observed. The spectrum of neat ODPABA (Figure 4.3C), also shows four strong peaks at 1183, 1277, 1607 and 1701 cm^{-1}, in addition to other medium and weak intensity peaks. Again, based on the IR assignments for ODPABA (34) and Raman assignments for DMABEE (62), these peaks are assigned to the C-H bend, C-O stretch, C=C stretch, and C=O stretch, respectively, while the peak at 861 cm^{-1} is assigned to the O-C-O bending mode.

Unlike OCS, OMC, and ODPABA which were liquid samples, BZ3 and DBM were solid samples. Figure 4.4 shows the Raman spectra of BZ3 and DBM in hexane, the least polar solvent used in this study. All the peaks are due to BZ3 and DBM, respectively, and are reproducibly seen in other solvents. For BZ3, four intense peaks are seen at 1228, 1305, 1602 and 1622 cm^{-1}, with other medium and weak intensity bands. From the Raman spectra (21) and IR assignments (34) of BZ3, the doublet at 1602/1622 cm^{-1} is the C=O stretch mixed with the C=C stretches. From Raman assignments for DMABEE (62), the modes at 1305 and 1228 cm^{-1} could be the aliphatic and aromatic C-O stretch, respectively, with the C-H bend at 1164 cm^{-1}. The spectrum of DBM, shows two strong peaks at 1280 and 1601 cm^{-1}. From the IR assignments of butyl methoxy dibenzoyl methane (34), the modes at 1601 and 1498 cm^{-1} are assigned to the C=O stretch and a ring vibration, respectively. The peaks at 1278 and 1181 cm^{-1} are assigned to the C-O stretch and the C-H bend, respectively, from the Raman assignments of DMABEE (62).

The Raman spectra of DBM, ODPABA, OMC and BZ3 were also obtained in the ten solvents whose parameters are given in Table 4.1. The Raman spectra of the solvents are presented in Figure 4.5, while the Raman spectra of DBM, ODPABA, OMC and BZ3 solutions are presented in Figures 4.6-4.9, respectively. Good quality spectra of the sunscreens are obtained in all cases. The spectral patterns are similar for each sunscreen active ingredient in all the solvents. However, significant frequency shifts and some intensity changes are observed for ODPABA, OMC and BZ3. Only the Raman spectra of DBM in hexane, acetonitrile and methanol shows no change (Figure 4.6) in either

Figure 4.4 - Raman spectra of oxybenzone (BZ3, A) and dibenzoyl methane (DBM, B) in hexane.

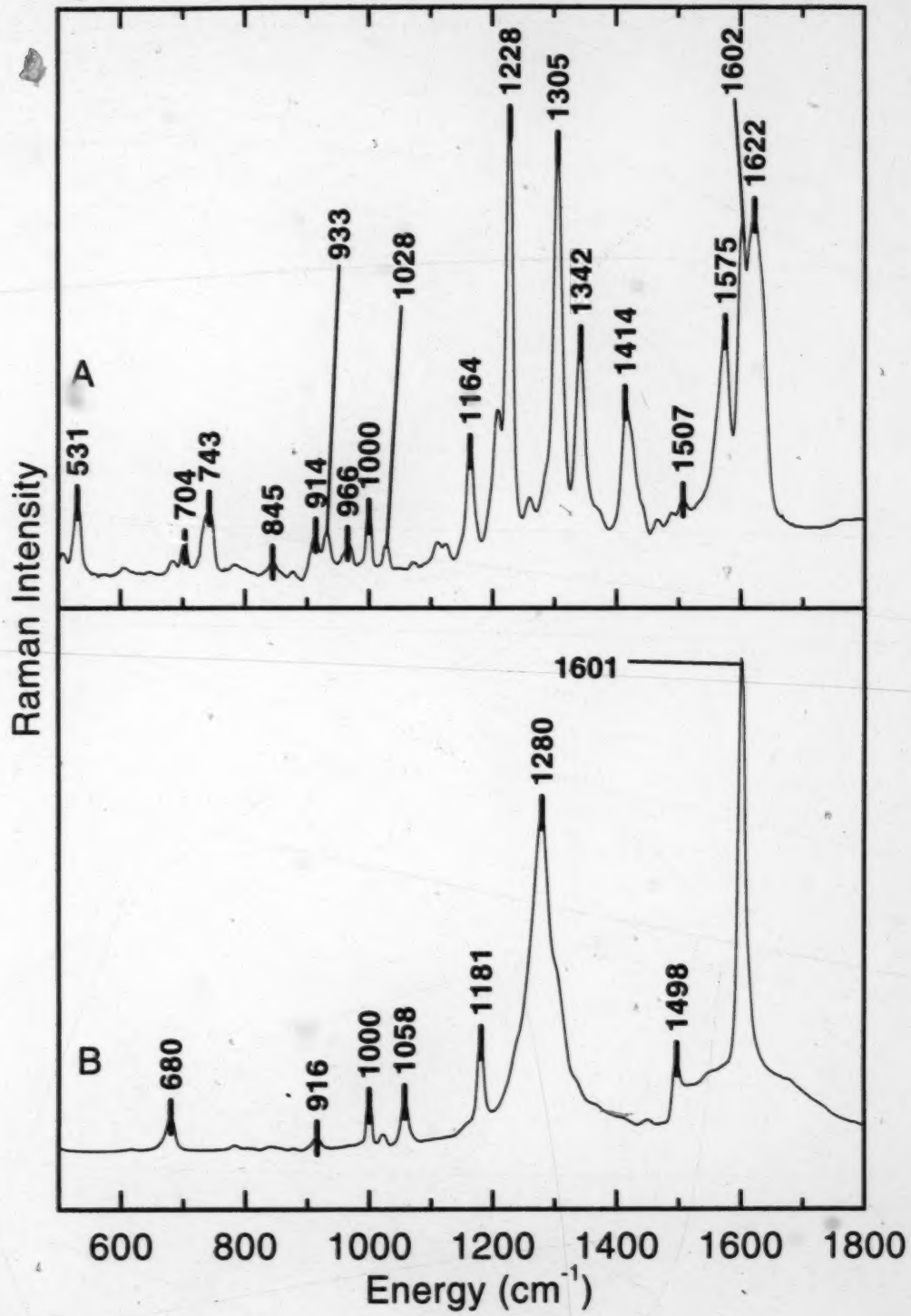
Raman Intensity
A
531
704
743
845
914
933
966
1000
1028
1164
1228
1305
1342
1414
1507
1575
1602
1622
B
680
916
1000
1058
1181
1280
1498
1601
600
800
1000
1200
1400
1600
1800
Energy (cm-1)

Figure 4.5 - Raman spectra of solvents used: hexane (A), diethyl ether (B), benzene (C), THF (D), 1,4-dioxane (E), acetone (F), N,N-DMF (G), acetonitrile (H), dichloromethane (I), and methanol (J). Solvents are arranged in increasing acceptor number (AN) from Table 4.1.

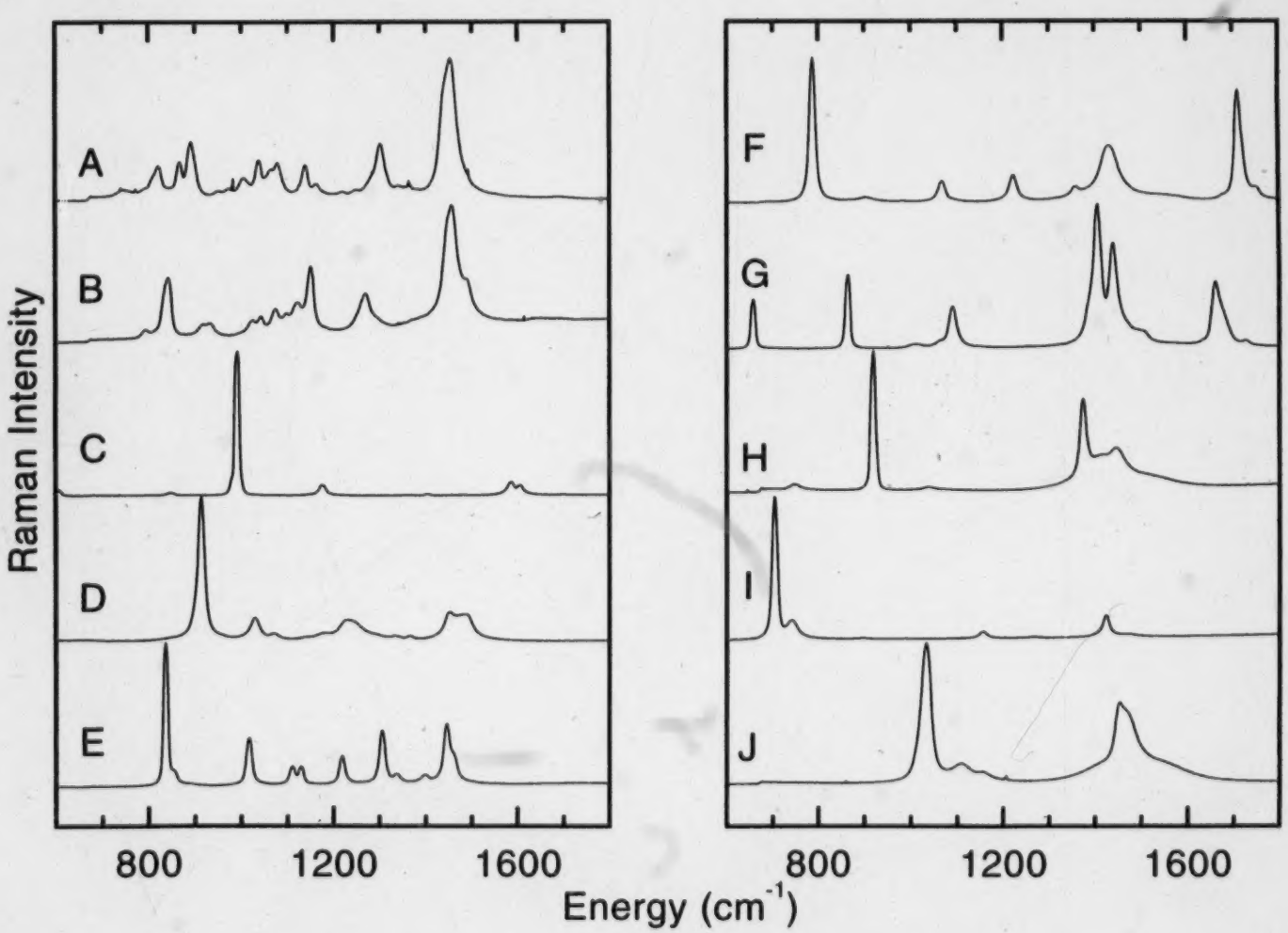
A
B
C
D
E
F
G
H
I
J
Raman Intensity
800
1200
1600
800
1200
1600
Energy (cm-1)

Figure 4.6 - Raman spectra of DBM in hexane (A), acetonitrile (B), and methanol (C).

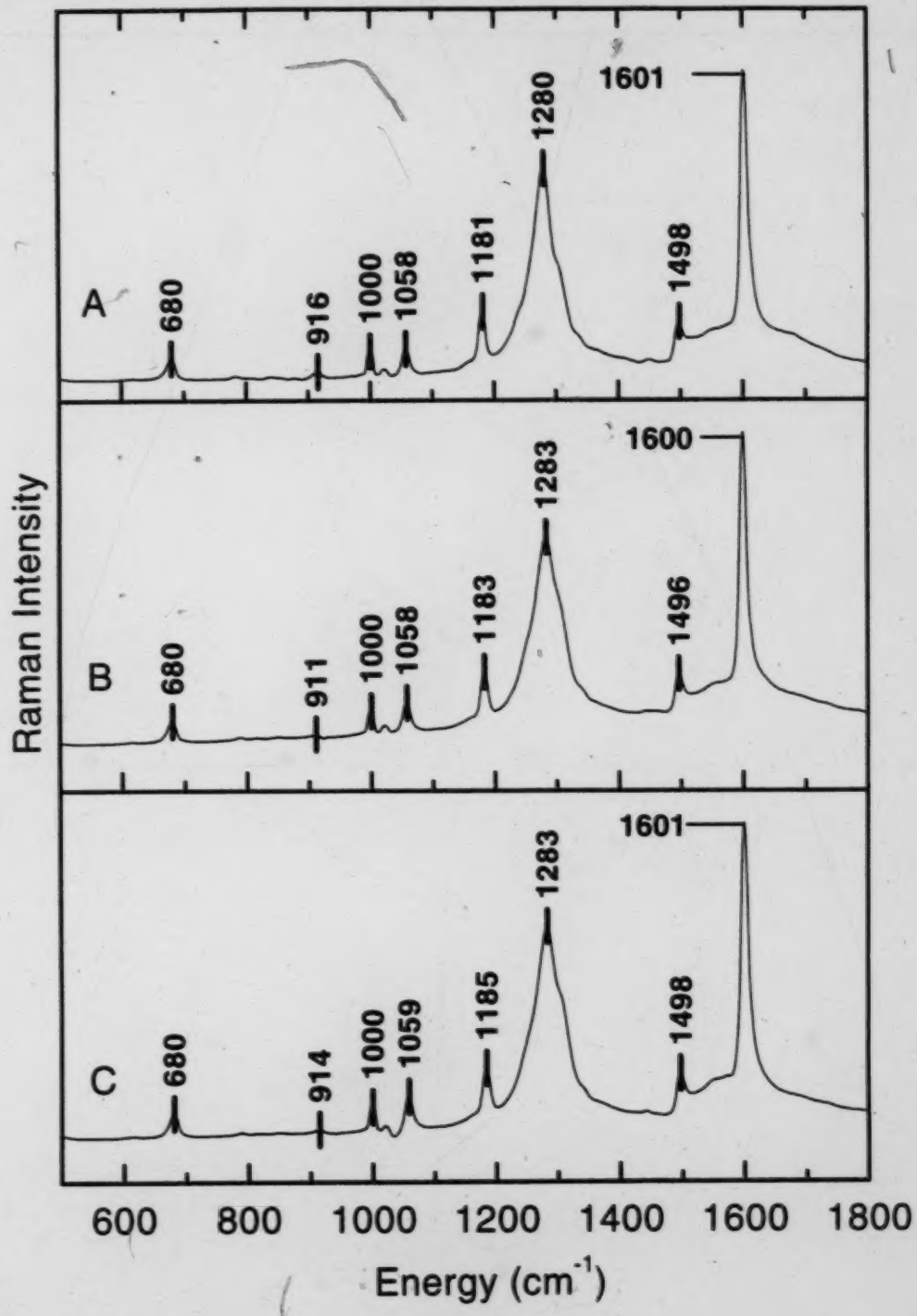
A
680
916
1000
1058
1181
1280
1601
1498
B
680
911
1000
1058
1183
1283
1600
1496
C
680
914
1000
1059
1185
1283
1601
1498
Raman Intensity
600
800
1000
1200
1400
1600
1800
Energy (cm-1)

frequency or intensity with change of solvent from non-polar hexane to highly polar methanol. Although there is a slight frequency shift of the 1181 and 1280 cm^{-1} peaks assigned to the C-H bend and C-O stretch respectively, this shift is so small compared to the shifts seen for ODPABA and OMC (see below), and also in the range of the limit of error of this parameter of ±1.5, that it is negligible.

In ODPABA (Figure 4.7), the four most intense peaks appear around 1180, 1280, 1600, and 1700 cm^{-1}. Table 4.3 compiles the peaks from the spectra in Figure 4.7. The ca. 1700 cm^{-1} C=O band is observed at 1716 cm^{-1} in hexane, decreases to 1698 cm^{-1} in acetonitrile and to 1681 cm^{-1} in methanol, the most polar solvent. Also, this band at 1700 cm^{-1} splits into a doublet in methanol only. No shift in frequency is observed for any of the other modes. Intensity changes are also observed for some of the peaks. Slight relative intensity changes are observed for the 1600 and 1700 cm^{-1} peaks. Although the 1600 cm^{-1} peak is more intense in all cases, there is a change in the relative intensity of the two peaks with change in solvent polarity. The 1700 cm^{-1} peak is far less intense in dichloromethane and methanol, compared to the other solvents. These results are consistent with those obtained for DMABEE (46), except that there is no frequency shift of the O-C-O and C-O modes in our results. This difference may be due to the bulkier octyl substituent in ODPABA compared to the ethyl substituent on DMABEE.

For OMC (Figure 4.8), the three most intense peaks appear around 1170, 1600 and 1630 cm^{-1}, with a weak, important peak at 1700 cm^{-1}. The peaks in Figure 4.8 are compiled in Table 4.4. As for ODPABA, there is a shift in the frequency of the 1700 cm^{-1} mode to lower frequency with increasing solvent polarity. This C=O stretching mode is observed at 1720 cm^{-1} in hexane, at 1704 cm^{-1} in acetonitrile and at 1688 cm^{-1} in methanol. Again, the 1700 cm^{-1} peak appears to split in methanol. There is little or no frequency shift in any of the other modes with change of solvent polarity. However, significant intensity changes are observed for the 1600 and 1630 cm^{-1} peaks. In hexane, the 1630 cm^{-1} peak is more intense than the 1600 cm^{-1}, they have almost equal intensity in diethyl ether and benzene, and for the rest of the solvents, the 1630 cm^{-1} peak keeps decreasing in intensity with increasing solvent polarity.

The Raman spectra of BZ3 in eight solvents are shown in Figure 4.9. Table 4.5 is

Figure 4.7 - Raman spectra of ODPABA solutions: hexane (A), diethyl ether (B), benzene (C), THF (D), 1,4-dioxane (E), acetone (F), N,N-DMF (G), acetonitrile (H), dichloromethane (I), and methanol (J).

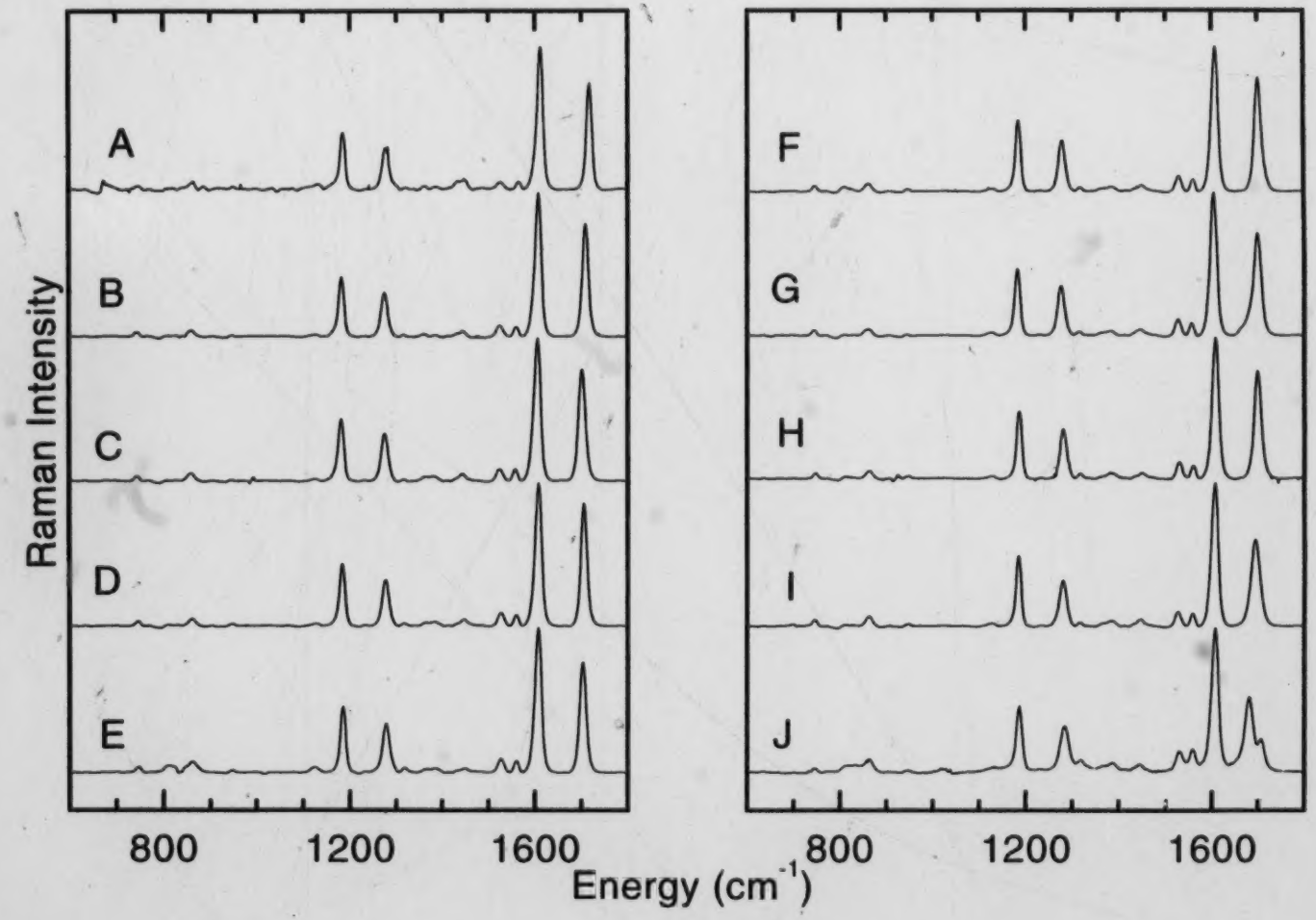
A
B
C
D
E
F
G
H
I
J
Raman Intensity
800
1200
1600
800
1200
1600
Energy (cm-1)

Table 4.3: ODPABA Peaks in Various Solvents from the Spectra in Figure 4.7

Solvent	Vibrational Band Frequency (cm^{-1})													
	746	861	946	1128	1183	1277	1317	1380	1444	1526	1559	1608	1700	1707
hexane	745	862	947	1134	1184	1276	1320	1384	1446	1526	1565	1612	1716	
diethyl ether	744	860			1183	1275		1385	1445	1525	1561	1610	1711	
benzene	746	860			1183	1275		1383	1446	1527	1560	1608	1703	
THF	746	862	946	1127	1184	1277	1317	1384	1448	1526	1559	1608	1705	
1,4-dioxane	746	862	948	1123	1185	1279	1317	1386	1449	1528	1561	1608	1704	
acetone	746	862	946	1128	1185	1279	1317	1386	1449	1528	1559	1608	1701	
N,N-DMF	746	863		1128	1185	1279	1317	1384	1448	1528	1558	1607	1701	
acetonitrile	746	860	945	1126	1186	1280	1317	1381	1449	1529	1559	1607	1698	
dichloromethane	746	862	946	1128	1185	1280	1317	1386	1446	1526	1559	1608	1694	
methanol	746	861	948		1187	1283	1319	1387	1443	1528	1560	1608	1681	1707

Figure 4.8 - Raman spectra of OMC solutions: hexane (A), diethyl ether (B), benzene (C), THF (D), 1,4-dioxane (E), acetone (F), N,N-DMF (G), acetonitrile (H), dichloromethane (I), and methanol (J).

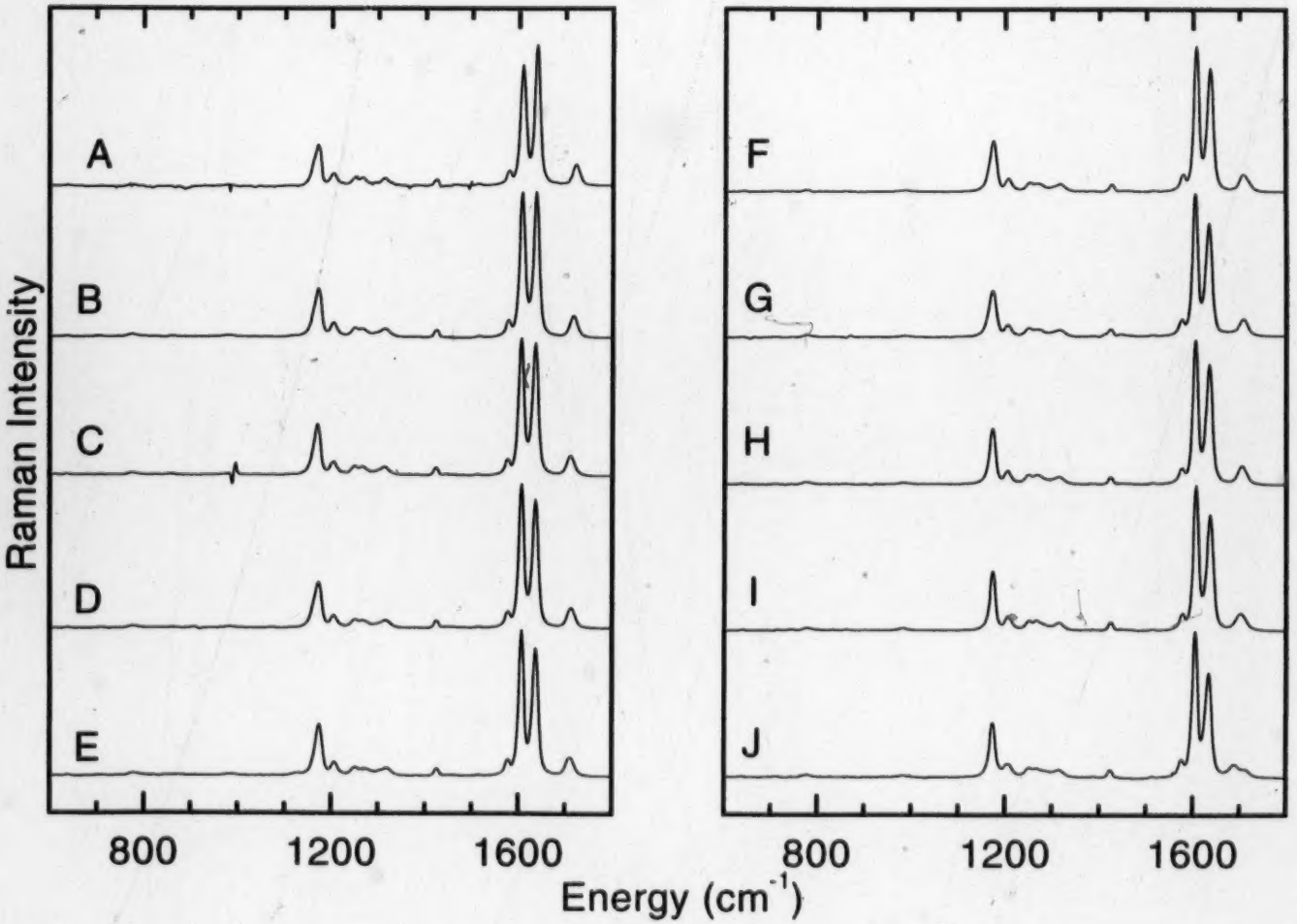
A
B
C
D
E
F
G
H
I
J
Raman Intensity
800
1200
1600
800
1200
1600
Energy (cm-1)

Table 4.4: OMC Peaks in Various Solvents from the Spectra in Figure 4.8

Solvent	Vibrational Band Frequency (cm^{-1})															
	555	774	860	984	1172	1204	1250	1266	1316	1422	1514	1576	1604	1634	1707	1709
hexane		771		977	1169	1201	1253	1267	1312	1422	1514	1579	1608	1638	1722	
diethyl ether	551	774		981	1170	1203	1250	1265	1312	1422	1514	1577	1607	1636	1715	
benzene	553	774	856		1169	1204	1250	1266	1312	1422	1511	1576	1605	1635	1711	
THF	553	775		982	1171	1203	1250	1266	1314	1422	1512	1576	1604	1634	1710	
1,4-dioxane	554	775		984	1172	1205	1250	1270	1317	1424	1514	1576	1604	1634	1708	
acetone	554	773		984	1172	1205	1250	1268	1316	1424	1514	1576	1604	1634	1705	
N,N-DMF	554	776	870	986	1172	1204	1250	1267	1316	1424	1514	1577	1603	1633	1708	
acetonitrile	554	774		986	1172	1204	1250	1268	1316	1424	1515	1577	1605	1634	1705	
dichloromethane	554	776		981	1172	1205	1250	1266	1314	1422	1512	1577	1604	1634	1699	
methanol	553	778		984	1174	1204	1251	1266	1316	1424	1514	1576	1605	1633	1689	1709

Figure 4.9 - Raman spectra of BZ3 solutions: hexane (A), benzene (B), THF (C), 1,4-dioxane (D), acetone (E), acetonitrile (F), dichloromethane (G), and methanol (H).

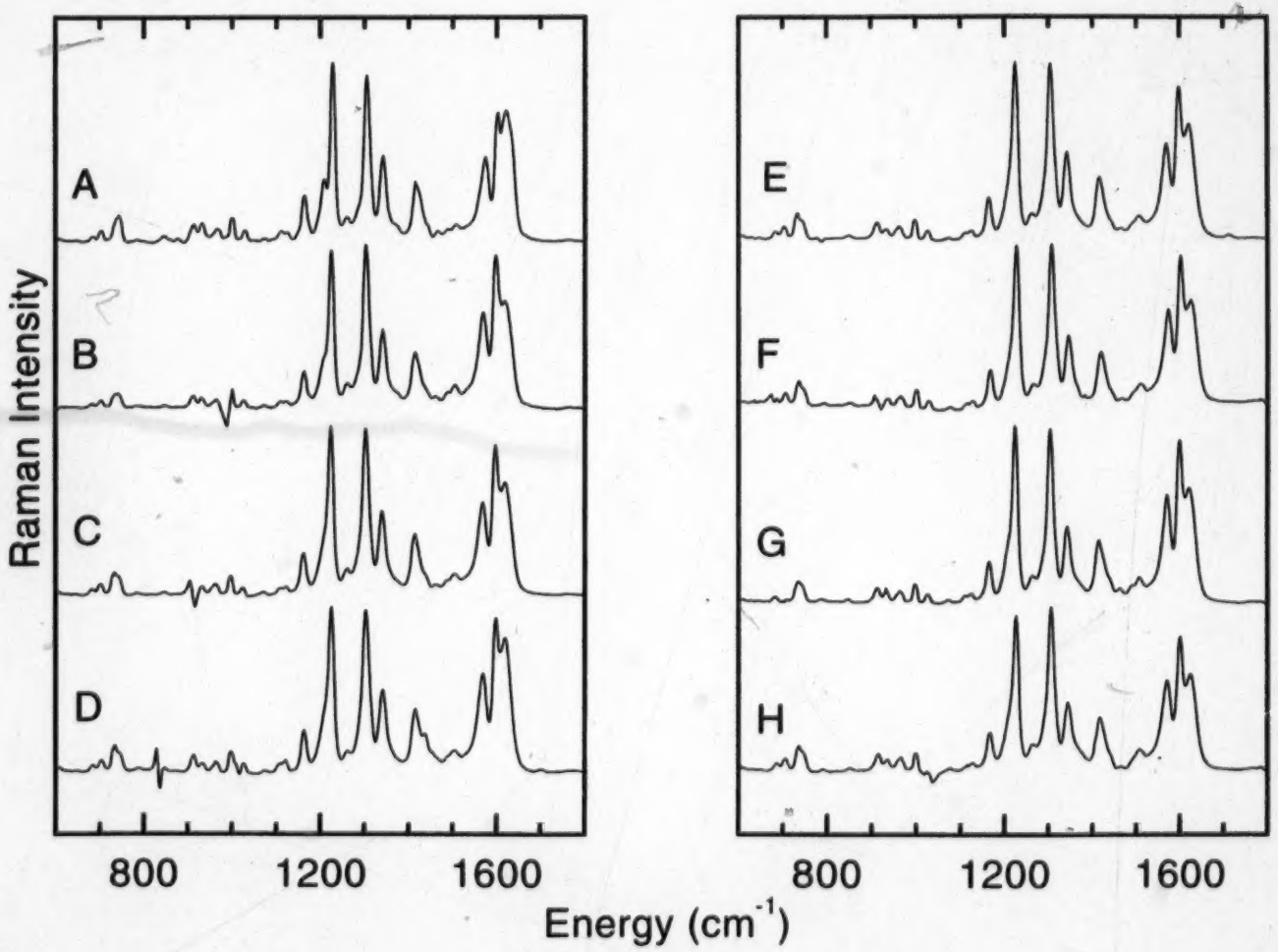
A
B
C
D
E
F
G
H
Raman Intensity
800
1200
1600
800
1200
1600
Energy (cm-1)

TABLE 4.5: BZ3 Peaks in Various Solvents from Spectra in Figure 4.9

Solvent	Vibrational Band Frequency (cm^{-1})									
	734	1164	1223	1304	1342	1414	1504	1568	1598	1620
hexane	743	1164	1228	1305	1342	1414	1507	1575	1602	1622
benzene	737	1164	1223	1302	1341	1414	1504	1568	1598	1619
THF	734	1162	1223	1302	1339	1414	1504	1568	1600	1621
1,4-dioxane	734	1164	1225	1304	1342	1416	1504	1568	1598	1620
acetone	734	1164	1225	1304	1341	1416	1506	1568	1598	1621
acetonitrile	737	1167	1227	1307	1344	1419	1509	1572	1600	1623
dichloromethane	736	1164	1223	1304	1342	1414	1506	1568	1598	1620
methanol	737	1167	1227	1306	1344	1416	1509	1570	1600	1623

a compilation of the peaks from the spectra in Figure 4.9. From Figure 4.9 and Table 4.5, we observe no shift in frequency of any of the modes with increasing solvent polarity. However, slight relative intensity changes are observed. The 1230 cm^{-1} peak is slightly more intense than the 1300 cm^{-1} in hexane. However, in the rest of the solvents, they are of almost equal intensity except in methanol where the 1300 cm^{-1} peak has a greater intensity. Also, the intensity of the bands at 1600 and 1620 cm^{-1} differ in hexane and 1,4-dioxane compared to the other solvents.

All of these results indicate that the Raman spectra of the sunscreens are sensitive to the solvent environment. Therefore, they may be good *in situ* probes of DNA-sunscreen interaction. To determine the nature of DNA-sunscreen interactions, Raman spectra were obtained of DNA solutions containing various amounts of sunscreen. These results are shown in Figure 4.10-4.13 for the 900-1800 cm^{-1} region. The four most intense peaks of both ODPABA and OMC appear clearly in all the spectra including the solutions containing the sunscreen-DNA mixtures of 2:1, 1:1 and 1:5 concentration ratios (Figure 4.10-4.13).

Figure 4.10-4.11 show the spectra of ODPABA/methanol/water with and without DNA. The methanol peaks have been expanded off-scale to show the ODPABA peaks. In Figure 4.10, we have the spectra for ODPABA-DNA concentration ratio of 2:1, while the spectra for 1:1 and 1:5 ratios are shown in Figure 4.11. Spectra were also obtained for concentration ratios of 1:2.5 and 1:10 (not shown) and the results were found to be consistent with what is seen for the 2:1, 1:1 and 1:5 ratios. A spectrum of calf thymus DNA solution shows no peaks at a 1 mM concentration and weak peaks for 2 and 5 mM DNA solutions compared to the intensity of the ODPABA peaks under our experimental conditions. The spectrum of 5 mM DNA (Figure 4.10) agrees with Raman spectra that have been previously reported for DNA (56, 64). None of the DNA peaks appear in the sunscreen-DNA spectra. A comparison of the four most intense modes of ODPABA shows no significant difference in frequency of the marker band, the C=O mode, nor in any of the other modes, in the absence or presence of DNA. A similar result was obtained for sunscreen-DNA concentration ratios ranging from 2:1 to 1:10.

Figure 4.12-4.13 show the spectra of OMC/methanol/water with and without

Figure 4.10 - Raman spectra of DNA-ODPABA. The Figure shows the spectra of methanol (CH_3OH), a mixture of 200 µl 0.01 M ODPABA in CH_3OH + 1 ml H_2O, a mixture of ODPABA and DNA in a ratio of 2:1, and 5 mM DNA.

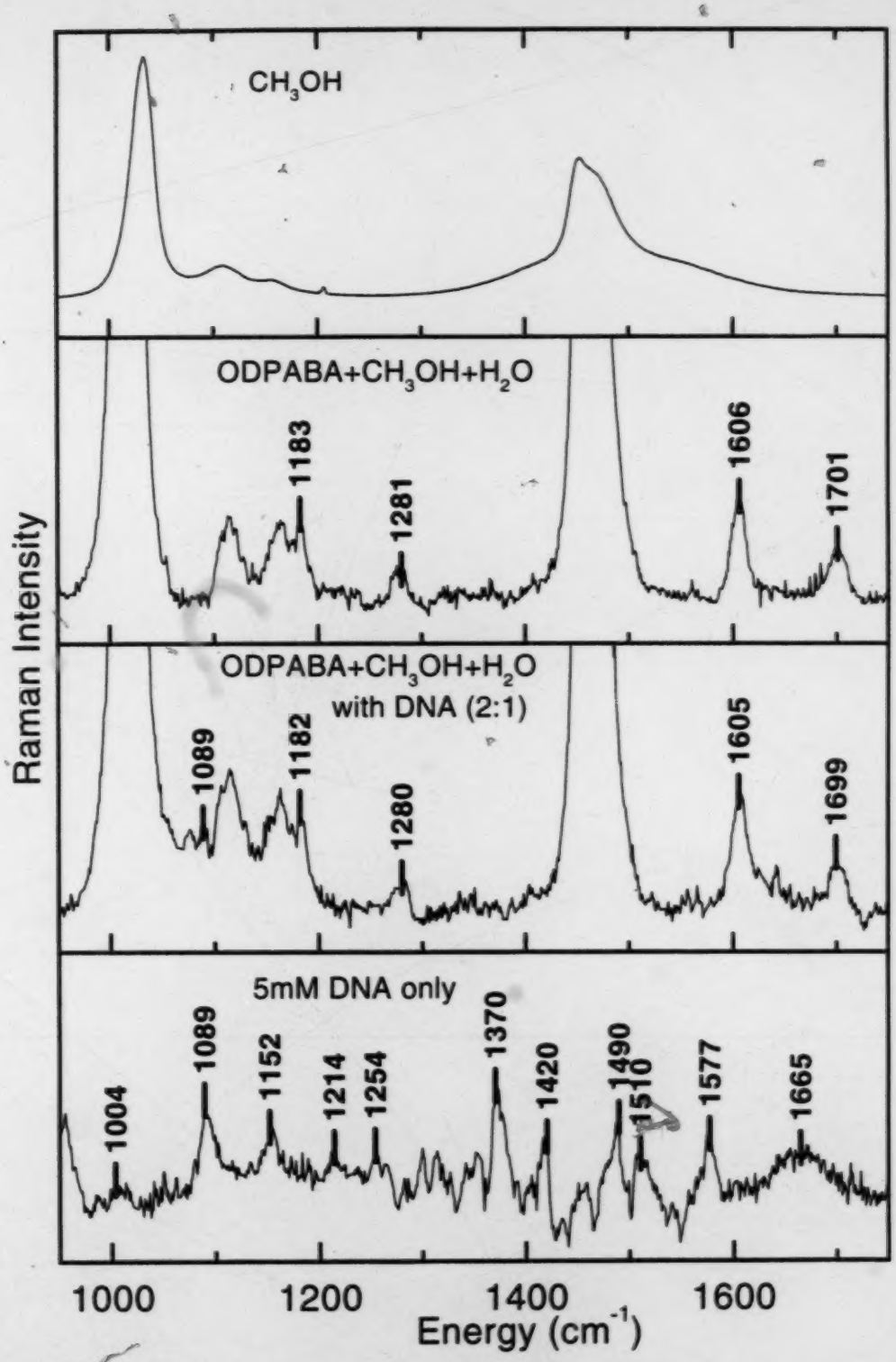
CH3OH
ODPABA+CH3OH+H2O
1183
1281
1606
1701
ODPABA+CH3OH+H2O
with DNA (2:1)
1089
1182
1280
1605
1699
5mM DNA only
1004
1089
1152
1214
1254
1370
1420
1490
1510
1577
1665
Raman Intensity
1000
1200
1400
1600
Energy (cm-1)

Figure 4.11 - Raman Spectra of ODPABA-DNA. The Figure shows the spectra of a mixture of 200 µl 0.01 M ODPABA in CH_3OH + 1 ml H_2O, a mixture of ODPABA and DNA in a ratio of 1:1, a mixture of 100 µl 0.01 M ODPABA in CH_3OH + 1 ml H_2O, and a mixture of ODPABA and DNA in a ratio of 1:5.

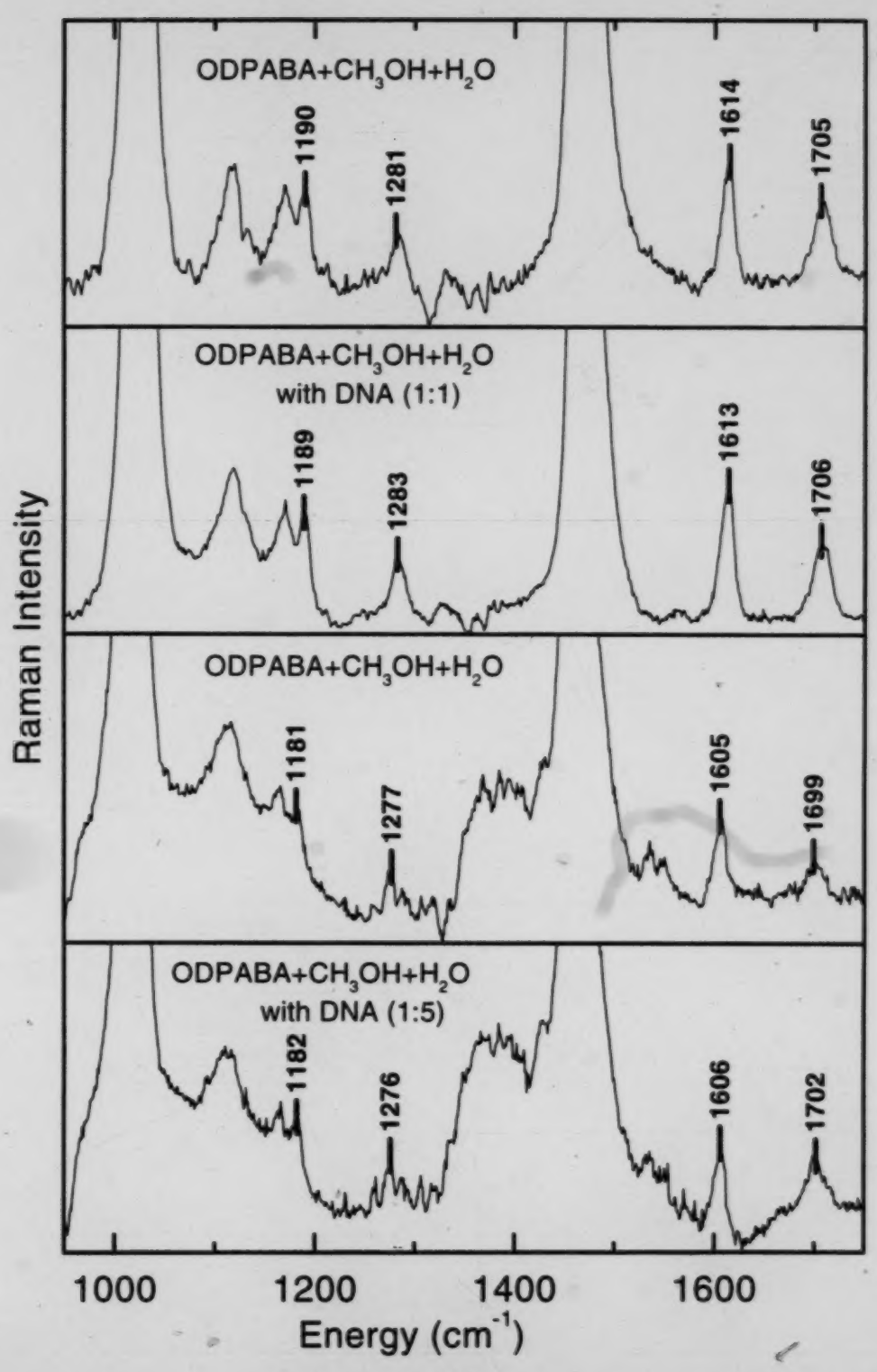
ODPABA+CH3OH+H2O
1190
1281
1614
1705
ODPABA+CH3OH+H2O
with DNA (1:1)
1189
1283
1613
1706
ODPABA+CH3OH+H2O
1181
1277
1605
1699
ODPABA+CH3OH+H2O
with DNA (1:5)
1182
1276
1606
1702
Raman Intensity
1000
1200
1400
1600
Energy (cm-1)

Figure 4.12 - Raman spectra of DNA-OMC. The Figure shows the spectra of methanol (CH_3OH), a mixture of 200 µl 0.01 M OMC in CH_3OH + 1 ml H_2O, a mixture of OMC and DNA in a ratio of 2:1, and 5 mM DNA.

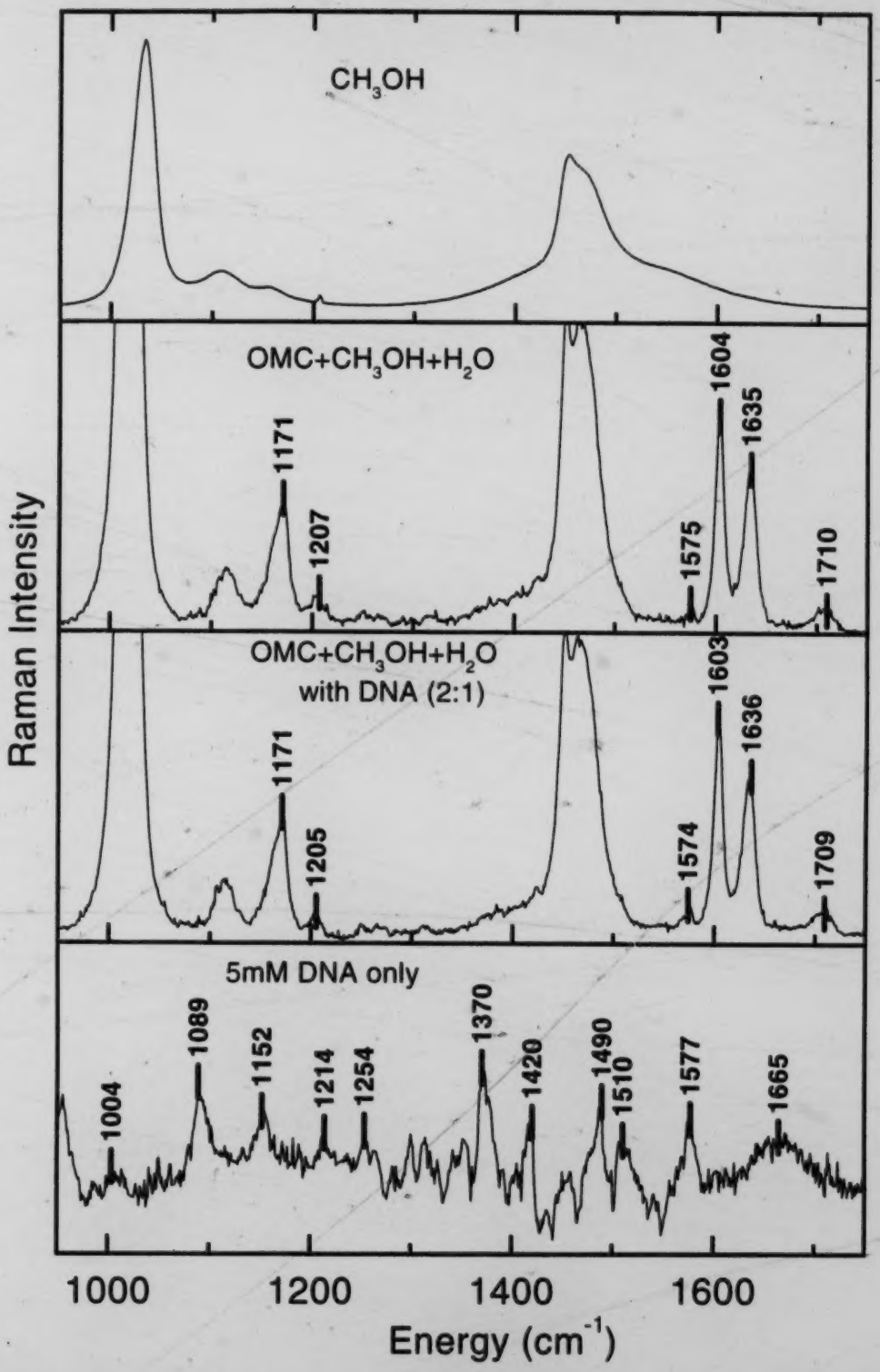
CH3OH
OMC+CH3OH+H2O
1171
1207
1575
1604
1635
1710
OMC+CH3OH+H2O
with DNA (2:1)
1171
1205
1574
1603
1636
1709
5mM DNA only
1004
1089
1152
1214
1254
1370
1420
1490
1510
1577
1665
Raman Intensity
1000
1200
1400
1600
Energy (cm-1)

Figure 4.13 - Raman spectra of DNA-OMC. The Figure shows the spectra of a mixture of 200 µl 0.01 M OMC in CH_3OH + 1 ml H_2O, a mixture of OMC and DNA in a ratio of 1:1, a mixture of 100 µl 0.01 M OMC in CH_3OH + 1 ml H_2O, and a mixture of OMC and DNA in a ratio of 1:5.

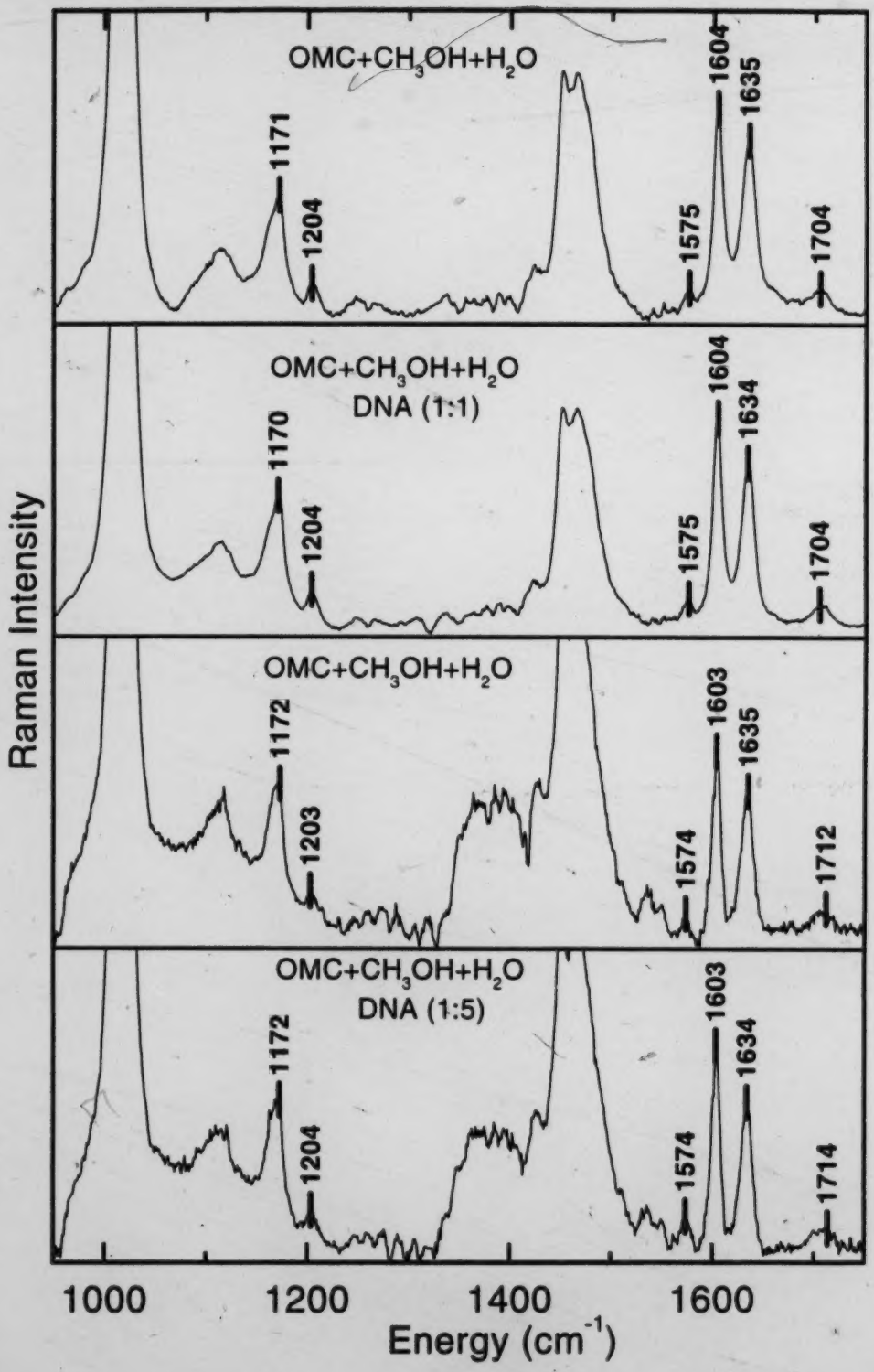
OMC+CH3OH+H2O
1171
1204
1575
1604
1635
1704
OMC+CH3OH+H2O
DNA (1:1)
1170
1204
1575
1604
1634
1704
OMC+CH3OH+H2O
1172
1203
1574
1603
1635
1712
OMC+CH3OH+H2O
DNA (1:5)
1172
1204
1574
1603
1634
1714
Raman Intensity
1000
1200
1400
1600
Energy (cm-1)

DNA for OMC-DNA concentration ratios of 2:1, 1:1 and 1:5, with the methanol peaks expanded off-scale. The four most intense OMC peaks appear clearly in all the spectra. Again, spectra were also obtained for a concentration ratio of 1:2.5 and 1:10 (not shown) and the results found to be consistent with those shown for sunscreen-DNA concentration ratios of 2:1, 1:1 and 1:5. As for ODPABA, the C=O stretch marker band around 1700 cm^{-1} shows no significant shift in frequency in the absence or presence of DNA. There is also no shift in frequency or change in intensity of any of the other modes. No shift in any of the ODPABA and OMC modes were observed upon letting the solutions sit for up to seven days. This result was obtained for sunscreen-DNA concentration ratios ranging from 2:1 to 1:10.

4.4 DISCUSSION

4.4.1 Solvent Interactions

Most sunscreen formulations are creams, lotions or gels, with the active ingredients dissolved in a mixture of solvents of different polarities and properties such as water, glycerin, mineral oils and alcoholic solvents. Since sunscreens function by absorbing the harmful short-wave (high energy) UV rays (250-340 nm) and convert the remaining energy into longer-wave (lower energy) radiation, (usually above 380 nm), the effectiveness of the sunscreen may be influenced by the solvents/vehicle in which they are dissolved. The effect of vehicle on the UV-absorbance of sunscreens depends on factors such as pH, solvent(s), and extinction coefficient of the sunscreen. There are two groups of sunscreens; one that is more polar and the other that is considered to be less polar. The main ingredient in cosmetic preparations that will cause a change in the absorption maximum (λ_{max}) of sunscreens is the solvent. Each solvent may perturb the electron configuration of the molecule in its ground and excited states. In addition to this dielectric effect of the solvent environment, there can be spectral changes due to solvent-solute interaction resulting in changes in the permanent or induced dipoles in one solvent to a greater extent than in another solvent. Other influences are possible, such as hydrogen bonding effects, aggregation and similar molecular interactions all of which can

cause spectral changes. For polar sunscreens such as the benzophenones, interaction with polar solvents cause a shift in the λ_{max} to shorter wavelengths (hypsochromic shift). On the other hand, for the less polar sunscreens such as PABA derivatives, cinnamates, and DBM, interactions with polar solvents shifts the λ_{max} to longer wavelengths (bathochromic shift) (34, 37, 38). Solvent effects on the Raman spectra of thymine and thymidine have been reported (47), while some Raman modes of DMABEE (46) were found to be sensitive to solvent environment. Spectral changes in both the UV absorption and Raman spectra of the sunscreens are therefore expected.

From the UV-absorption spectra of the sunscreens in the solvents studied (Table 4.2), no shift is observed in λ_{max} of OCS with increasing solvent polarity. These results are in agreement with literature data (34, 38), which reported no significant shift in λ_{max} for OCS and other salicylate derivatives on going from hexane to ethanol. As well, no shift was observed in λ_{max} when the solvent range was expanded from mineral oil to 70 % ethanol-30% water mixture. Due to the ortho-substituted configuration of OCS (Figure 4.1), the lone pair of electrons of the C=O oxygen atom are involved in a six-membered cyclic arrangement as a result of intramolecular hydrogen bonding, making them unavailable for interaction with polar solvents. Because the UV-absorption results for OCS showed no shift in λ_{max}, solvent effects on the Raman spectra are expected to be minimal and were not studied.

For DBM, from Table 4.2, there is a bathochromic shift in λ_{max} on going from non-polar hexane to very polar methanol of 6 nm. Although this shift is small compared to the shifts in ODPABA and OMC (see below), the results are in agreement with those obtained for butyl methoxy dibenzoyl methane (34, 38), where a bathochromic shift of 7 nm was observed on going from hexane to methanol. From the Raman spectra of DBM in representative solvents (Figure 4.6), hexane (non-polar), acetonitrile (medium polarity) and methanol (very polar), we observe no shift in frequency of the C=O mode at 1600 cm^{-1} or in any of the other modes. There are also no intensity changes in any of the modes with change in solvent polarity. DBM is a diketone which exists mainly in the enol form. In this configuration, intramolecular hydrogen bonding leading to six-membered ring formation makes the lone pairs of electrons on the C=O oxygen less

available for interaction with solvent. Hence, no solvent sensitivity of the C=O mode in the Raman spectra and little sensitivity in the absorption spectrum is observed.

For the less polar ODPABA, a bathochromic shift in λ_{max} of 12 nm is observed as the solvent varies from non-polar hexane to very polar methanol. Again, this is in agreement with the bathochromic shift in λ_{max} of 11 nm reported for ODPABA (34, 38), on going from hexane to ethanol. For the less polar sunscreen compounds (DBM, ODPABA, and OMC), the excited state is expected to be more polar than the ground state. Therefore, the solvent-solute interaction (mainly hydrogen bonding) results in a greater stabilization of the excited state by polar solvents. This interaction lowers the energy of the electronic transition (between the ground and excited state), and a higher λ_{max} (bathochromic shift) would be expected. From the solvation effects on the absorption λ_{max} of ODPABA, spectral changes are expected in the Raman spectra of ODPABA in the different solvents. From Figure 4.7 and Table 4.3, a shift in frequency of the C=O mode from 1716 cm^{-1} in hexane to 1681 cm^{-1} in methanol is observed. This shift is due to interaction of the C=O bond with polar solvents leading to a weakening of the C=O bond strength in these polar solvents, hence it appears at a lower frequency. This bond weakening can be explained by considering the possible resonance structures of ODPABA shown in Figure 4.14A. In the less or non-polar solvents, the structure of ODPABA closely resembles structure I, while in the polar solvents, it more closely resembles structure II due to stabilization of the zwitterionic charges by solvent hydrogen bonding. Thus, the frequency of the C=O stretch decreases with increasing stabilization of structure II. In the less polar solvents, where structure I is a better representation of ODPABA, less interaction between solvent and the C=O oxygen results in a stronger C=O bond and a C=O stretch at higher frequency. However, in polar solvents with structure II as a better representation of ODPABA, more hydrogen bonding interaction weakens the C=O bond and the C=O stretch appears at a lower frequency.

Mitambo and Loppnow (46) observed frequency shifts with varying solvent polarity in the Raman modes of DMABEE (similar structure to ODPABA with ethyl substituent in place of octyl) at 852, 1282, and 1698 cm^{-1}, assigned to the O-C-O bend, C-O stretch and C=O stretch, respectively. However, there is little or no apparent

Figure 4.14 - Resonance structures of ODPABA (A) and OMC (B).

A

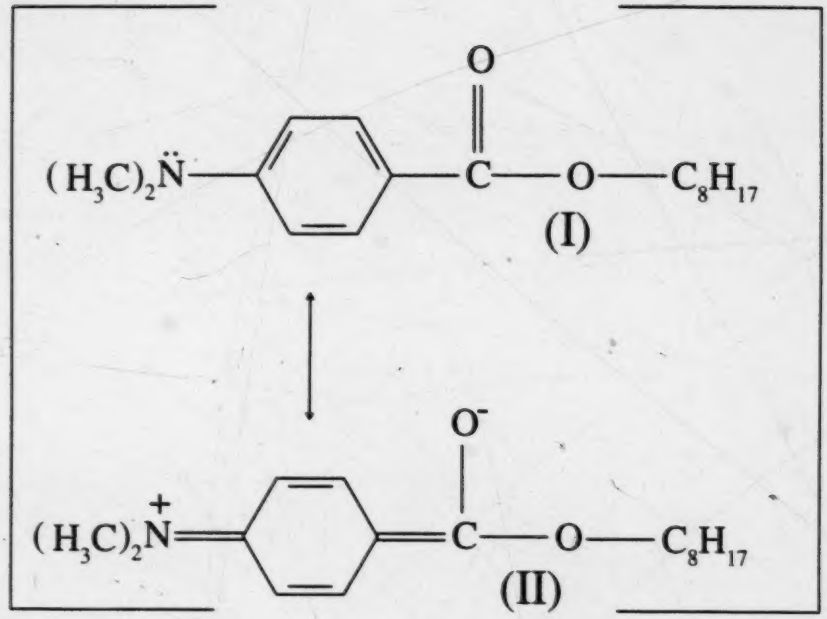
O
(H3C)2N
C
O
C8H17
(I)
O-
(H3C)2N+
C
O
C8H17
(II)

B

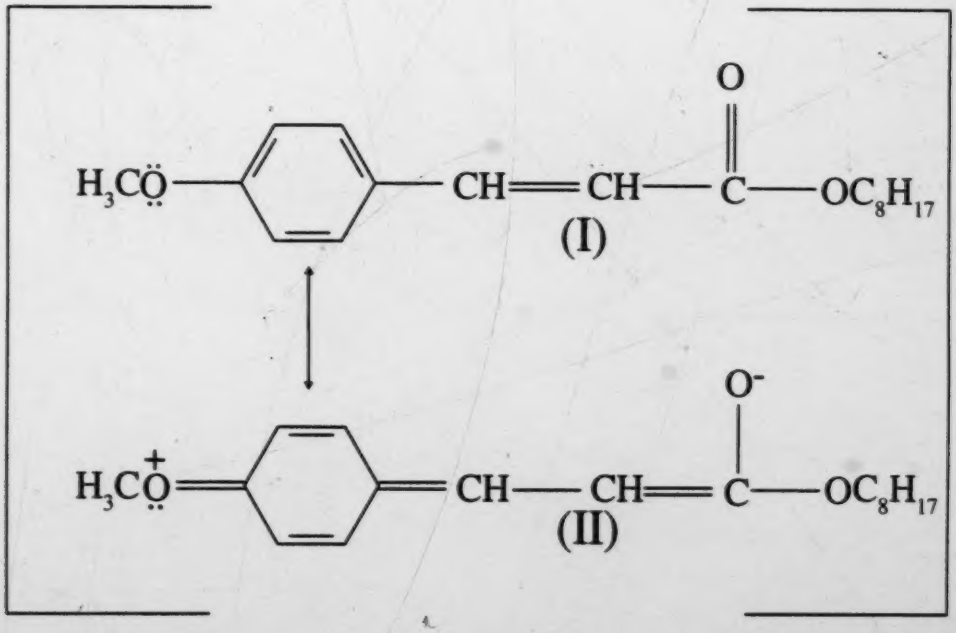
O
H3CO
CH
CH
C
OC8H17
(I)
O-
H3CO+
CH
CH
C
OC8H17
(II)

frequency shift in the ODPABA modes at 861 and 1277 cm^{-1}, assigned to the O-C-O bend and C-O stretch, respectively. The bulkier octyl substituent of ODPABA compared to an ethyl substituent in DMABEE may be responsible for this change. Due to this heavy substituent, the interaction of solvent with ODPABA does not result in as large a perturbation of these modes with solvent polarity/hydrogen bonding strength. Further work is required to understand the slight intensity changes in the ratio of the peaks at 1608 and 1700 cm^{-1} in dichloromethane and methanol, compared to the other solvents. The Fermi resonance (65, 66), resulting from a combination of the first overtone of the O-C-O mode and the fundamental of the C=O stretch, results in the 1707 cm^{-1} shoulder in methanol, again in agreement with the DMABEE results (46).

From Table 4.2, we also observe a bathochromic shift in the λ_{max} of OMC from non-polar hexane to very polar methanol of 20 nm. These results are in agreement with the bathochromic shift of 22 nm reported in the λ_{max} of OMC (34, 38), on going from hexane to ethanol. The same reasoning for the absorption λ_{max} shift holds for this less polar sunscreen as for ODPABA above. Hence, we would expect solvent effects on the Raman spectra of OMC. As for ODPABA, from Figure 4.8 and Table 4.4, we observe frequency shifts in the C=O mode of OMC from 1722 cm^{-1} in hexane to 1689 cm^{-1} in methanol. Also, the 1709 cm^{-1} shoulder in methanol due to Fermi resonance is observed. Similar arguments as in ODPABA account for the frequency shift of the C=O mode with solvent and the Fermi resonance, as well as for the lack of sensitivity of the O-C-O bending and C-O stretching modes with change in solvent polarity. From the resonance structures of OMC in Figure 4.14B, structure I is a better representation of OMC in the less or non-polar solvents. The stronger C=O bond stretch therefore appears at a higher frequency. However, in the more polar solvents the structure of OMC more closely resembles structure II, due to greater stabilization of the zwitterionic charges by the more polar solvent, resulting in a lower frequency C=O stretch. The intensity changes in the ratio of the peaks at 1604 and 1634 cm^{-1} assigned to the aromatic and conjugated C=C stretches, respectively, can partly be explained by considering the resonance structures of OMC in Figure 4.14B. In non-polar hexane, where the structure of OMC more closely resembles structure I, the 1634 cm^{-1} mode has a higher intensity. However, with

increasing solvent polarity, there is some degree of solvent interaction with OMC decreasing the resemblance of OMC to structure I. The structure of OMC now begins to more closely resemble structure II. Hence, the intensity of the 1604 cm^{-1} mode increases and becomes equal to 1634 cm^{-1}. With further increase in solvent polarity and greater solvent-solute interaction, structure II now better represents OMC in the more polar solvents resulting in the 1604 cm^{-1} mode being more intense throughout, with the 1634 cm^{-1} mode being of lesser intensity and reducing gradually in intensity. We therefore attribute the intensity changes to a change in vibrational character with changing solvent. The aliphatic C=C stretch in structures I and II is the same mode, since it does not shift in frequency with changing solvent polarity (Table 4.4). However, it changes its vibrational character depending on which structure is a better representation of OMC and the polarity of the solvent. In structure I, this C=C stretch is in conjugation with the aromatic ring and the C=O of the ester group, while in structure II, it is directly attached to a carbon atom bonded to two highly electronegative oxygen atoms (the enolate ion). Ideally, the C=C stretch in both structure I and II should contribute equally to the overall intensity of this C=C stretch. However, unequal contributions in the different solvents due to changing vibrational character causes the loss in intensity in the polar solvents and gain in intensity in the less polar solvents.

For BZ3, which has two absorption bands with λ_{max} at 288 and 326 nm, there is a bathochromic shift in the 288 nm-band λ_{max} with increasing solvent polarity of 5 nm. However, there is a slight shift of the λ_{max} at 326 nm to shorter wavelength with increase in solvent polarity of ~3 nm. This hypsochromic shift is so small and in the limit of error of this parameter of ±2 nm. However, the results agree with other works (34, 38), although these workers only reported the λ_{max} at 326 nm without considering the influence of the 288 nm band. They reported a hypsochromic shift of 3 nm on going from hexane to ethanol, in agreement with our results. In addition, on extension of the solvent range from mineral oil to an ethanol(7):water(3) mixture, a hypsochromic shift of 8 nm was reported, an indication that the shift is real, unlike in OCS where an extension of the solvent range resulted in no significant change. BZ3, being a polar compound, is expected to have extensive interaction with polar solvents. This extensive solvation

stabilizes the ground state more than the less polar excited state, thereby inhibiting electron delocalization resulting in a larger energy difference between the ground and excited states, hence a hypsochromic shift of λ_{max}. This extensive interaction (mainly hydrogen bonding) between BZ3 and the solvent would hinder electron delocalization, thereby the formation of the excited state. From the Raman spectra of BZ3 (Figure 4.9, Table 4.5) we observe no shift in frequency of the C=O mode or of any other mode with changing solvent polarity. More work is required to explain the slight intensity changes in the ratio of the peaks at 1570, 1600 and 1620 cm^{-1} in hexane and 1,4-dioxane compared to the other solvents. These results show no solvent effects on the Raman spectra of BZ3. BZ3, like OCS also forms six-membered cyclical arrangement, similar to salicylates, and although the added polarity due to the additional hydroxy and methoxy groups contributes to the slight shifts in UV-absorption maxima observed, these groups apparently do not contribute to any solvent effects in the Raman spectra.

4.4.2 Sunscreen interaction with DNA

From the Raman spectra of the sunscreens above, we observe solvent effects on the C=O mode of ODPABA and OMC. Thus, the C=O frequency and relative intensity can be used to probe the sunscreen's molecular environment. Based on these results and using the C=O as a marker band, DNA-sunscreen interaction experiments were performed with the sunscreens ODPABA and OMC, and calf thymus DNA. From the spectra in Figure 4.10-4.11 and 4.12-4.13, we observe no change in the C=O mode frequency or intensity in the presence of DNA for either ODPABA or OMC. There are also no changes in any of the other modes. No change in any ODPABA or OMC mode frequency or intensity occurred in the presence of DNA after sitting for up to seven days. These negative results can be interpreted in three possible ways: (a) the interaction is not effectively monitored by Raman spectroscopy, (b) there is no interaction between the sunscreens and DNA, or (c) the solvent environment around the sunscreens interacting with DNA is similar to bulk solvent. These alternative interpretations are discussed in detail below.

Previous experiments with DMABEE (46), thymine and thymidine (47) and the psoralens (52), have shown that Raman spectroscopy is a sensitive probe of solvent-solute interaction. The sensitivity of the C=O mode to solvent in the Raman spectra of the sunscreens ODPABA and OMC reported here also confirms this. We therefore expect that interaction of the DNA with sunscreens will cause a significant change in the sunscreen's molecular environment and would be reflected in the Raman spectrum. These results suggest Raman spectroscopy is a powerful probe of the bulk environment in these specific systems.

Logically, then, only two alternatives remain. Either there is no interaction between the sunscreens and DNA, or the environment of the complexed sunscreen is similar to the bulk environment. Raman/UVRR studies of the interaction of DNA and intercalating agents such as anticancer/antitumor drugs (53-56), shows intensity changes and frequency shifts in some Raman modes of the DNA and/or the drug. There are also reports that PABA and the cinnamates bind covalently to DNA bases and DNA itself (21-24) and thymine-PABA and thymidine-PABA photoadducts have been isolated. These past studies provide enough evidence of interaction between sunscreens and DNA.

There have been numerous reports of psoralen-DNA adducts in the literature (48-52). Recently, the solvent sensitivity of the C=O Raman mode of the psoralens has been observed in our lab (52). In this study, the C=O mode of the psoralens was observed to be sensitive to solvent in much the same way as the sunscreens reported here. However, no change in the psoralens C=O frequency was observed upon non-covalent binding with DNA. Although the C=O modes of the psoralens and sunscreens are sensitive to the bulk solvent environment, no change in the Raman spectra of the sunscreens or psoralens, even though they are interacting with the DNA, are observed. These results imply that the DNA environment may be similar to the bulk solvent environment.

4.5 Conclusion

UV-absorption and Raman spectra were obtained for the five common sunscreen active ingredients ODPABA, OMC, BZ3, DBM and OCS in ten different solvents. Bathochromic shifts were observed in the absorption maxima of ODPABA, OMC and DBM, hypsochromic shifts for BZ3 and no change in the maximum absorbance of OCS with increasing solvent polarity. Raman spectra of DBM in three solvents showed no solvent effects, while Raman spectra of BZ3 in eight solvents showed only slight intensity changes, but no frequency shifts in any of the modes. The Raman spectra of ODPABA and OMC in ten solvents showed frequency shifts in the C=O mode as well as intensity changes. Using the C=O mode as a marker band, sunscreen-DNA interaction spectra were obtained for sunscreen-DNA concentration ratios ranging from 2:1 to 1:10. For both ODPABA and OMC, no frequency shifts in the C=O mode, in any other mode, nor intensity changes were observed. These results, bolstered by other studies in our group, suggest the microenvironment in DNA is similar to the bulk environment.

4.6 References

1. Hidaka, H.; et al. *J. Photochem. Photobiol. A: Chem.* **1997**, *111*, 205.
2. Allen, J. M.; Engenolf, S.; Allen, S. K. *Biochem. Biophys. Res. Commun.* **1995**, *212*, 1145.
3. Allen, J. M.; Gossett, C. J.; Allen, S. K. *Chem. Res. Toxicol.* **1996**, *9*, 605.
4. Schauder, S.; Ippen, H. *Contact Dermatitis* **1997**, *37*, 221.
5. Gasparro, F. P.; et al. *Photochem. Photobiol.* **1998**, *68*, 243.
6. Shaath, N. A. In *Sunscreens: Development, Evaluation, and Regulatory Aspects*; Lowe, N. J., Shaath, N. A., Eds.; Marcel Dekker: New York, 1990, p 211.
7. Martincigh, B. S.; Aleen, J. M.; Allen, S. K. In *Sunscreen Photobiology*; Gasparro, F. P., Ed.; Landes Press: Georgetown, TX. 1997; chapter 2.
8. Kligman, L. H.; Akin, F. J.; Kligman, A. M. *J. Am. Acad. Dermatol.* **1980**, *3*, 30.
9. Kligman, L. H.; Akin, F. J.; Kligman, A. M. *J. Invest. Dermatol.* **1982**, *78*, 181.
10. Whitmore, S. E.; Morison, W. L. *Arch. Dermatol.* **1995**, *131*, 1128.
11. Wolf, P.; Donawho, C. K.; Kripke, M. L. *J. Invest. Dermatol.* **1993**, *100*, 254.
12. Naylor, M. F.; et al. *Arch. Dermatol.* **1995**, *131*, 170.
13. Morliere, P.; Avice, O.; Melo, T. S. E.;et al. *Photochem. Photobiol.* **1982**, *36*, 395.
14. Allen, J. M.; Gossett, C. J.; Allen, S. K. *J. Photochem. Photobiol. B: Biol.* **1996**, *32*, 33.
15. Halliwell, B.; Gutteridge, J. M. C. *Free Radicals in Biology and Medicine*, 2nd. Ed.; Clarendon Press: Oxford, 1995, p. 1.
16. Gasparro, F. P. *Photodermatology* **1985**, *2*, 151.
17. Shaw, A. A.; Wainschel, L. A.; Sheltar, M. D. *Photochem. Photobiol.* **1992**, *55*, 647.
18. Knowland, J.; McKenzie, E. A.; McHugh, P. J.; Cridland, N. A. *FEBS*, **1993**, *324*, 309.
19. Roscher, N. M. ; Lindemann, M. K. O.; Kong, S. B.; et al. *Photochem. Photobiol.* **1994**, *80*, 417.

20. Schallreuter, K. U.; Wood, J. M.; Farewell, D. W.; et al. *J. Invest. Dermatol.* **1996**, *106*, 538.

21. Gasparro, F. P.; Battista, J. *Photochem. Photobiol.* **1987**, *45*, 49S.

22. Shaw, A. A.; Wainschel, L. A.; Sheltar, M. D. *Photochem. Photobiol.* **1992**, *55*, 657.

23. Broadbent, J. K.; Martincigh, B. S.; Raynor, M. W.; et al. *J. of Chromatography A* **1996**, *732*, 101.

24. Mohammad, T.; Baird, W. M.; Morrison, H. *Bioorganic Chem.* **1991**, *19*, 88.

25. Selles, E.; Aberturas, M. R.; Fresno, M. J. *An. R. Acad. Farm* **1987**, *53*, 153.

26. Kammeyer, A.; Westerhof, W.; Bolhuis, P. A. *Cos. Sc.* **1987**, *9*, 125.

27. Shaath, N. A.; Fares, H. M.; Klein, K. *Cosmetics and Toiletries*, **1990**, *105*, 41.

28. Deflandre, A.; Lang, G. *Cos. Sci.* **1988**, *10*, 53.

29. Rutherford, C. E.; Salter, L. F.; Thomas, R. C. *Photochem. Photobiol.* **1990**, *52*, 337.

30. Bolton, K.; Martincigh, B. S.; Salter, L. F. *Photochem. Photobiol. A: Chem.* **1992**, *63*, 241.

31. Martincigh, B. S.; Salter, L. F. *Photochem. Photobiol. A: Chem.* **1993**, *71*, 137.

32. Aliwell, S. R.; Martincigh, B. S.; Salter, L. F. *Photochem. Photobiol. A: Chem.* **1994**, *83*, 223.

33. Sutherland, B. M. *Photochem. Photobiol.* **1982**, *36*, 95.

34. Shaath, N. A.; et al. In *Sunscreens: Development, Evaluation and Regulatory Aspects*; Lowe, N. J.; Shaath, N. A. Eds.; New York: Marcel Dekker, 1990, p. 537.

35. Shaath, N. A. *Cosmet. Toilet.*, **1987**, *102*, 21.

36. Dubois, J. E.; Goetz, E.; Bienvenue, A. *Spectrochimica Acta*, **1964**, *20*, 1815.

37. Riegelman, S., Penna, R. P. *J. Soc. Cosmet. Chem.* **1960**, *11*, 280.

38. Agrapidis-Paloympis, L. E., Nash, R. A. *J. Soc. Cosmet. Chem.* **1987**, *38*, 209.

39. Kolling, O. W. *J. Phys. Chem.* **1996**, *100*, 16087.

40. Nyquist, R. A. *Appl. Spectrosc.* **1990**, *44*, 433.

41. Nyquist, R. A. *Appl. Spectrosc.* **1992**, *46*, 306.

42. Nyquist, R. A. *Appl. Spectrosc.* **1991**, *45*, 92.

43. Picquart, M.; Lefevre, T.; Lacrampe, G. *Appl. Spectrosc.* **1995**, *49*, 1268.

44. Fawcett, W. R.; Kloss, A. A. *J. Phys. Chem.* **1996**, *100*, 2019.

45. Yamaguchi, T.; Kimura, Y.; Hirota, N. *J. Phys. Chem. A:* **1997**, *101*, 9050.

46 Mitambo, M. M.; Loppnow, G. R. *Chem. Phys. Lett.* **1996**, *261*, 691.

47. Beyere, L. H.; et al. In preparation.

48. Young, A. R. In *Sunscreens: Development, Evaluation and Regulatory Aspects;* Lowe, N. J.; Shaath, N. A. Eds.; New York: Marcel Dekker, 1990, p. 299.

49. Hearst, J. E. *Ann. Rev. Biophys. Bioeng.* **1981**, *10*, 69.

50. Sastry, S. S.; Spielmann, H. P.; Hearst, J. E. *Adv. In Enzymol. Relat. Areas Mol. Biol.* **1993**, *66*, 85.

51. Spielmann, H. P.; Dwyer, T. J.; Hearst, J. E.; Wemmer, D. E. *Biochemistry*,**1995**, *34*, 12937.

52. McWatt, T.; Rafai, S.; Loppnow, G. R. Unpublished work.

53. Manfait, M.; Theophanides, T. In *Advances in Infrared and Raman Spectroscopy*; Clark, R. J. H.; Hester, R. E., Eds.; John Wiley, 1986, Vol 13; p. 311

54. Nabiev, I.; Chourpa, I.; Manfait, M. *J. Phys. Chem.* **1994,** *98*, 1344.

55. Motohashi, N.; Kamata, K.; Meyer, R. *Anticancer Research*, **1990**, *10*, 1611.

56. Zhao, X.; Lu, D.; et al. *Science in China, Series B:* **1995**, *38*, 555.

57. Weast, R. *Handbook of Chemistry and Physics* CRC Press, 54th Ed.,1977.

58. Riddle, F. L. Jr.; Fowkes, F. M. *J. Am. Chem. Soc.*, **1990**, *112*, 3259.

59. Gutmann, V. *The Donor-Acceptor Approach to Molecular Interactions*; Plenum: New York, 1978, p.17

60. Kamlet, M. J., Abboud, J-L. M., Taft, R. W. *J. Am. Chem. Soc.*, **1977**, *99*, 6027.

61. Kamlet, M. J., Abboud, J-L. M., Abraham, M. H., and Taft, R. W. *J.Org. Chem.*, **1983,** *48*, 2877.

62. Hester, E.; Forster, M. *J. Chem. Soc., Faraday Trans. 2*, **1981**, *77*, 1535.

63. Lin-Vien, D.; Colthup, N. B.; Fateley, W. G.; Grasselli, J. G. *The Handbook of Infrared and Raman Characteristic Frequencies of Organic Molecules;* Academic Press, Inc.: San Diego, 1991.

64. Oconnor, T.; et al. *Biophysical Chemistry* **1981**, *15*, 53.

65. Rao, C.; Venkataghavan, R. *Spectrochim. Acta* **1962**, *18*, 273.

66. McHale, J. L. *Molecular Spectroscopy;* Prentice-Hall Inc.: New Jersey, 1st ed., 1999, p. 270.

Chapter 5 - Conclusions and Future Work

5.1 Thymine and Thymidine Raman Spectra

As a preliminary step in the better understanding of the interaction of DNA with exogenous substances and DNA damage and repair mechanisms, the solvent effects on the Raman spectra of thymine, the most photoreactive DNA base and its nucleotide thymidine, were obtained with visible excitation (457.9 nm). For thymine, Raman spectra in eight solvents, acid and base were obtained. The frequency of several peaks in the 700-1800 cm^{-1} region were observed to shift to higher frequency with increasing hydrogen-bonding ability of the solvent. Drastic intensity changes were also observed in the 1600-1800 cm^{-1} region. Correlation of the observed frequency shifts of specific vibrational modes with various solvent properties showed good correlation of modes containing N-H and C=O stretching coordinates with the specific solvent property of hydrogen-bonding (AN and DN). This hydrogen bonding interaction of solvent with thymine at the N-H and C=O sites also accounts for the intensity changes observed in the 1600-1800 cm^{-1} region.

Raman spectra were obtained for thymidine in nine solvents, acid and base. Similar frequency shifts and slight intensity changes were also observed in the Raman spectra of thymidine in the different solvents, as in thymine. However, unlike thymine, correlation of the observed frequency shifts with various solvent properties showed good correlation with the specific solvent property of hydrogen-bonding, as well as with a few "non-specific" solvent properties such as polarity and polarizability. We attributed this effect to the larger solute. The major interaction of solvent with thymidine was found to be at the proton accepting/donating sites of the thymine base, at both the N-H and C=O sites, with little or no apparent interaction with the proton accepting/donating sites of the deoxyribose sugar ring.

These results suggest that Raman spectroscopy is a sensitive, mode-specific technique for probing solvent-solute interactions and thus can be used to probe the interaction of DNA with exogenous molecules. The interaction of DNA with exogenous molecules in different chemical environments should result in frequency shifts and intensity changes in the Raman modes of the bases and/or the sugar-phosphate backbone,

enabling us to predict the nature and mechanism of interaction from these changes in the Raman spectra. Indeed, solvent effects on the Raman spectra of ethyl 4-(dimethylamino)benzoate (DMABEE,) have been reported by Mitambo and Loppnow (1) in this lab. As well, frequency shifts and intensity changes have been reported in the Raman and resonance Raman spectra for the interaction of DNA and anticancer drugs (2-5).

5.2 DNA and Sunscreen Interaction

For a better understanding of how sunscreens contribute to DNA damage, solvent effects on the UV-visible absorption and Raman spectra of the five most commonly used active sunscreen ingredients ODPABA, OMC, BZ3, OCS and DBM were obtained. UV-visible absorption spectra of these sunscreens in ten solvents of varying parameters showed shifts in absorption maxima (λ_{max}) of the lowest-energy electronic transition related to the structure and polarity of these sunscreens. Bathochromic shifts in λ_{max} were observed for the less polar sunscreens ODPABA, OMC, and DBM with increasing solvent polarity, hypsochromic shift for the more polar BZ3, while there was no shift in λ_{max} for the ortho-substituted OCS. These results are in agreement with solvent effects on the UV absorption spectra of these sunscreens previously reported (6-8).

Raman spectra were obtained for these sunscreens in various solvents of varying parameters at visible excitation (406.7 nm). No frequency shifts or intensity changes were observed for DBM in any of the Raman modes. The Raman spectra of ODPABA and OMC in 10 solvents showed frequency downshifts in the C=O stretching mode with increasing solvent hydrogen-bonding. Intensity changes in the C=O and C=C stretching modes were also observed. For BZ3, the Raman spectra in eight solvents showed no apparent frequency shift in the C=O stretching mode nor in any other mode with increasing solvent polarity. However, slight intensity changes were observed in the peaks in the 1100-1700 cm^{-1} region.

These results again show that Raman spectroscopy is a sensitive method for probing solvent-solute interactions, in agreement with the thymine and thymidine data, as

well as with the Raman results for DMABEE (1). Based on these results, Raman spectra with visible excitation (514 nm) were obtained for solutions containing sunscreens and DNA, for two sunscreens ODPABA and OMC alone, and for calf thymus DNA alone. The sunscreen-DNA solution results showed no shift in frequency of the C=O mode marker band or in any other band, nor intensity changes for sunscreen:DNA concentration ratios ranging from 2:1 to 1:10, for both ODPABA and OMC in the presence of DNA. These negative results can be interpreted in three possible ways. First, that the interaction is not effectively monitored by Raman spectroscopy. However, this is not possible since previous experiments with thymine and thymidine (9), the psoralens (10), DMABEE (1), anticancer drugs (2-5) and the sunscreens themselves all confirm the suitability and sensitivity of Raman spectroscopy for monitoring the interaction of solutes with their environment. Second, the results may imply that there is no interaction between the sunscreens and DNA. However, there are numerous reports of sunscreen-DNA interaction and PABA-thymine/thymidine adducts have been isolated (11-14). The third possibility is that the solvent environment around the sunscreens interacting with DNA is similar to bulk solvent. For this possibility, no changes in the spectrum would be predicted, even though the DNA and sunscreens are interacting.

Sunscreen damage to DNA is thought to occur either by the formation of photoproducts/photoadducts or the generation of ($^1O_2$) and other reactive species which attack the DNA backbone causing damage. The results presented here are ambiguous and subject to several interpretations, so no clear evidence for one damage mechanism or the other can be discerned. Further work is therefore required to probe the sunscreen-induced DNA damage mechanism.

5.3 Future Work

The ultimate goal of this research is to obtain a better understanding of DNA damage and repair mechanisms, and the role sunscreens play in DNA damage. This work provides preliminary results which demonstrate that Raman spectroscopy can be a useful probe of environment and suggests further work which may achieve this ultimate goal.

Raman experiments for the interaction of anticancer drugs and DNA (2-5), have used the dual approach of obtaining Raman spectra of the free drug and the drug-DNA complex at a wavelength where the drug modes are probed, as well as obtaining spectra of the free DNA and the drug-DNA complex at a suitable wavelength where only changes in the DNA Raman modes are monitored. Our experiments have only tried to probe the changes in the Raman spectra of the sunscreens. Further experiments in which changes occur only in the DNA Raman spectra on interaction with the sunscreens are required. Raman spectra should be taken of the DNA only, DNA/water/methanol mixtures with and without the sunscreens, at excitation wavelengths where the DNA modes appear clearly, such that only changes in the DNA Raman modes can be monitored. Frequency shifts and intensity changes of some of the Raman modes of the DNA bases and/or sugar-phosphate backbone will indicate the sites and nature of interaction of the sunscreens with DNA.

Since the sunscreens absorb solar UV radiation, UVRR experiments of the sunscreen-DNA interaction are required for the sunscreen-DNA mixtures. Taking advantage of the more rigorous selectivity of the UVRR technique, changes in the sunscreens Raman modes on interaction with DNA can be selectively probed at an excitation wavelength around 300 nm, while changes in the DNA Raman spectrum on interaction with the sunscreens can be probed at 260 nm. The sunscreens absorb maximally around 300 nm, while all the DNA bases have an absorption maximum band around 260 nm. Hence, selective excitation at these wavelengths will result in resonance enhancement of some of the sunscreens and DNA modes, respectively. This also enables the use of lower concentrations of sunscreens to reflect the amounts actually used in sunscreen preparations. Finally, using other techniques such as electron microscopy (TEM and SEM, 15) and gel sequencing experiments which have already been applied to sunscreen-DNA studies (16-18), the sites of physical and chemical damage inflicted on DNA by sunscreens, as well as some of the decomposition products formed and any photoproducts/photoadducts will be identified. This additional information together with the Raman results will indicate the mechanisms by which sunscreens damage DNA, leading to a better understanding of the role of sunscreens in DNA damage.

5.4 References

1 Mitambo, M. M.; Loppnow, G. R. *Chem. Phys. Lett.* **1996**, *261*, 691.

2. Manfait, M.; Theophanides, T. In *Advances in Infrared and Raman Spectroscopy*; Clark, R. J. H.; Hester, R. E., Eds.; John Wiley, 1986, Vol 13; p. 311

3. Nabiev, I.; Chourpa, I.; Manfait, M. *J. Phys. Chem.* **1994,** *98*, 1344.

4. Motohashi, N.; Kamata, K.; Meyer, R. *Anticancer Research*, **1990**, *10*, 1611.

5. Zhao, X.; Lu, D.; et al. *Science in China, Series B:* **1995**, *38*, 555.

6. Shaath, N. A. In *Sunscreens: Development, Evaluation, and Regulatory Aspects*; Lowe, N. J., Shaath, N. A., Eds.; Marcel Dekker: New York, 1990, p 211.

7. Riegelman, S., Penna, R. P. *J. Soc. Cosmet. Chem.* **1960**, *11*, 280.

8. Agrapidis-Paloympis, L. E., Nash, R. A. *J. Soc. Cosmet. Chem.* **1987**, *38*, 209.

9. Beyere, L. H.; Monga, V.; Loppnow, G. R.; et al. In preparation.

10. McWatt, T.; Rafai, S.; Loppnow, G. R. Unpublished work.

11. Gasparro, F. P.; Battista, J. *Photochem. Photobiol.* **1987**, *45*, 49S.

12. Shaw, A. A.; Wainschel, L. A.; Sheltar, M. D. *Photochem. Photobiol.* **1992**, *55*, 657.

13. Broadbent, J. K.; Martincigh, B. S.; Raynor, M. W.; et al. *J. of Chromatography A* **1996**, *732*, 101.

14. Mohammad, T.; Baird, W. M.; Morrison, H. *Bioorganic Chem.* **1991**, *19*, 88.

15. Hidaka, H.; et al. *J. Photochem. Photobiol. A: Chem.* **1997**, *111*, 205.

16. McHugh, P. J., Knowland, J. *Photochem. Photobiol.* **1997**, *66*, 276.

17. Stevenson, C.; Davies, R.J.H. *Chem. Res. Toxicol.* **1999**, *12*, 38.

18. Knowland, J.; McKenzie, E. A.; McHugh, P. J.; Cridland, N. A. *FEBS*, **1993**, *324*, 309.